EDITORIAL BOARD OF THE JOURNAL OF AGRICULTURE AND DEVELOPMENT

EDITORIAL SECRETARIAT

Contact information:
Nong Lam University
Room 404, Thien Ly Building
Linh Trung Ward, Thu Duc City, Ho Chi Minh City, Vietnam
Tel: (84-28)37245670
Email: jad@hcmuaf.edu.vn

The Journal of Agriculture and Development
Volume 20 - Issue 3 (2021)
pISSN 2615-9503
eISSN 2615-949X

CONTENT

Animal Sciences, Veterinary Medicine, Aquaculture and Fisheries

1 Relationship between the ratio of villous height:crypt depth and gut bacteria counts as well production parameters in broiler chickens
Dung T. N. Nguyen, Ngoc H. Le, Vinh V. Pham, Parra Eva, Forti Alberto, & Hien T. Le

11 Identification of porcine circovirus type 2 (PCV2), type 3 (PCV3) and porcine parvovirus (PPV) in swine by multiplex PCR test
Thoai K. Tran, Trang T. T Nguyen, Hiep L. X. Vu, & Phat X. Dinh

18 Genetic analysis of African swine fever virus based on major genes encoding p72, p54 and p30
Hop Q. Nguyen, Duyen M. T. Nguyen, Nam M. Nguyen, Dung N. T. Nguyen, Han Q. T. Luu, & Duy T. Do

26 Quantities and antibiotic resistance of microorganisms in some microbial products for animals in Vietnam
Nhi T. T. Nguyen, Ngoc H. Le, & Hoa T. K. Ho

32 Efficacy of a commercial supplement added to drinking water in broilers fed aflatoxin-contaminated diets
Tung M. Che, Hien T. Le, Vi Q. Tran, Matthieu Le-Goff, & Phat T. Luong

Biotechnology

41 Genetic relationship analysis of *Dendrobium anosmum* Lindl. var. semialba based on the chloroplast *matK* and *rbcL* genes
Dien T. K. Pham, Biet V. Huynh, & Truong Mai

50 Accumulation and distribution of lead (Pb) in different tissues of Lucky bamboo plants (*Dracaena sanderiana*)
Lien B. Ho, Biet V. Huynh, & Tuyen C. Bui

Food Science and Technology

61 Influence of spray-drying conditions on the physicochemical properties of red-fleshed dragon fruit (*Hylocereus polyrhizus*) powder made from peel and flesh
Trang T. N. Tran, Quan A. Do, Ngoan H. Nguyen, Tram N. Pham, Trang L. H. Do, Diep T. N. Duong, & Binh Q. Hoang

Relationship between the ratio of villous height:crypt depth and gut bacteria counts as well production parameters in broiler chickens

Dung T. N. Nguyen[1*], Ngoc H. Le[1], Vinh V. Pham[2], Parra Eva[3], Forti Alberto[3], & Hien T. Le[1]

[1]Faculty of Animal Science and Veterinary Medicine, Nong Lam University, Ho Chi Minh City, Vietnam
[2]Animaid Ltd, Vietnam
[3]Ascor-Vetoquinol, Italia

ARTICLE INFO

Research Paper

Received: March 08, 2021
Revised: May 13, 2021
Accepted: May 24, 2021

Keywords

Broilers
Crypt depth
Gut health
Meat quality
Villous height

***Corresponding author**

Nguyen Thi Ngoc Dung
Email: dungnguyenngoc2004@gmail.com

ABSTRACT

The villous height to crypt depth (V:C) ratio is one of the most significant parameters which is associated with the nutrients' absorption and greater body weight. The objective of this study was to assess the relationship between V:C ratio, gut bacteria counts and production parameters in broiler chickens. A total of 100 individual broilers were randomly selected from a farm with 40,000 Ross 308 chickens and slaughtered for sampling at three different ages including 14, 28 and 37 day old. Villous height and crypt depth were measured for each section of the small intestine to calculate V:C ratio. Intestinal score and gut microbiology including total coliforms, lactic acid bacteria and Salmonella prevalence were assessed. At day 37, besides those parameters, the carcass, breast, legs and wings were taken for weight measurements. Leg and breast color was also measured. Data were statistically analyzed by STATA software to explore the relationship between V:C and those parameters. The results showed the positive correlation between V:C of duodenum and the number of lactic acid bacteria at 28 days of age ($P < 0.05$). Moreover, the leg yield was negatively related to the V:C ratio of jejunum ($P < 0.05$). No significant correlations were found between V:C ratio and other parameters. The results indicated the potential of controlling V:C ratio to improve gut health and meat quality of broiler chickens and thus, further studies should be conducted to fully evaluate these correlations.

Cited as: Nguyen, D. T. N., Le, N. H., Pham, V. V., Eva, P., Alberto, F., & Le, H. T. (2021). Relationship between the ratio of villous height:crypt depth and gut bacteria counts as well production parameters in broiler chickens. *The Journal of Agriculture and Development* 20(3), 1-10.

1. Introduction

The poultry sector is one of the most rapidly growing food-producing animal industries worldwide. A primary emphasis of the commercial broiler industry has been to maximize the growth, meat yield and quality of birds while maintaining their health at an optimal level. The small intestine is a vital organ that is the major site for digestion and absorption of nutrients which is related to growth performance. The chickens'gut health provides broad implications for their systemic health and the correlation between animal performance and gut health is universally accepted. The definition of gut health contains microbiology, immunology, morphology and physiology of the intestinal tract. Because a part of the digestive and also all of the absorptive capac-

ity of the small intestine occur around and near villi and crypts, it is well-known that the villus height:crypt depth ratio is the gut health index (Pluske, 1996).

At hatch, the gastrointestinal tract of broilers is completely undeveloped, affecting the ability of the animal to digest and absorb nutrients. There are drastic changes in the first few days of age in physiological characteristics, such as expression of membrane transporters, endogenous enzyme activities and cell differentiation, and physical characteristics, including villus and crypt development and the size of the digestive tract (Uni et al., 2001). The growth of intestinal villus length is correlated to the enhanced digestive and absorptive functions of the intestine, leading to an increase in total luminal villus absorptive area and an increased activity among intestinal brush border enzymes (Prakatur et al., 2019). While the decrease in the crypt depth achieves an increase in the enzymatic activity of the small intestine which affects to absorption ability (Kelly et al., 1991). In addition, a higher ratio between villous height and crypt depth leads to a slower maintenance requirement and consequently, reaches a higher growth efficiency of the animal as a result of a decreased turnover of the intestinal mucosa (Van Nevel et al., 2005).

In literature, there are only a few studies that have previously described the identified influence of chickens' histological feature changes on the growth of poultry and gut microbiota, but rarely on meat quality. Additionally, in Vietnam, the investigations with regards to these relationships have not been carried out yet. In the strategy of antibiotic alternatives, several products such as probiotics, prebiotics and phytochemicals were proven that had positive impacts on V:C ratio. According to Awad et al. (2009), the supplementation of either synbiotic or probiotic reveals the improvement in the villus height:crypt depth ratio and villus height in both duodenum and ileum. Demir et al. (2003) indicated that there was a reduction in crypt depth in the ileum of broilers given dietary natural growth promoters such as garlic. Therefore, the specific objectives of the present study were to reveal the relationship between the ratio of villus height to crypt depth and other parameters related to chicken performance, gut microbiota and meat quality in the field condition which has become the foundation for this strategy.

2. Materials and Methods

2.1. Animals

Broiler chickens were collected from a commercial farm in Vung Tau province. A total of 40000 day-old Ross 308 broiler chickens of the farm were housed in 2 buildings with a dimesion of 15 m x 100 m and 6 m height, and equipped with 212 feeders and 382 drinkers (approximately 95 birds per feeder and 52 birds per drinker) for each. Temperature, humidity, and lighting in the facility were maintained according to the manufacturer's recommendations for the Ross 308 hybrid (Aviagen, 2018). Chickens were raised from day-old to 37 days (ready for slaughter) and provided with water as well as diet ad libitum. Feed used for broiler was from Kyodo Sojitz and the size of feed was changed based on the age of animals (Table 1). Feed had correctly small size and contained high level of probiotic with the purpose support digestive function for baby chicken. From 1 to 14 days, pellet of feed should be 1.5 - 3.0 mm diameter, 1.5 - 3.0 mm length, while it should be 3.0 - 4.0 mm in diameter, 4.0 - 7.0 mm in length and a change in texture as well as nutrition composition at grower period (15 - 21 days). From 22 days to finish, the birds were fed with pellet which should be 3.0 - 4.0 mm in diameter, 5.0 - 8.0 in length. Breeding was conducted on straw (5 cm depth) and lasted for more than 5 weeks (37 days).

Table 1. Nutritional compositions of feed at three different stages

Compositions	Stage		
	Starter	Grower	Finisher
Crude protein (%)	21	19.5	19
Metabolizable energy (kcal/kg)	3000	3100	3150

2.2. Sample collection, measurements, and analysis

A total of 100 birds, 30 birds at 14 and 28 days of age and 40 birds at 37 days of age was randomly selected and tranported by car from farm to the lab of Nong Lam University HCMC. These points of time were representative for the three stages of development: starter (not fully devel-

oped), grower (developing) and finisher (developed). Feed should be removed from the flock 12 h before the expected time of processing to reduce the risk of fecal contamination. Chickens were transported in the hostile temperature and given a 2-hour rest before slaughtering to minimize stress for chickens which can cause a huge impact on results. Before bleeding, birds were weighed to record their live weight. After that, birds were quickly scalded at 54°C, defeathered in a rotary drum picker and manually eviscerated. This was a normal slaughter process and did not effect to the intestinal microbiota and morphology.

2.2.1. Intestinal histomorphology

Three segments of about 5 cm removed from the small intestine (duodenum, jejunum and ileum) were at the following locations: (i) the middle part of the duodenal loop, (ii) midpoint between the endpoint of the duodenal loop and Meckel's diverticulum (jejunum) and (iii) midway between the Meckel's diverticulum and the ileocaecal junction (Choe et al., 2012). The ingesta in the lumen washed away using normal saline and fixed in 10% buffered formalin. Then, all intestinal portions were dehydrated in an increasing series of ethanol, cleared in xylene, embedded in paraffin block and then cut into 5 µm sections. After drying, paraffin-embedded sections that were stained with hematoxylin and eosin (H & E) and examined under a light microscope (Olympus CX40). The procedure was a modified method from HairBejo (1990), as described by Thanh et al. (2009). A computer morphometric program, Optika Vision Pro 3.0, was used for morphometric measuring the villi height and crypt depth. The villus height was measured from the tip to the base of the villus and crypt depth was measured from the base of the villus to the mucosa. For each section, averaged height and depth measurements of 10 randomly selected villi and crypts were expressed. The ratio of villus to crypt was estimated by dividing the villus height by the crypt depth.

2.2.2. Microbiology

The ceca were dissected and the content was extracted into 50 mL sterilized falcon conical tubes for subsequent analysis of the bacterial populations by serial dilution. Microbiological parameters included total coliforms, *Salmonella* and lactic acid bacteria. Total coliforms were isolated from cecal feces by multiple tube fermentation in lauryl tryptone broth (LTB) and brilliant green bile broth (BGBB) and enumerated by most-probable-number (MPN) estimated by using standard techniques. *Salmonella* was isolated by standard microbiological methods and was confirmed by biochemical and slide agglutination tests using commercial polyvalent O. Lactic acid bacteria were isolated on *Lactobacillus* agar DE Man, ROGOSA and SHARPE (MRS-agar) plates and then, incubated under anaerobic conditions at 37°C for 48 h. Samples were diluted in saline and chosen at least three continuous dilutions (10^{-4}, 10^{-5}, 10^{-6}) to spread 0.1 mL samples directly onto the surface of MRS-agar plates. Each dilution was repeated in duplicate. All colony forming units (CFU) on selected plates were counted and recorded. The number of colonies from 30 to 300 were accepted. All morphologies of colonies were observed including the shape and color, then selected to perform gram-stain and observed under microscope to confirm.

2.2.3. Intestinal scores

All internal organs of slaughtered chickens were observed and recorded any abnormal lesions. Intestinal lesion scores were classified into 4 scales from 0 to 3 corresponding from normal to multifocal hemorrhage in intestinal tract (Table 2).

Table 2. Clinical scoring of intestines

Score	Description
0	Normal, no hemorrhage, normal content
1	Focal hemorrhage (petechial hemorrhage) in a part of intestinal tract
2	More hemorrhage and/or hemorrhage and swollen lymphoid patches
3	Multifocal hemorrhage in large area of the intestinal tract, as well as in lymphoid patches and/or gas in lumen

2.2.4. Carcass traits

At 37 days, carcass and meat qualities were evaluated. After defeathering, eviscerating and removal of the head and paws, carcass weight was determined. The breast, wings, legs muscles of each birds were dissected and weighed. Carcass yield (CY) corresponded to the ratio between

carcass weight (CW) and body weight at slaughter (BW), and was calculated according to the following formula: CY (%) = CW/BW × 100. Parts yield (breast, wings and legs) was calculated as the ratio between the part weight and carcass weight, according to the formula: Part yield (%) = PY/ CW × 100 (PY is the representative value of each part). Breast and leg colors were also assessed by DSM broiler color fan which is expressed in a 101 - 110 scale corresponding from white to marigold color (Figure 1).

Figure 1. DSM broiler color fan.

2.2.5. Meat quality parameters

Drip loss and pH measurements were performed on the major pectoralis muscle of broiler breast. Breast muscles were removed by severing the humeral-scapular joint and pulling downward to strip the meat from the breast. After excision, the ultimate pH and drip loss evaluation were measured. The pH was assessed directly by inserting the probe of portable meat pH meter HI99163 in the same points in the breast at three different points of time including after 0 h, 4 h and 8 h post-mortem. All samples were keep at room temperature. Drip loss was measured using the filter paper press method (Kauffman et al., 1986), which evaluated the amount of moisture loss from the surface of the breast shortly after cutting (15 min, 4 h and 8 h). The size of sample for drip loss measurement was approximately 10 g.

2.3. Statistical analysis

Data collected from the study were entered into Microsoft Excel (2016). For each measured parameter, basic descriptive statistics would be performed for undestanding its distribution to use as either a continuous or categorical variable. The interested outcome variable was V:C ratio – a continuous variable. The relationship between this one with other parameters (dependent variables) would be explored by certain methods. In particular, the one between V:C ratio and dependent variables (intestinal score, logColiforms, logLAB, BW, carcass, breast, wing, leg yield, breast and leg color) would be assessed by correlation coefficient (R) and slope coefficient of Univariate linear regression. With categorical variable (*Salmonella* prevalence), the mean of V:C ratio of each category would be calculated and one-way ANOVA would be used to compare the difference of the means. The P value less than 0.05 would be considered statistical significance. All analysis would be performed on STATA 14.2 software (College Station, Texas 77845 USA).

3. Results

3.1. Evaluation of the relationship between the V:C ratio and gut health

The relationships among V:C ratio and gut health were presented in three tables. At the age of 14, no significant correlation was detected ($P > 0.05$) (Table 3), while the positive correlation was found between V:C ratio of duodenum and the number of lactic acid bacteria at the day of 28 (Fig 2). This relationship was statistically significant ($P < 0.05$) (Table 4). It meant that the greater V:C ratio, the higher number of lactic acid bacteria. At 37 days, the correlation between V:C ratio of ileum and intestinal score was significantly positive ($P < 0.05$) (Table 5). The increased V:C ratio could result in the increase in intestinal score.

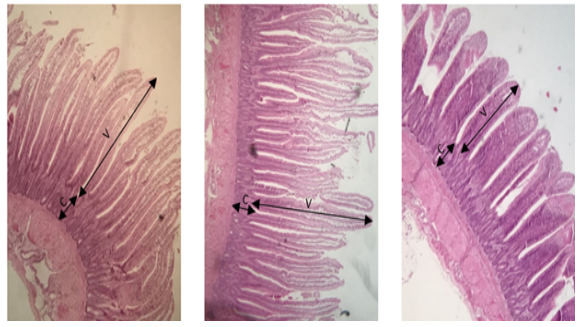

Figure 2. The representative histomorphometry of duodenum, jejunum and ileum (in order from left to right) at 28 days of age (V: villous height, C: crypt depth) (x40).

Table 3. The relationship between the villous height:crypt depth ratio and gut health at the age of 14 days

Segments	Dependent Variables	Mean	R	Slope Coefficient	95% Confidence Interval		*P*
					Lower	Upper	
Duodenum	Intestinal score	1.067	- 0.2341	- 0.2581	- 0.6814	0.1651	0.222
	LogColiforms (CFU/g)	8.337	0.2770	0.3367	- 0.1245	0.7979	0.146
	LogLAB (CFU/g)	8.965	- 0.0922	- 0.1350	- 0.7108	0.4408	0.634
Jejunum	Intestinal score	1.067	0.0449	0.0495	- 0.3767	0.4758	0.814
	LogColiforms (CFU/g)	8.337	- 0.2487	0.3367	- 0.1245	0.7979	0.146
	LogLAB (CFU/g)	8.965	- 0.0121	- 0.1782	- 0.5866	0.5509	0.949
Ileum	Intestinal score	1.067	- 0.1761	- 0.2347	- 0.7528	0.2834	0.361
	LogColiforms (CFU/g)	8.337	- 0.0836	- 0.1233	- 0.7037	0.4571	0.666
	LogLAB (CFU/g)	8.965	- 0.0506	- 0.0899	- 0.7905	0.6106	0.794

Table 4. The relationship between the villous height:crypt depth ratio and gut health at the age of 28 days

Segments	Dependent Variables	Mean	R	Slope Coefficient	95% Confidence Interval		*P*
					Lower	Upper	
Duodenum	Intestinal score	1.8	0.2138	0.2227	- 0.2658	0.7112	0.352
	LogColiforms (CFU/g)	8.200	0.2087	0.4043	- 0.5054	1.3140	0.364
	LogLAB (CFU/g)	7.909	0.4585	0.3284	0.0227	0.6340	0.037
Jejunum	Intestinal score	1.8	0.2227	0.1879	- 0.1369	0.5127	0.246
	LogColiforms (CFU/g)	8.200	0.0955	0.1728	- 0.5384	0.8841	0.622
	LogLAB (CFU/g)	7.909	- 0.1015	- 0.0725	- 0.3528	0.2079	0.600
Ileum	Intestinal score	1.8	0.1506	0.1274	- 0.2172	0.4721	0.453
	LogColiforms (CFU/g)	8.200	0.2879	0.4971	- 0.1839	1.1782	0.145
	LogLAB (CFU/g)	7.909	0.2025	0.1472	- 0.1460	0.4405	0.311

Table 6. *Salmonella* occurence at means of the villous height (V):crypt depth (C) ratio of intestinal segments

Segments	*Salmonella*	n	Mean of V:C	SD	*P*
Duodenum	Negative	68	4.659	0.775	0.6027
	Positive	18	4.768	0.822	
Jejunum	Negative	79	4.027	0.873	0.2853
	Positive	19	4.250	0.485	
Ileum	Negative	77	3.449	0.786	0.4187
	Positive	19	3.606	0.585	

Table 5. The relationship between the villous height:crypt depth ratio and gut health at the age of 37 days

Segments	Dependent Variables	Mean	R	Slope Coefficient	95% Confidence Interval		*P*
					Lower	Upper	
Duodenum	Intestinal score	1.675	0.3433	0.2765	0.0129	0.5401	0.040
	LogColiforms (CFU/g)	8.476	- 0.1716	- 0.3275	- 0.9831	0.3279	0.317
	LogLAB (CFU/g)	7.973	- 0.2154	- 0.1778	- 0.4586	0.1031	0.207
Jejunum	Intestinal score	1.675	- 0.1203	- 0.1001	- 0.3751	0.1750	0.466
	LogColiforms (CFU/g)	8.476	- 0.0624	- 0.1226	- 0.7765	0.5312	0.706
	LogLAB (CFU/g)	7.973	- 0.0176	- 0.0150	- 0.3004	0.2704	0.916
Ileum	Intestinal score	1.675	0.0995	0.0902	- 0.2061	0.3865	0.541
	LogColiforms (CFU/g)	8.476	0.2390	0.5217	- 0.1744	1.2179	0.137
	LogLAB (CFU/g)	7.973	0.1559	0.1521	- 0.1645	0.4686	0.337

3.2. Evaluation of the relationship between the V:C ratio and *Salmonella* occurence

In this study, there was no significant correlation between V:C ratio and Salmonella occurence ($P > 0.05$; Table 6).

3.3. Evaluation of the relationship between the V:C ratio, carcass yield and meat quality

The leg and breast color did not show any correlations with V:C ratio in all three sections of small intestines ($P > 0.05$; Table 7). Carcass, breast and wing weight had no correlation with V:C ratio in three sections of small intestine. While leg weight was negatively related to the V:C ratio of jejunum ($P < 0.05$), which indicated that the proportion of leg weight and carcass weight decreased 1.13% due to one-unit increased in jejunum V:C ratio. No significant correlation among V:C ratio, pH and drip loss.

4. Discussion

Intestine morphology may be mediated via alteration of intestinal microbiota. Based on the results of this study, the improvement of intestinal histomorphometry had a significant correlation with gut microbiota such as lactic acid bacteria. Previous studies have been reported that lactic acid bacteria could affect to intestinal histomorphometry (Chichlowski et al., 2007). According to Liao et al. (2020), the *Lactobacillu*s was positively correlated with V:C ratio in the ileum of the growing broilers which is consistent with the results of this study at the day of 28 ($P < 0.05$). The LAB supplement increased the V:C ratio, thereby positively affecting the development morphology of the small intestine in the study of Gāliņa et al. (2020).

The relative increase in the percentage of the carcass could be related to gut health as well. The improvement in digestion and absorption efficiency of different nutritional materials due to the development of intestinal morphometry, consequently, leads to the improvement in carcass characteristics of broiler chickens (Hosseini et al., 2017). The results of this study did not found any correlation between V:C ratio and carcass yields, except the negative association between V:C ratio of the jejunum and leg yield ($P < 0.05$). Moreover, the wing and leg yields in this study had negative relationship as well, while the breast yield was positive relationship . This finding could be considered as the increase in carcass quality. Despite the small sample size, these findings probably indicated that the improvement in carcass quality may result from the development of the gastrointestinal tract.

Some useful parameters for evaluating quality and consumer acceptability such as pH and drip loss can be affected by the supplementation of antioxidants such as vitamin E, selenium. The association between muscle vitamin E and lower drip loss has been described (Ashgar et al., 1991) and also a trend toward higher muscle pH at 24 h postmortem (5.7 vs. 5.5) (Lu et al., 2014). Although there is no further information about the relationship among the V:C ratio, pH and drip loss, those coefficient seem to be at the direction of improvement of meat quality (higher pH ($P = 0.051$) and reduction of drip loss in the duodenum and ileum). Thus it can be thought that the higher V:C ratio, the greater absorption of antioxidants supplied in the diet which probably impacts on meat quality.

Furthermore, the number of previous studies specified that the main compound with coloring function in meat and eggs is the carotenoids (Blanch & Hernandez, 2000). Carotenoids are essential for the immune system, have antioxidant effects and cannot be synthesized by poultry that therefore needs to obtain these compounds from the diet (Kim et al., 2012). The skin color may be related to the absorption of carotenoids of chicken intestines. According to Lloyd (1970), most of the absorption of xanthophylls (one of the forms of carotenoids) takes place in the area of the jejunum-ileum in which *E. maxima* infections occur and very little xanthophylls are absorbed in the duodenum, ceca, and large intestine. Nevertheless, there were no significantly positive correlations between skin color and intestinal histomorphometry in this study.

It has been proven that shorter intestinal villi relative to crypt depth are related to a smaller number of absorptive cells and a larger number of secretory cells which are responsible for the secretion of mucins. Mucin is the major constituent of the mucous layer (Iwashita et al., 2003) which is the first line of the host intestinal defense and influences nutrient digestion and absorption. Under normal physiological conditions, mucin secretion is necessary to replenish and maintain a suitable

Table 7. The relationship between the villous height:crypt depth ratio and meat quality

Segments	Dependent Variables		Mean	R	Slope Coefficient	95% Confidence Interval		*P*
						Lower	Upper	
	Leg color		74.9	- 0.0476	- 0.0511	- 4.2446	0.3224	0.783
	Breast color		30.1	- 0.1349	- 0.0524	- 0.1864	0.0816	0.433
	Carcass yield(%)		7.8	- 0.1673	- 0.0060	- 0.0185	0.0064	0.329
	Breast yield(%)		21.8	0.2042	0.0055	- 0.0037	0.0147	0.232
	Wing yield(%)		101.0	- 0.3222	- 0.0033	- 0.0066	0.0001	0.055
Duodenum	Leg yield(%)		103.3	- 0.0191	- 0.0005	- 0.0106	0.0095	0.912
		0	6.4	0.1890	0.0209	- 0.0271	0.0691	0.382
	pH	4 h	5.8	- 0.2221	0.0076	- 0.0467	0.0619	0.778
		8 h	5.7	- 0.2961	- 0.0086	- 0.0673	0.0502	0.769
	Drip loss(%)	4 h	5.7	- 0.2367	- 0.0093	- 0.0226	0.0040	0.165
		8 h	9.3	- 0.2122	- 0.0108	- 0.0282	0.0066	0.214
	Leg color		74.9	0.2677	0.2945	- 0.0586	0.6477	0.099
	Breast color		30.1	- 0.1324	- 0.0509	- 0.1781	0.0761	0.422
	Carcass yield(%)		7.8	0.0853	0.0031	- 0.0089	0.1517	0.606
	Breast yield(%)		21.8	0.1139	0.0031	- 0.0059	0.0119	0.490
	Wing yield(%)		101.0	- 0.0461	- 0.0005	- 0.0041	0.0031	0.781
Jejunum	Leg yield(%)		103.3	- 0.3851	- 0.0113	- 0.0204	-0.0023	0.015
		0	6.4	- 0.0221	- 0.0031	- 0.0502	0.0439	0.894
	pH	4 h	5.8	0.1810	0.0336	- 0.0272	0.0938	0.270
		8 h	5.7	0.0451	0.0083	- 0.0529	0.0695	0.785
	Drip loss(%)	4 h	5.7	0.1517	0.0068	- 0.0060	0.0197	0.292
		8 h	9.3	0.1837	0.0099	- 0.0067	0.0266	0.233
	Leg color		74.9	- 0.0556	- 0.0666	- 0.4594	0.3263	0.733
	Breast color		30.1	- 0.2383	- 0.0998	- 0.2332	0.0337	0.139
	Carcass yield(%)		7.8	- 0.1770	- 0.0070	- 0.0198	0.0058	0.275
	Breast yield(%)		21.8	- 0.0339	- 0.0009	- 0.0106	0.0086	0.835
	Wing yield(%)		101.0	0.1724	0.0020	- 0.0018	0.0058	0.287
Ileum	Leg yield(%)		103.3	0.0482	0.0016	- 0.0093	0.0124	0.768
		0	6.4	- 0.2524	- 0.0276	- 0.0807	0.0255	0.299
	pH	4 h	5.8	- 0.1206	- 0.0426	- 0.1075	0.0222	0.191
		8 h	5.7	0.1993	- 0.0620	- 0.1245	0.0004	0.051
	Drip loss(%)	4 h	5.7	- 0.1274	- 0.0069	- 0.0208	0.0069	0.318
		8 h	9.3	- 0.1251	- 0.0086	- 0.0266	0.0094	0.340

thickness of the mucous layer in the intestine because this layer is often sloughed off by intestinal movement, chemical compounds and microbially derived factors (Horn et al., 2009) to maintain gut health. Nevertheless, in this study, at the age of 37 day old, the greater the duodenum V:C ratio, the higher the intestinal lesion scores. This is not the desired finding but we believed that in the case of enteritis problems, the use of V:C value should be concerned in the case of without antibiotics in feed.

5. Conclusions

The results achieved from the study showed that the significantly positive correlations among the V:C ratio, the number of lactic acid bacteria, intestinal scores and the negative one between V:C ratio and the leg yield. No significant relationships between the V:C ratio and other parameters were found. In conclusion, the promising and encouraging results of this study emphasize the importance of the further evaluation of the relationship between the intestinal morphology and other parameters in order to maximize the gut health of chickens and, consequently, the overall health of broiler chickens in the field condition.

Conflict of interest

The authors declare no conflict of interest.

Acknowledgements

The authors would like to express their deep gratitude to Animaid Company and Ascor-Vetoquinol Company for funding for this study. This work was supported by the staff of the laboratory of Infectious Diseases and Veterinary Public Health Department for sample processing.

References

Ashgar, A., Gray, J. I., Miller, E. R., Ku, P. K., Booren, A. M., & Buckley, D. J. (1991). Influence of supranutritional vitamin E supplementation in the feed on swine growth, performance and deposition in different tissues. *Journal of Science of Food and Agriculture* 57(1), 19-29.

Aviagen. (2018). *Ross broiler management handbook*. Retrieved December 22, 2018, from https://en.aviagen.com/assets/Tech_Center/Ross_Broiler/Ross-BroilerHandbook2018-EN.pdf.

Awad, W. A., Ghareeb, K., Abdel-Raheem, S., & Bohm, J. (2009). Effects of dietary inclusion of probiotic and synbiotic on growth performance, organ weights, and intestinal histomorphology of broiler chickens. *Poultry Science* 88(1), 49-56.

Blanch, A., & Hernandez, J. M. (2000). Red carotenoids for optimal yolk pigmentation. *Feed Mix* 8(6), 9-12.

Chichlowski, M., Croom, W. J., Edens, F. W., McBride, B. W., Qiu, R., Chiang, C. C., Daniel, L. R., Havenstein, G. B., & Koci, M. D. (2007). Microarchitecture and spatial relationship between bacteria and ileal, cecal and colonic epithelium in chicks fed a direct-fed microbial, Primalac, and Salinomycin. *Poultry Science* 86(6), 1121-1132.

Choe, D. W., Loh, Dr T. C., Foo, H. L., Hair-Bejo, M., & Awis, Q. S. (2012). Egg production, faecal pH and microbial population, small intestine morphology, and plasma and yolk cholesterol in laying hens given liquid metabolites produced by *Lactobacillus* plantarum strains. *British Poultry Science* 53(1), 106-115.

Demir, E., Sarica, S., Ozcan, M. A., & Suicmez, M. (2003). The use of natural feed additives as alternatives for an antibiotic growth promoter in broiler diet. British Poultry Science 44(1), 44-45. Gāliņa, D., Ansonska, L., & Valdovska, A. (2020). Effect of probiotics and herbal products on intestinal histomorphological and immunological development in piglets. *Veterinary Medicine International* 2020, 3461768.

Hairbejo, M. (1990). *Gastrointestinal response to copper excess, studies on copper (and zinc) loaded rats* (Unpublished doctoral dissertion). University of Liverpool, Liverpool, United Kingdom.

Horn, N. L., Donkin, S. S., Applegate, T. J., & Adeola, O. (2009). Intestinal mucin dynamics, response of broiler chicks and white pekin ducklings to dietary threonine. *Poultry Science* 88(9), 1906-1914.

Hosseini, S., Chamani, M., Seidavi, A., Sadeghi, A. A., & Ansari-Pirsaraei, Z. (2017). Effect of feeding Thymolina® powder on the carcass characteristics and morphology of small intestine in ross 308 broiler chickens. *Acta Scientiarum Animal Sciences* 39(1), 45-50.

Iwashita, J., Yukita, S., Hiroko, S., Nagatomo, T., Hiroshi, S., & Tatsuya, A. (2003). mRNA of MUC2 is stimulated by IL-4, IL-13 or TNF-α through a mitogen-activated protein kinase pathway in human colon cancer cells. *Immunology and Cell Biology* 81(4), 275-282.

Kauffman, R. G., Eikelenboom, G., Van der Wal, P .G., Merkus, G., & Zaar, M. (1986). The use of filter paper to estimate drip loss of porcine musculature. *Meat Science* 18(3), 191-200.

Kelly, D., Smyth, J. A., & McCracken, K. J. (1991). Digestive development of the early-weaned pig. 1. Effect of continuous nutrient supply on the development of the digestive tract and on changes in digestive enzyme activity during the first week post-weaning. *British Journal of Nutrition* 65(2), 169-180.

Kim, J. E., Clark, R. M., Park, Y., Lee, J., & Fernandez, M. L. (2012). Lutein decreases oxidative stress and inflammation in liver and eyes of guinea pigs fed a hypercholesterolemic diet. *Nutrition Research Practice* 6(2), 113-119.

Liao, X., Shao, Y., Sun, G., Yang, Y., Zhang, L., Guo, Y., Luo, X., & Lu, L. (2020). The relationship among gut microbiota, short-chain fatty acids, and intestinal morphology of growing and healthy broilers. *Poultry Science* 99(11), 5883-5895.

Lloyd, H. L. (1970). *The site of absorption of xanthophylls and factors affecting pigmentation of chickens, egg yolks, and products made from egg yolks* (Unpublished doctoral dissertion). University of Tennessee, Knoxville, United States.

Lu, T., Harper, A. F., Scheffler, J. M., Corl, B. A., Estenne, M. J., & Zhao, J. (2014). Supplementing antioxidants to pigs fed diets high in oxidants: II. Effects on carcass characteristics, meat quality, and fatty acid profile. *Journal of Animal Science* 92(12), 5464-5475.

Pluske, J. R., Tompson, M. J., Atwood, C. S., Bird, P. H., Williams, I. H., & Hartmann, P. E. (1996). Maintenance of villus height and crypt depth, and enhancement of disaccharide digestion and monosaccharide absorption, in piglets fed on cow's whole milk after weaning. *British Journal of Nutrition* 76(3), 409-422.

Prakatur, I., Miškulin, M., Pavic, M., Marjanovic, K., Blazicevic, V., Miskulin, I., & Domacinovic, M. (2019). Intestinal morphology in broiler chickens supplemented with propolis and bee pollen. *Animals* 9(6), 301.

Thanh, N. T., Loh, T. C., Foo, H. L., Hair-Bejo, M., & Azhar, B. K. (2009). Effects of feeding metabolite combinations produced by *Lactobacillus* plantarumon growth performance, faecal microbial population, small intestine villus height and faecal volatile fatty acids in broilers. *British Poultry Science* 50(3), 298-306.

Uni, Z., Gal-Garber, O., Geyra, A., Sklan, D., & Yahav, S. (2001). Change in the growth and function of chick small intestine epithelium due to early thermal conditioning. *Poultry Science* 80(4), 438-445.

Van Nevel, C. J., Decuypere, J. A., Dierick, N. A., & Molly, K. (2005). Incorporation of galactomannans in the diet of newly weaned piglets, effect on bacteriological and some morphological characteristics of the small intestine. *Archives of Animal Nutrition* 59(2), 123-138.

Identification of porcine circovirus type 2 (PCV2), type 3 (PCV3) and porcine parvovirus (PPV) in swine by multiplex PCR test

Thoai K. Tran[1], Trang T. T Nguyen[1], Hiep L. X. Vu[2], & Phat X. Dinh[1*]

[1]Faculty of Biological Sciences, Nong Lam University, Ho Chi Minh City, Vietnam
[2]Nebraska Center for Virology, and School of Veterinary Medicine and Biomedical Sciences, University of Nebraska Lincoln, Nebraska, USA

ARTICLE INFO

Research Paper

Received: April 22, 2021
Revised: May 21, 2021
Accepted: June 01, 2021

Keywords

mPCR
PCV2
PCV3
PPV
Swine

[*]**Corresponding author**

Dinh Xuan Phat
Email: dinhxuanphat@hcmuaf.edu.vn

ABSTRACT

This study aimed to simultaneously detect three important viruses reported to be involved in the reproductive problems of sows. A multiplex PCR (mPCR) test was developed to provide rapid diagnosis of porcine circovirus type 2 and 3 (PCV2, PCV3) and to illustrate parvovirus (PPV) prevalence in sow herds. Three pairs of specific primers were designed to target PCV2 *Cap* gene, PCV3 *Cap* gene and PPV NS1 gene, with predicted mPCR products of 702 bp, 267 bp and 380 bp, respectively. The detection limit of mPCR was 100 copies/reaction per target gene. The mPCR was run against a panel of 94 swine serum samples whose infection status had been pre-determined by commercial real-time PCR kits. Sequencing of mPCR products performed with clinical serum samples accurately confirmed the results. Overall, the results indicated that the mPCR functioned accurately and specifically and matched 100% with the single-target real-time PCRs. The mPCR was developed successfully and can be used in routine diagnosis of PCV2, PCV3 and PPV.

Cited as: Tran, T. K., Nguyen, T. T. T., Vu, H. L. X., & Dinh, P. X. (2021). Identification of porcine circovirus type 2 (PCV2), type 3 (PCV3) and porcine parvovirus (PPV) in swine by multiplex PCR test. *The Journal of Agriculture and Development* 20(3), 11-17.

1. Introduction

Reproductive disorders are among the most concerned syndromes in sow herds, causing huge economic losses to swine producers. Many infectious pathogens are involved in the problems, including porcine parvovirus (PPV), porcine circovirus type 2 (PCV2) and porcine circovirus type 3 (PCV3), a newly discovered viral pathogen (Palinski et al., 2016).

Porcine circovirus type 2 and type 3 are non-enveloped and single-circular DNA viruses that belong to the family *Circoviridae* (Tisciier et al., 1986; Palinski et al., 2016). Porcine circovirus type 2 has been demonstrated to play significant roles in different swine syndromes such as postweaning multisystemic wasting syndrome (PMWS), porcine dermatitis and nephropathy syndrome (PDNS), or porcine circovirus associated diseases (PCVAD) in general (Allan et al., 1999; Allan et al., 2000; Rosell et al., 2000). The virus was first identified in western Canada in a case of wasting disease using electron microscopy, immunohistochemical, and in-situ hybridization methods (Ellis et al., 1998). Later, various publications illustrated the circulation and the pathogenesis of PCV2 in abortion cases or weak piglets at birth (West et al., 1999; Calsamiglia et al.,

2007; Oropeza-Moe et al., 2017). Porcine circovirus type 3 was recently detected in a case of PDNS syndrome in a sow farm in North Carolina (USA) (Palinski et al., 2016). The virus was found in the skin, kidneys, lungs, and lymph nodes of the affected pigs without the existence of PCV2. From this observation, PCV3 was also suspected to play a pathogenic role in swine, especially in the sow herds, although the evidence of its pathogenesis remains to be elusive. In addition, another virus in the list of causative agents for reproductive disorders in swine is PPV, a member of the *Parvoviridae* family, that was identified at the end of the 1960s (Cartwright et al., 1967; Cartwright et al., 1969; Johnson & Collings, 1969). Typical manifestations associated with a PPV infection in pregnant sows are collectively identified as SMEDI syndrome which includes stillbirths, mummification, embryonic death, and infertility. These viruses are currently circulating in Vietnam and cause significant losses (Huynh et al., 2014; Dinh et al., 2021). Co-infection among these viruses may result in a different impact on the swine farms. Co-infection of swine with PCV2 and PCV3 does not result in significantly enhanced disease outcomes compared to individual infection with one of these two viruses (Wozniak et al., 2019). However, co-infection of swine with PCV2 and PPV led to the increased viremia level of PCV2 (Milek et al., 2020).

Several conventional and real-time PCRs have been developed for molecular diagnosis of these three viruses (Chen et al., 2009; Zhao et al., 2010; Yang et al., 2019). However, those PCRs are designed for the detection of a single or double pathogens at a time. In the present study, we report the development and validation of a mPCR that allows simultaneous detection of these three viruses in field samples.

2. Materials and Methods

2.1. Controls and clinical samples

Positive controls: DNA fragments of PCV3 *Cap* gene and PPV *NS1* gene were synthesized by Integrated DNA Technologies (IDT - USA) based on the sequences of PCV3 (MH184542.1) and PPV (MK993540.1), respectively. The DNA template of PCV2 was originally obtained from a field isolate followed by sequencing confirmation. The resulting sequence exhibited 99.72% identity to the previously reported PCV2 (Gene Accession no. LC383449.1).

Unrelated DNA from other pathogens used for specificity evaluation: bacteria and viruses that are commonly present in swine farm environment and potentially contaminated into the samples were used to confirm the specificity of the mPCR. *Staphylococcus aureus* (ATCC 6338) and *Escherichia coli* (ATCC 25922) were offered by Sanphar Vietnam laboratory (belonging to Erber group, Austria); *Streptococcus suis* and *Clostridium perfringens* were obtained from a previous study (Nguyen et al., 2018). The bacterial DNA was extracted with phenol-chloroform-isoamyl alcohol (25:24:1) solution (Cat#P1037, Sigma; Cat#25666, Merck). Pseudorabies virus *gE* gene was synthesized by Integrated DNA Technologies (IDT - USA).

Field samples: Ninety-four serum samples from sows were collected and used to evaluate this mPCR procedure. These sow farms were located in the South of Vietnam. Each serum sample was pooled from five individual sows. All samples were submitted to the laboratory and the senders signed an agreement for the laboratory to use the result data for teaching and publication. The infectious status of these 94 samples was predetermined by using commercial real-time PCR kits or master mix, as per the manufacturers' instructions. The real-time kits used for detection of PCV2, PPV and PCV3 were PowerChekTM PCV2 real-time PCR kit (Cat#R0809, Primerdesign), PowerChekTM ADV/PPV real-time PCR kit (Cat#R0832, Primerdesign) and Luna® Universal qPCR Master Mix (Cat#M3003S, NEB), respectively.

2.2. DNA preparation from clinical samples

The DNA was extracted from test serum samples by using the advanced phenol-chloroform method. The extracted DNA was stored at -20°C for subsequent assays.

2.3. Primers

The primers used in this study are listed in Table 1. For PCV2, primers were designed based on the consensus of 65 PCV2 *Cap* gene sequences in the NCBI GenBank with a PCR product of 702 bp. For PPV, primers were designed based on the consensus of 67 PPV *NS1* sequences in the NCBI GenBank with an expected product of 380 bp. Lastly, for PCV3, primers were obtained from

Table 1. Primer sequences and estimated product sizes

Virus	Primers	Gene	Primer sequences (5' – 3')	Product size (bp)	Reference
PCV2	PCV2	*Cap*	F:ATGACGTATCCAAGGAGGCG R: TTAAGGGTTAAGTGGGGGGTC	702	Present study
PCV3	PCV3	*Cap*	F: TTCCGGGACATAAATGCT R: GGGCACACAGCCATAGAT	267	Chen et al., 2017
PPV	PPV	*NS1*	F: GCTTTAGCCTTGGAGCCGTGGA R: CGTGTTCTTTTGCTGCGGCGTC	380	Present study

Chen et al. (2017). They were designed based on the PCV3 *Cap* gene with a product size of 267 bp.

2.4. Multiplex PCR (mPCR)

After multiple rounds of optimization, a primer mix containing three primer pairs were created at a mixing ratio of 1 PPV : 2 PCV2 : 4 PCV3. Accordingly, the final concentrations of the PPV, PCV2 and PCV3 primer pairs in the mixture were 0.2 µM, 0.4 µM, 0.8 µM, respectively. The mPCR was performed in a 20 µL reaction volume containing 10 µL of DreamTaq 2X (Cat#K1072, No MAN0012702, Thermo Scientific), 1.4 µL of the primer mix, 3 µL DNA template, and 5.6 µL of nuclease free water (Thermo Fisher). After initial denaturation at 94°C for 5 min, 35 cycles were conducted at 94°C for 30 sec, 56°C for 30 sec, and 72°C for 40 sec, followed by a final extension at 72°C for 5 min. The amplified products were then analyzed by electrophoresis in a 1.5% (w/v) agarose gel in 1X Tris-Boric-EDTA (TBE) containing Midori Green Advance DNA stain (Cat#MG04, Nippon Genetics). The standard DNA (Cat#10787018, Invitrogen) was included in each DNA gel electrophoresis to indicate the PCR product size.

2.5. Evaluation of the specificity of the mPCR

The target viruses of this study can be found in blood, saliva, feces, vulval discharge in live pigs. In disease surveillance, these types of samples are favored due to the less invasive advantages. However, sampling procedures in practice are prone to contamination with other bacteria or viruses popularly distributed in pig farms. Therefore, genomic DNA of *S. aureus*, *E. coli*, *S. suis*, *C. perfringens* and PRV *gE* gene were used as templates in the mPCR to determine the specificity of the test. The concentration of DNA templates used in the reaction was 30 ng per reaction in the cases of bacterial target and 10^8 copies per reaction in the case of *gE* gene.

2.6. Evaluation of the detection limit of the mPCR

Ten-fold serial dilutions of each positive control DNA templates ranging from 10^7 to 10^0 copies were used as the DNA template in the mPCR to determine its limit of detection. The minimum number of template copies that enable successful amplification of all products was considered as the limit of detection of the mPCR.

2.7. DNA sequencing

Sequencing of each PCR product was performed by using both forward and reverse primers used in the corresponding PCR (Table 1). The sequencing results were aligned with the reference PCV2 (accession no. MH470234.1), PCV3 (accession no. MK058529.1) and PPV (accession no. MK378155.1) using Clustal Omega program.

3. Results

3.1. Optimal conditions for the mPCR

Before the optimal ratio of primers for mPCR was achieved, each primer pair was tested for its performance in single PCR (sPCR) at different annealing temperatures. Gel analysis indicated that only one DNA product was generated in each sPCR, with the product sizes of 267 bp for PCV3, 380 bp for PPV and 702 bp for PCV2 (Figure 1). It appeared that the three primer pairs worked well at the annealing temperatures between 52°C - 58°C.

Subsequently, the annealing temperature of 56°C was chosen for mPCR. As shown in Figure 2, the mPCR produced three amplicons that were

clearly visible and easily distinguishable. Importantly, the sizes of the amplicons were as expected and were similar to the ones observed in the corresponding sPCRs (Figure 2). These three products in mPCR were recovered from agarose gel and subjected to sequencing. The results confirmed that the three PCR amplicons from the mPCR aligned well with the three respective target DNA sequences, indicating that the primer pairs functioned as anticipated.

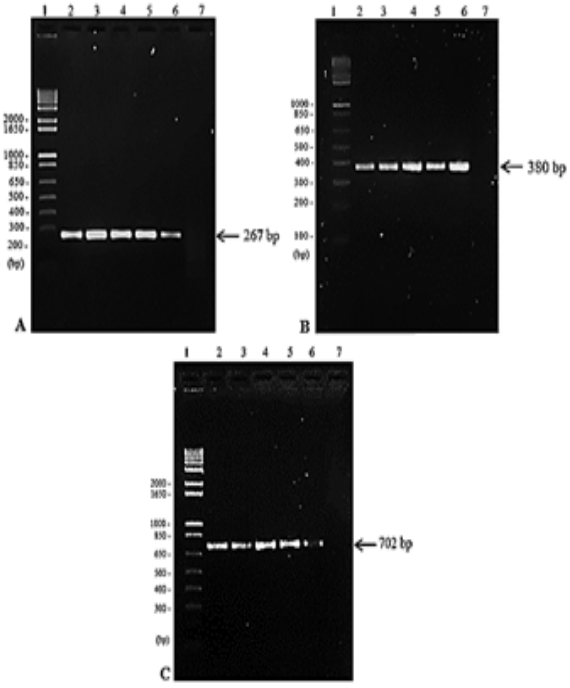

Figure 1. Optimization of annealing temperature in s-PCR. (A) PCV3, (B) PPV, (C) PCV2. (Lane 1): DNA ladder 1 Kb plus, (Lane 2): 50°C, (Lane 3): 52°C, (Lane 4): 54°C, (Lane 5): 56°C, (Lane 6): 58°C, (Lane 7): negative control with pure water. The thermal cycling conditions were 94°C/5 min; 35 cycles of 94°C/30 sec, 50-58°C/30 sec and 72°C/40 sec, a final extension at 72°C/5 min.

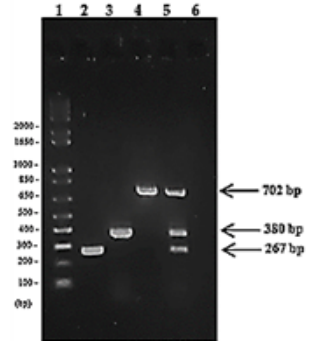

Figure 2. Products of sPCRs and mPCR. (Lane 1): DNA ladder, (Lane 2): PCV3 267 bp, (Lane 3): PPV 380 bp, (Lane 4): PCV2 702 bp, (Lane 5): mPCR of all three targets, (Lane 6): negative control with pure water. The thermal cycling conditions were 94°C/5 min; 35 cycles of 94°C/30 sec, 56°C/30 sec and 72°C/40 sec, a final extension at 72°C/5 min.

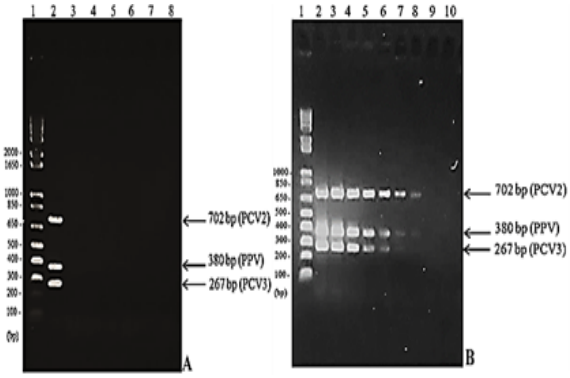

Figure 3. Specificity and detection limit of the mPCR. (A) Result of specificity test. (Lane 1): DNA ladder, (Lane 2): positive control, (Lane 3): *E. coli*, (Lane 4): *Streptococcus suis*, (Lane 5): *Staphylococcus aureus*, (Lane 6): *C. perfringens*, (Lane 7): Pseudorabies virus, (Lane 8): negative control. (B) Detection limit of the mPCR. (Lane 1): DNA ladder, (Lane 2-9): DNA template of PCV2, PCV3 and PPV at 10^7 - 10^0 copies/reaction; (Lane 10): negative control with pure water.

3.2. Specificity and detection limit of the mPCR

Next, we wanted to evaluate the specificity of this mPCR by running the assay with DNA templates extracted from bacteria and viruses commonly present in swine farm environment including *Staphylococcus aureus*, *Escherichia coli*, *Streptococcus suis*, *Clostridium perfringens* and Pseudorabies virus. Results showed that the three primer pairs did not cross-react with any of these DNA templates (Figure 3A), indicating the mPCR established in this study was highly specific.

We then evaluated the limit of detection of the mPCR by performing the assay with a set of 10-fold serially diluted positive control DNA samples with the copy numbers ranging from 10^7 to 10^0 copies per reaction. As shown in Figure 3B, three distinct DNA bands at the expected size were observed at the concentration of 10^2 copies per reaction. It demonstrated that this mPCR

could detect the viral genes at the limit of 100 copies/gene/reaction.

3.3. Performance of the mPCR with clinical samples

The ultimate aim of this experiment was to evaluate the diagnostic performance of the mPCR using field samples. A total of 94 sow serum samples whose infectious status was predetermined by commercial single-target real-time PCR kits were used to evaluate the established mPCR. The DNA electrophoresis of mPCR results was partially illustrated in Figure 4 and the sample that was infected with one single pathogen such as PPV (Figure 4A, lane 6) or samples that were dually infected with two pathogens (Figure 4B, lane 4 and 11) or three pathogens (Figure 4A, lane 8 and 10). The mPCR results matched completely with the results generated by commercial real-time PCR. The infection rates for PCV2, PCV3 and PPV in these 94 samples were 43.6%, 39.4% and 55.3%, respectively. Combined infection of the three tested viruses (PCV2, PCV3 and PPV) was 17.0% while the dual infection between PCV2 and PCV3, PCV3 and PPV, or PCV2 and PPV were 7.4%, 5.3%, and 11.7%, respectively.

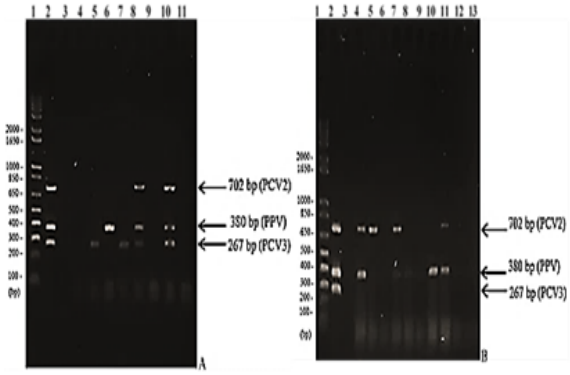

Figure 4. Diagnosis of PCV2, PCV3, PPV in clinical samples. (A) mPCR result of samples 1-9. (Lane 1): DNA ladder; (Lane 2): positive control; (Lane 3): negative control. (Lane 4 - 11): samples 1 to 9. (B) mPCR result of samples 10-19. (Lane 1): DNA ladder; (Lane 2): positive control; (Lane 3): negative control with pure water. (Lane 4 - 13): samples 10-19.

3.4. Sequence analysis of the PCR amplicons

To further confirm the specificity of the mPCR assay, PCR products of PPV, PCV3 and PCV2 amplified from the field samples were excised from the agarose gel and subjected to DNA sequencing. The resulting sequences exhibited 100%, 98.88%, 98.95% identity to the reference sequences for PCV2 (MH470234.1); PCV3 (MK058529.1) and PPV (MK378155.1), respectively.

4. Discussion

Swine reproductive failure is a common disorder in sow herds in Vietnam at present. Various pathogens can be found in such cases including classical swine fever virus, Aujeszky's disease virus, PRRSV (Porcine reproductive and respiratory syndrome virus), PPV, PCV2, PCV3 and some bacteria (Christianson, 1992; Dinh et al., 2021). Currently, single real-time PCRs are available for molecular detection of these viruses. Nevertheless, single real-time PCRs are relatively expensive, thereby deterring swine producers from using these services. Multiplex PCRs can significantly reduce the cost spent in single PCR for each target. Technically, it is easier to develop a multiplex PCR for viruses that are in the same category of either RNA or DNA genome. Therefore, the goal of this study was to develop a quick and reliable mPCR that allows simultaneous detection of PCV2, PCV3 and PPV, the three DNA viruses that are commonly involved in reproductive failure.

Since its initial identification in the US (Palinski et al., 2016), PCV3 has been found in various pig-producing countries. The 39.4% detection rate for PCV3 in our study was also comparable to other reports elsewhere, such as 44.2% in Korea (Kwon et al., 2017); 31.18% in Central China (Xu et al., 2018); 50% in Germany (Prinz et al., 2019); 56.4%, 37.4%, 14.8% in Denmark, Italy, Spain, respectively (Franzo et al., 2018); 61.1% in United States (Arruda et al., 2019); and 47.8% in Brazil (Saraiva et al., 2019). Concurrent infections between PCV2 and other bacteria or viruses have been reported widely in swine herds (Ouyang et al., 2019; Dinh et al., 2021). One of the plausible reasons for this is that PCV2 can suppress the host immune system, therefore rendering the host more susceptible to infections with other microorganisms. The PPV is one of the common swine pathogens that are detected in PCV2 infected pigs (Ouyang et al., 2019). Previous studies showed that co-infections of pigs with PCV2 and PPV were more effective in inducing PMWS disease than coinfection between

PCV2 and other pathogens (Milek et al., 2020). Consequently, PPV could be used in combination with PCV2 to induce PMWS in experimental studies (Palinski et al., 2016). Coinfection of PCV2 and PCV3 is also commonly observed. Several surveillances from China have reported the PCV2/PCV3 co-infection rates varying from 27.6 - 39.39% (Ouyang et al., 2019). Those numbers were higher than what we found in this study (7.4%). In addition, it has been demonstrated that PCV2, PCV3 and PPV are endemic in Vietnam (Huynh et al., 2015; Pham et al., 2017; Nguyen et al., 2020), but the co-infection rates of these 3 viruses in sow herds have not been studied. Our preliminary demonstration of 17% of sow samples to be simultaneously positive for these three viruses illustrated the complex prevalence of various pathogens involved in porcine reproductive syndrome in Vietnam and highlighted the need for further investigations for a better understanding and control strategies.

The detection limit of our mPCR is 100 copies for each target gene per reaction. Liu et al. (2015) established a mPCR to detect and differentiate PCV2, PRRSV, PPV and Pseudorabies virus in pigs with PMWS manifestation. The authors reported that the sensitivity of their mPCR was 4.0×10^3 and 3.0×10^2 copies to PCV2 and PPV, respectively. Recently, Yang et al. (2018) developed a mPCR for simultaneous detection of PCV1, PCV2 and PCV3 with the detection limit of 50 copies of each target gene per reaction. Thus, our mPCR reported in this communication possesses a fairly good detection limit and certainly can be useful for pathogen monitoring in the field or used for predetermination of pathogen occurrence before further viral analysis of field samples.

5. Conclusions

In summary, we have successfully developed and validated a mPCR assay to simultaneously detect PCV2, PCV3 and PPV, the three common swine DNA viruses in field samples. This mPCR should provide a quick and reliable molecular diagnostic tool for reproductive failure in sow herds.

Conflict of interest

The authors declare no conflict of interest.

References

Allan, G. M., McNeilly, E., Kennedy, S., Meehan, B., Moffett, D., Malone, F., Ellis, J., & Krakowka, S. (2000). PCV-2-associated PDNS in Northern Ireland in 1990. Porcine dermatitis and nephropathy syndrome. *Veterinary Record* 146(24), 711-712.

Allan, G. M., McNeilly, F., Meehan, B. M., Kennedy, S., Mackie, D. P., Ellis, J. A., Clark, E. G., Espuna, E., Saubi, N., & Riera, P. (1999). Isolation and characterisation of circoviruses from pigs with wasting syndromes in Spain, Denmark and Northern Ireland. *Veterinary Microbiology* 66(2), 115-123.

Arruda, B., Piñeyro, P., Derscheida, R., Hause, B., Byers, E., Dion, K., Long, D., Sievers, D., Tangen, J., Williams, T., & Schwartz, K. (2019). PCV3-associated disease in the United States swine herd. *Emerging Microbes & Infections* 8(1), 684-698.

Calsamiglia, M., Fraile, L., Espinal, A., Cuxart, A., Seminati, C., Martín, M., Mateu, E., Domingo, M., & Segalés, J. (2007). Sow porcine circovirus type 2 (PCV2) status effect on litter mortality in postweaning multisystemic wasting syndrome (PMWS). *Research in Veterinary Science* 82(3), 299-304.

Cartwright, S. F., & Huck, R. A. (1967). Viruses isolated in association with herd infertility abortions and stillbirths in pigs. *Veterinary Record* 81(1967), 196-197.

Cartwright, S. F., Lucas, M., & Huck, R. A. (1969). A small haemagglutinating porcine DNA virus: I. Isolation and properties. *The Journal of Comparative Pathology* 79(3), 371-377.

Chen, G. H., Mai, K. J., Zhou, L., Wu, R. T., Tabg, X. Y., Wu, J. L., He, L. L., Lan, T., Xie, Q. M., Sun, Y., & Ma, J. Y. (2017). Detection and genome sequencing of porcine circovirus 3 in neonatal pigs with congenital tremors in South China. *Transboundary and Emerging Diseases* 64(6), 1650-1654.

Chen, H. Y., Li, X. K., Cui, B. A., Wei, Z. Y., Li, X. S., Wang, Y. B., Zhao, L., & Wang, X. Y. (2009). A TaqMan-based real-time polymerase chain reaction for the detection of porcine parvovirus. *Journal of Virological Methods* 156(1-2), 84-88.

Christianson, W. T. (1992). Stillbirths, mummies, abortions, and early embryonic death. *Veterinary Clinics of North America: Food Animal Practice* 8(3), 623-639.

Dinh, P. X., Nguyen, N. M., Nguyen, T. H., Tran, V. H., Tran, Q. D., Dang, K. H., Vo, D. T., Le, H. T., Nguyen, N. T. T., Nguyen, T. T., & Do, D. T. (2021). Porcine circovirus genotypes and their copathogens in pigs with respiratory disease in southern provinces of Vietnam. *Archives of Virology* 166(2), 403-411.

Ellis, J., Hassard, L., Clark, E., Harding, J., Allan, G., Willson, P., Strokappe, J., Martin, K., McNeilly, F., & Meehan, B. (1998). Isolation of circovirus from lesions of pigs with postweaning multisystemic wasting syndrome. *Canadian Veterinary Journal* 39(1), 44-51.

Franzo, G., Legnardi, M., Hjulsager, C. K., Klaumann, F., Larsen, L. E., Segales, J., & Drigo, M. (2018). Full-genome sequencing of porcine circovirus 3 field strains from Denmark, Italy and Spain demonstrates a high within-Europe genetic heterogeneity. *Transboundary and Emerging Diseases* 65(3), 602-606.

Huynh, T. M. L., Le, V. P., Nguyen, V. G., & Trinh, D. T. (2015). Variety selection porcine circovirus type 2 (PCV2) for producing vaccines against piglets. *Journal of Scientific Research and Development* 13, 406-415.

Huynh, T. M., Nguyen, B. H., Nguyen, V. G., Dang, H. A., Mai, T. N., Tran, T. H., Ngo, M. H., Le, V. T., Vu, T. N., Ta, T. K., Vo, V. H., Kim, H. K., & Park, B. K. (2014). Phylogenetic and phylogeographic analyses of porcine circovirus type 2 among pig farms in Vietnam. *Transboundary and Emerging Diseases* 61(6), e25-34.

Johnson, R., & Collings, D. (1969). Experimental infection of piglets and pregnant gilt with a parvovirus. *Veterinary Record* 85(16), 446-447.

Kwon, T., Yoo, S. J., Park, C. K., & Lyoo, Y. S. (2017). Prevalence of novel porcine circovirus 3 in Korean pig populations. *Veterinary Microbiology* 207, 178-180.

Liu, J. K., Wei, C. H., Yang, X. Y., Dai, A. L., & Li, X. H. (2015). Simultaneous detection and differentiation of porcine circovirus type 2, type 2 porcine reproductive and respiratory syndrome virus, porcine parvovirus and pseudorabies virus in pigs with post-weaning multisystemic wasting syndrome (PMWS) by multiplex PCR. *The journal Veterinarski arhiv* 85(5), 511-521.

Milek, D., Wozniak, A., Podgorska, K., & Stadejek, T. (2020). Do porcine parvoviruses 1 through 7 (PPV1-PPV7) have an impact on porcine circovirus type 2 (PCV2) viremia in pigs? *Veterinary Microbiology* 242, 108613.

Nguyen, D. H. M., Luong, Q. T. X., Hoang, P. T., Do, D. T. T., Tran, T. K., & Dinh, P. X. (2018). Detecting toxin genes of Clostridium perfringens isolated from diarrhea piglets using multiplex PCR. *The Journal of Agriculture and Development* 17(6), 24-30.

Nguyen, V. G., Mai, T. N., Le, V. T., Vu, T. N., Vo, V. H., Ta, T. K. C., Vu, D. H., & Huynh, T. M. L. (2020). Presence of porcine parvovirus 1 (PPV1) in domestic pigs in Ha Noi and the neighborhood. *Vietnam Journal of Agricultural Sciences* 18, 495-503.

Oropeza-Moe, M., Oropeza Delgado, A. J., & Framstad, T. (2017). Porcine circovirus type 2 associated reproductive failure in a specific pathogen free (SPF) piglet producing herd in Norway: a case report. *Porcine Health Management* 3(1), 2-6.

Ouyang, T., Zhang, X., Liu, X., & Ren, L. (2019). Co-Infection of swine with porcine circovirus type 2 and other swine viruses. *Viruses* 11(2), 185.

Palinski, R., Piñeyro, P., Shang, P., Yuan, F., Guo, R., Fang, Y., Rui, G., Ying, F., Emily, B., & Ben, M. H. (2016). A novel porcine circovirus distantly related to known circoviruses is associated with porcine dermatitis and nephropathy syndrome and reproductive failure. *Journal of Virology* 91(1), e01879-16.

Pham, H. Q., Nguyen, V. G., Nguyen, T. T. T., Pham, C. H., & Huynh, T. M. L. (2017). Study the circulation of new viruses (porcine circovirus 3 - PCV3) in pigs raised in some northern provinces of Vietnam. *Vietnam Journal of Agricultural Science* 15(11), 1520-1528.

Prinz, C., Stillfried, M., Neubert, L. K., & Denner, J. (2019). Detection of PCV3 in German wild boars. *Virology Journal* 16, (1), 25.

Rosell, C., Segales, J., Ramos-Vara, J. A., Folch, J. M., Rodriguez-Arrioja, G. M., Duran, C. O., Balasch, M., Plana-Duran, J., & Domingo, M. (2000). Identification of porcine circovirus in tissues of pigs with porcine dermatitis and nephropathy syndrome. *Veterinary Record* 146(2), 40-43.

Saraiva, G. L., Vidigal, P. M. P., Assao, V. S., Fajardo, M. L. M., Loreto, A. L. S., Fietto, J. R. L., Bressan, G. C., Lobato, Z. I. P., Almeida, M. R. D., & Silva-Júnior, A. (2019). Retrospective detection and genetic characterization of porcine circovirus 3 (PCV3) strains identified between 2006 and 2007 in Brazil. *Viruses* 11(3), 201.

Tisciier, I., Mields, W., Wolff, D., Vagt, M., & Griem, W. (1986). Studies on epidemiology and pathogenicity of porcine circovirus. Archives of *Virology* 91(3-4), 271-276.

West, K. H., Bystrom, J. M., Wojnarowicz, C., Shantz, N., Jacobson, M., & Allan, G. M. (1999). Myocarditis and abortion associated with intrauterine infection of sows with porcine circovirus 2. *Journal of Veterinary Diagnostic Investigation* 11(6), 530-532.

Wozniak, A., Milek, D., Baska, P., & Stadejek, T. (2019). Does porcine circovirus type 3 (PCV3) interfere with porcine circovirus type 2 (PCV2) vaccine efficacy? *Transboundary and Emerging Diseases* 66(4), 1454-1461.

Xu, P. L., Zhang, Y., Zhao, Y., Zheng, H. H., Han, H. Y., Zhang, H. X., Chen, H. Y., Yang, M. F., & Zheng, L. L. (2018). Detection and phylogenetic analysis of porcine circovirus type 3 in central China. *Transboundary and Emerging Diseases* 65(5), 1163-1169.

Yang, K., Jiao, Z., Zhou, D., Guo, R., Duan, Z., Yuan, F., & Tian, Y. (2018). Detection of porcine circoviruses in clinical specimens using multiplex PCR in Hubei, central China. *PeerJ Preprints* 6, e27145v1.

Yang, K., Jiao, Z., Zhou, D., Guo, R., Duan, Z., & Tian, Y. (2019). Development of a multiplex PCR to detect and discriminate porcine circoviruses in clinical specimens. *BMC Infectious Diseases* 19, 778.

Zhao, K., Han, F., Zou, Y., Zhu, L., Li, C., Xu, Y., Zhang, C., Tan, F., Wang, J., Tao, S., He, X., Zhou, Z., & Tang, X. (2010). Rapid detection of porcine circovirus type 2 using a TaqMan-based real-time PCR. *Virology Journal* 7, 374.

Genetic analysis of African swine fever virus based on major genes encoding p72, p54 and p30

Hop Q. Nguyen[1], Duyen M. T. Nguyen[1], Nam M. Nguyen[2], Dung N. T. Nguyen[1], Han Q. T. Luu[1], & Duy T. Do[1*]

[1]Faculty of Animal Science and Veterinary Medicine, Nong Lam University, Ho Chi Minh City, Vietnam
[2]Research Center for Genetics and Reproductive Health, School of Medicine, Vietnam National University, Ho Chi Minh City, Vietnam

ARTICLE INFO

Research Paper

Received: April 24, 2021
Revised: June 01, 2021
Accepted: June 08, 2021

Keywords

ASFV
Genotyping
p30
p54
p72

***Corresponding author**

Do Tien Duy
Email: duy.dotien@hcmuaf.edu.vn

ABSTRACT

African swine fever (ASF) is reported as a highly contagious hemorrhage lethal disease of domestic and wild swine. The causative agent of ASF is a large enveloped DNA virus with a complex structure. There are twenty-four ASFV genotypes described to date. However, in Vietnam, only genotypes II had been previously described. The genetic characterization of ASFV enhances the understanding of ASF epidemiology in terms of the extent, severity, source, and potential genetic variations among ASFV strains circulating in Southern Vietnam. Twenty ASFV strains were collected from pigs with ASFV-infected clinical signs from 10 provinces during 2019 - 2020. Partial B646L (p72) gene, complete E183L (p54), and CP204L (p30) genes were amplified, purified, and sequenced. Phylogenetic analysis confirmed the circulation of genotype II by both the partial B646L (p72) and full-length E183 (p54) gene sequencing. Analysis of the p72, p54, and p30 regions did not indicate any change in the nucleotide and amino acid sequences among these strains. The results of this study revealed that these ASFVs shared high homology to ASFV isolates detected in Northern Vietnam and China.

Cited as: Nguyen, H. Q., Nguyen, D. M. T., Nguyen, N. M., Nguyen, D. N. T., Luu, H. Q. T., & Do, D. T. (2021). Genetic analysis of African swine fever virus based on major genes encoding p72, p54 and p30. *The Journal of Agriculture and Development* 20(3), 18-25.

1. Introduction

African swine fever (ASF) is reported as a highly contagious hemorrhage lethal disease by the World Organization for Animal Health (OIE, 2019). First described in Kenya in 1921, it happened on the African continent until 1957, when it spread from Angola to Lisbon. From then on, African swine fever virus (ASFV) has been repeatedly identified in many countries of Europe, Central America, and South America. The introduction of ASFV into Georgia from Southeast Africa in 2007 was described by Rowlands (2008). After that, ASFV crossed into the Eastern European Union (EU) territory in 2014 and affected Lithuania, Poland, Latvia, and Estonia in 2014, the Czech Republic and Romania in 2017, and Hungary and Bulgaria in 2018 (Gallardo et al., 2017; OIE, 2018). In 2018, the disease reached China having the largest pig production (Ge et al., 2018), followed by Vietnam (2019) (Le et al., 2019), and other Asian countries, which caused the devastation of pig industry, leading to substantial economic loss due to the lack of an effective vaccine (FAO, 2020).

African swine fever is caused by the ASFV that is the only member of the family *ASFarviridae* (Dixon et al., 2020). ASFV was classified into 24 genotypes (Quembo et al., 2018). The different strains lead to variable pathogenesis ranging

from highly lethal to asymptomatic. The highly virulent genotype II is confirmed as a circulating strain in China, and Vietnam which showed high mortality (91-100%), making ASF the most severe restriction on domestic pig production, food security, and livelihood and socioeconomic effects (Ge et al., 2018; Gallardo et al., 2019).

In Vietnam, the previously characterized ASFV have been reported only genotype II based on sequencing of the C-terminal region of the B646L gene (Le et al., 2019; Tran et al., 2020; Mai et al., 2021). Further differentiation between close strains and identifying virus subtypes of the 24 genotypes was achieved by nucleotide sequencing of the whole E183L gene regions encoding p54 proteins and the CP204L gene encoding the phosphoprotein p30. Previous studies have shown that using the three encoding regions of the ASFV DNA including p72, p54, and p30, to characterize ASFV is much sufficient despite the presence of many other markers (Nix et al., 2006; Gallardo et al., 2009).

This study was set out to characterize African swine fever virus genotypes from 20 farms in 10 provinces, which occurred ASF outbreaks in 2019 and 2020. The results are expected to contribute sequence data for molecular epidemiology studies and provide further understanding of ASF disease patterns in Southern Vietnam.

2. Materials and Methods

2.1. Study design and sample collection

This study was conducted in 10 Southern provinces of Vietnam (Figure 1). Samples were collected from clinical pigs in ASF outbreaks reported in the period of 2019 - 2020. Sets of lymph nodes, spleens, kidney, lung, and whole blood from 20 pigs were collected for diagnosis according to the OIE-recommendation, then the whole blood used for DNA extraction submitted to sequencing. PCR amplification of ASFV detection was performed using primers PPA-1/PPA-2 described in previous studies (Table 1). Sample source, temporal and spatial distribution of specimens were summarized in Table 2.

Table 1. Primers used for PCR detection and PCR genomic characterization

Gene name	GPrimers	Sequences (5'-3')	Size of products	References
B646L	PPA-1	AGTTATGGGAAACCCGACCC	257bp	Aguero et al., 2004
	PPA-2	CCCTGAATCGGAGCATCT		
B646L	P72U	GGCACAAGTTCGGACATGT	478bp	Bastos et al., 2003
	P72D	GTACTGTAACGCAGCACAG		
E183L	PPA722	CGAAGTGCATGTAATAAACGTC	676bp	Gallardo et al., 2008
	PPA89	TGTAATTTCATTGCGCCACAAC		
CP204L	P30F	ATGAAAATGGAGGTCATCTTCAAAAC	521bp	Rowlands et al., 2008
	P30R	AAGTTTAATGACCATGAGTCTTACC		

2.2. DNA extraction and PCR assay

The genomic DNA of ASFV was extracted following the manufacturer's instructions of the commercial kit Promega^{TM} Wizard^{TM} SV

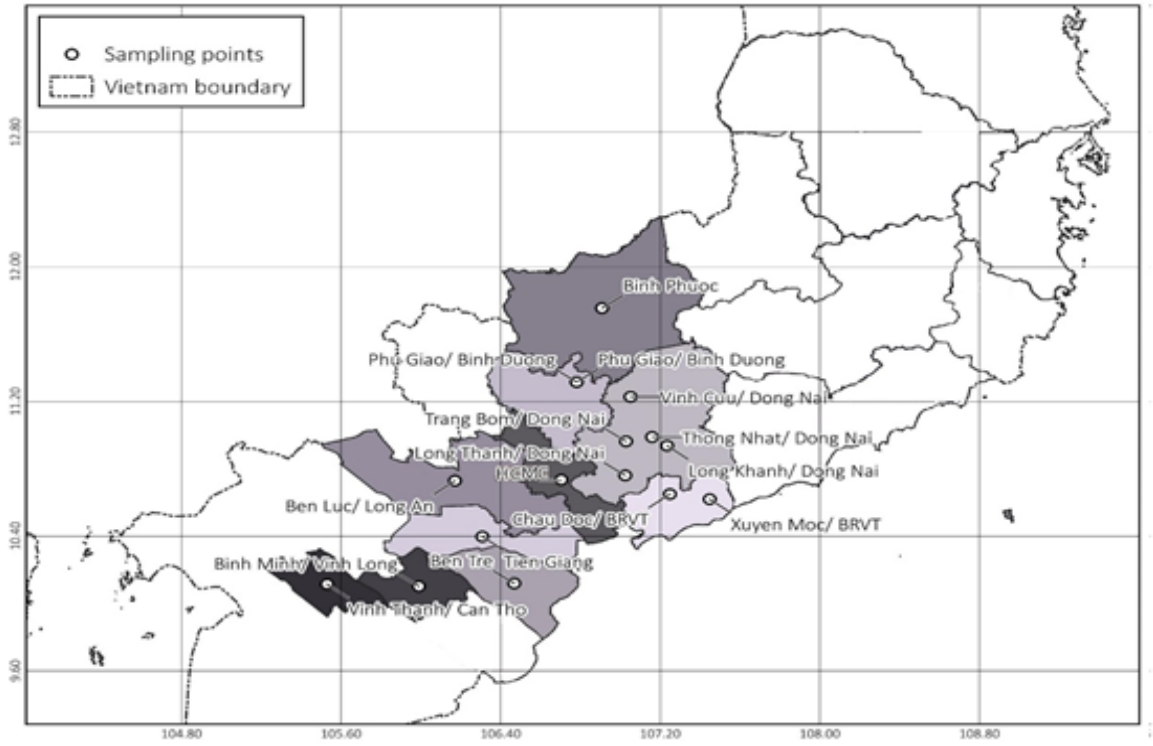

Figure 1. Map of Vietnam showing locations where field strains were obtained and genotyped.

Table 2. Summary of African swine fever viruses used in this study

ASFV strains	District/province	Sampling date	Sample obtained from each pig	Host
VN/HCMC/2019-ASF1	Binh Tan/HCMC	July, 2019	S	DP
VN/BRVT/2019-ASF1	Chau Doc/BRVT	August, 2019	S	DP
VN/BRVT/2019-ASF2	Xuyen Moc/BRVT	November, 2019	S	DP
VN/BD/2019-ASF1	Phu Giao/Binh Duong	September, 2019	S, Sp, K, L, LN	DP
VN/BD/2019-ASF2	Phu Giao/Binh Duong	July, 2019	S, Sp, K, L, LN	CP
VN/BD/2020-ASF3	Phu Giao/Binh Duong	July, 2020	S	DP
VN/BD/2020-ASF4	Phu Giao/Binh Duong	June, 2020	S	CP
VN/BP/2019-ASF1	Binh Phuoc	June, 2019	S	DP
VN/DN/2019-ASF1	Trang Bom/Dong Nai	June, 2020	S	CP
VN/DN/2019-ASF2	Vinh Cuu/Dong Nai	June, 2019	S	DP
VN/DN/2019-ASF3	Long Thanh/Dong Nai	August, 2019	S	DP
VN/DN/2020-ASF4	Long Khanh/Dong Nai	May, 2020	S	CP
VN/DN/2020-ASF5	Thong Nhat/Dong Nai	July, 2020	S	DP
VN/BenTre/2020-ASF1	Ben Tre	December, 2020	WB	DP
VN/CT/2019-ASF1	Vinh Thanh/Can Tho	July, 2019	S	DP
VN/LA/2019-ASF1	Ben Luc/Long An	September, 2019	S, Sp, K, L, LN	DP
VN/LA/2019-ASF2	Ben Luc/Long An	October, 2019	S, Sp, K, L, LN	DP
VN/LA/2019-ASF3	Ben Luc/Long An	September, 2019	S	DP
VN/TG/2020-ASF1	Tien Giang	July, 2020	S, Sp, K, L, LN	DP
VN/VL/2019-ASF1	Binh Minh/Vinh Long	August, 2019	S	DP

DP: Domestic pig; CP: Convalescent pig; WB: whole blood; S: serum, LN: lymph node; Sp: pleen; L: lung; K: kidney; WB: whole blood.

Genomic DNA Purification System (Promega, USA). PCR amplification for the genomic characterization of ASFV was performed to amplify the variable 3'-end of the B646L gene, whole gene E183L encoding the p54 protein, and the CP204L (p30) gene using primers that showed in Table 1.

All PCR amplifications were performed using kit MyTaq TM HS Mix, 2x (Bioline, USA). Reactions contained 12 µL MyTaq TM HS Mix, 5 µL DNA, 1 µL of 10 µM Forward primer, 1 µL of 10 µM Reverse primer, and 6 µL free-DNA water in a total reaction volume of 25 µL. The positive control DNA was given by Veterinary Hospital Laboratory of Nong Lam University (Vietnam). DNA extracts were substituted by nuclease free water in negative control reaction. Thermocycling condition for PCR detection of ASFV included a 10 min initial denaturation step of 95°C, followed by 40 cycles of 15 sec at 95°C, 30 sec at 62°C, and 30 sec at 72°C with a 5-min elongation step at 72°C. Thermocycling condition for amplification of the p72, p54, and p30 genes, the initial denaturation at 95°C for 5 min, followed by 40 of 30 sec at 95°C, 30 sec at 55°C, and 1 min at 72°C, and a final elongation at 72°C for 10 min. Afterward, PCR products were mixed with GelRed nucleic acid stain (Merck, Germany) and electrophoresed in a 1% agarose gel electrophoresis (Invitrogen, Thermo Fisher Scientific, USA) using 1 Kb Plus ladder (Invitrogen, Thermo Fisher Scientific, USA) to indicate the sizes of amplification products.

2.3. Genetic sequence and analysis

The PCR products of 3 gene regions (p72, p54, and p30) were purified using the Top-PURER PCR/GEL DNA PURIFICATION kit (ABT, Vietnam) and were sent to sequencing laboratory (Macrogen, Korea). Both sequences from the forward strand and the reverse complement sequences were manually overlapped to obtain a single sequence. The nucleotide sequences of the B646L, E183L and CP204L genes of the collected ASFV strains were compared with previous Vietnamese strains and with other sequences published available in GenBank (NCBI) (Table 3). The nucleotide sequences of three defined genes obtained were aligned using the CLUSTAL W package and phylogenetic analyses were conducted according to the maximum likelihood approach with a bootstrap value of 1000 in the MEGA X software (https://www.megasoftware.net).

3. Results

3.1. Confirmation of ASF using PCR

The 20 pigs included sows, fattening pigs, and nursing pigs that showed specifically pathological and clinical signs of ASF, including fever (41 - 42°C), loss of appetite, vomiting, skin hemorrhages, bloody discharge from the nose, and joint swelling. PCR revealed a band size of 257 bp, hence 20 pigs tested positive for ASF viral DNA (gel not shown).

3.2. Nucleotide and amino acid sequence analyis

3.2.1. Sequence alignment

Nucleotide and amino acid sequences of partial p72, full-length p54, and p30 of the 20 strains shared 100% sequence identity with each other. They shared 98.63% - 100% nucleotide and amino acid identity with the partial p72, full-length p54, and p30 sequences of genotype II reference isolates. The amino acid sequence alignment revealed that 20 strains shared 96.42% - 100% p72 sequence identity, 100% p54 sequence identity, and 99.42% - 100% p30 sequence identity within p72 genotype II. Interestingly, nucleotide and amino acid sequences of partial p72, full-length p54, and p30 of CN201801 (MH735140) and Jilin/2018 (MK189456) ASFV strains from China shared 100% sequence identity with 20 strains in this study (Figure 2).

3.2.2. Phylogenetic analysis

P72 phylogenetic tree: The p72 genotyping PCR results indicated a band size of 478 bp from all the samples using primers P72U/P72D (gel not shown). Phylogenetic analysis and comparison of these sequences to other isolates of known genotypes identified the 20 sequences belonging to B646L genotype II as shown in Figure 2A.

P54 phylogenetic tree: A band size of 676 bp was amplified using primers PPA722/PPA89 (gel not shown). Analysis of whole-length p54 sequences confirmed that the circulating virus belongs to genotype II (Figure 2B).

P30 phylogenetic tree: PCR amplification of CP204L gene from each of 20 field strains pro-

Table 3. References of ASFV isolates from Vietnam and over the world from Genbank

Isolates	Year of isolation	Countries	P72 genotype	P72 gene Genbank accession number	P54 genotype	P54 gene Genbank accession number	P30 gene Genbank accession number
Hanoi/2019	2019	Vietnam	II	MT332151	II	MT166692	MT166692
NgheAn/2019	2019	Vietnam	II	MT180393	II	MT180393	MT180393
VN/Pig/NA/1393	2020	Vietnam	II	MN711740	-	NA	NA
CN201801	2018	China	II	MH722357	II	MH735140	MH735141
Wuhan/2019	2019	China	II	MN393476	II	MN393476	MN393476
Jilin/2018	2018	China	II	MK189456	-	-	MK214680
Pol18	2018	Poland	II	MT847621	II	MT847621	MT847621
Georgia_2007/1	2007	Georgia	II	NC_044959	-	-	NC_044959
Etalle/2018	2018	Belgium	II	MK543947	II	MK543947	MK543947
LT14/1490	2014	Lithuania	II	MK628478	II	MK628478	MK628478
ZAM/14/Chipata	2014	Zambia	II	LC174751	-	NA	LC213611
OURT_88/3	1989	Portugal	I	AM712240	Ic	AM712240	AM712240
Li20/1	1983	Malawi	VIII	AY261361	VIII	AY261361	AY261361
Kenya-1950	1950	Kenya	X	AY261360	X	AY261360	AY261360
MZUKI/1979	1979	South Africa	I	AY261362	Ib	AY261362	AY261362
Warthog	NK	Namibia	IV	AY261366	IVa	AY261366	AY261366
KAB/62	1983	Zambia	XI	AY351522	XI	EU874331	EU874289
SUM 14/11	1983	Zambia	XIII	AY351542	XIII	EU874357	EU874287
TMB 89/1	1989	Zambia	VIII	AY351557	-	NA	JQ76886
SPEC/53	NK	South Africa	XXI	DQ250111	XXI	KC662384	NA
Ken05/Tk1	2014	Kenya	X	KM111294	X	KM111294	KM111294
Ken06Bus	2014	Kenya	IX	KM111295	IX	KM111295	KM111295
ZAM/13/Kalomo	NK	Zambia	XIV	LC174752	XIV	LC174761	LC213612
ZAM/14/Kasempa	NK	Zambia	XIV	LC174753	XIV	LC174762	NA
R8	NK	Uganda	IX	MH025916	IX	MH025916	MH025916
RSA_2/2008	2008	South_Africa	XXII	MN336500	XXII	MN336500	MN336500
RSA_2/2004	2004	South_Africa	XX	MN641877	XX	MN641877	MN641877
Liv13/33		France	I	MN913970	Ia	MN913970	MN913970
RSA W1	1999	South_Africa	IV	MN641876	IVb	MN641876	MN641876

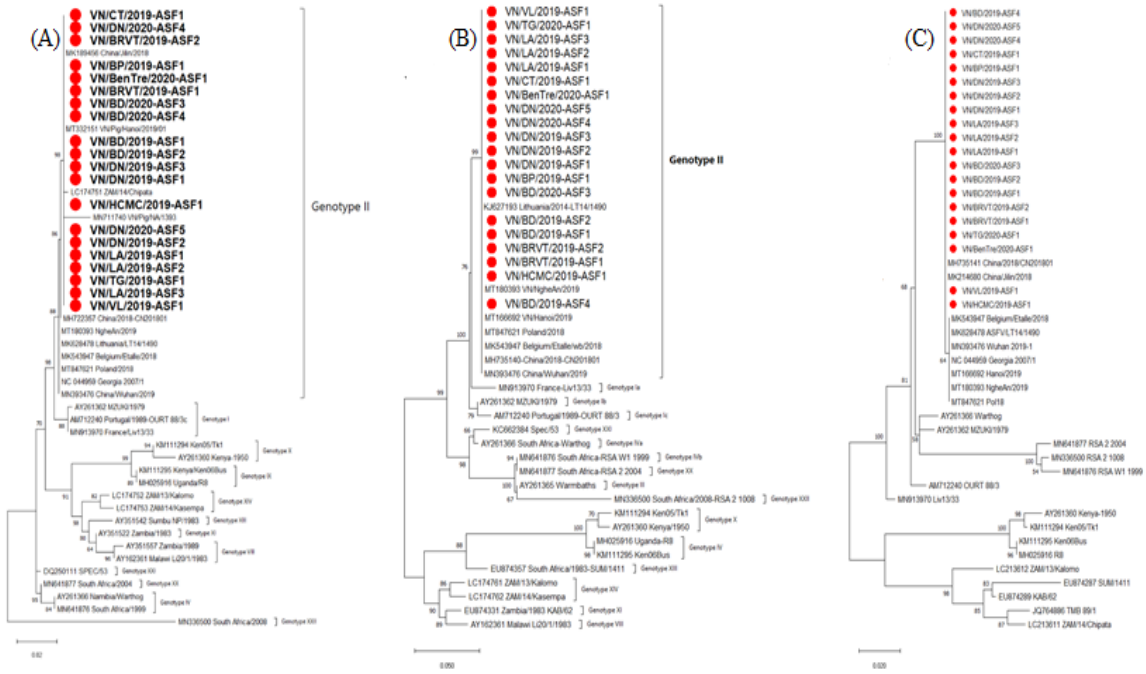

Figure 2. ASFV phylogenetic trees based on nucleotide sequences of genes encoding p72-p54-p30. (A) P72 genotype (B) P54 sub-group within p72 genotype, (C) P30 phylogenetic trees. The maximum likelihood approach was used for construction of phylogenetic trees in MEGA X software (https://www.megasoftware.net/). Numbers along branches indicate bootstrap values > 50% (1000 replicates). The red circles are ASFVs from this study. Scale bars indicate nucleotide substitutions per site.

duced a 521 bp band (gel not shown). All ASFVs collected from the 2019 - 2020 outbreaks in Southern Vietnam were indistinguishable in the p30 phylogeny. Except for one virus (ZAM14/Chipata, accession no. LC213611), all p72 genotype II ASFVs belonged to the same clade (Figure 2C).

4. Discussion

Phylogenetic analysis based on nucleotide sequences of the C-terminal of the B646L gene (p72), full-length E183L (p54) gene showed that all 20 Vietnamese ASFV field strains belonged to genotype II. The other analysis of p30 phylogeny showed that this genomic region could differentiate among closely related viruses (Simulundu et al., 2017). The findings are in contrast to those of a previous study in which p30 sequences obtained from ASFV collected from 10 different provinces over two years showed remarkable genetic stability and so could not obtain a finer level of discrimination among closely related viruses using this genomic region. The idea that illegal transportation of pork and pork products, triggering the outbreak in Southern Vietnam seems to support from this genetic analysis, which showed that the virus in this study was very similar in the comparison based on any of three selected gene fragments (B646L, E183L, and CP204L) to ASFVs which caused outbreaks in China during 2018 (CN201801 and Jilin/2018).

On the other hand, the analysis and comparison of the three independent regions of ASFV gene sequences in this study and other reports in Vietnam showed high stability of the ASFV genome (Le et al., 2019; Mai et al., 2021). However, the finding conflicted with the previous study in which p72 sequences obtained from ASFV collected from Nghe An province showed the presence of some nucleotide point substitution mutations (Tran et al., 2020). In general, the mutation rate of DNA viruses is lower than RNA viruses and ranges between 10^{-8} to 10^{-6} substitutions per nucleotide per cell infection (Sanjuan et al., 2010). Mowever, double-stranded DNA's evolutionary rate is difficult to estimate (Firth et al., 2010). The accurate proofreading of DNA polymerase and virus-encoded base excision DNA

repair system results in a low mutation rate in ASFV DNA. Our results may be rational to the previous description that ASFV is very stable and shows a very low mutation rate, which leads to low genetic variability in affected regions (Dixon et al., 2020). Interestingly, the virus collected from apparently convalescent pigs in a survey following this study had presented 100% of identity in the 3 ASFV genome regions of the 2019 - 2020 ASFV strains which induced an acute form of the infection for the 20 pigs. It could be assumed that after the first introduction of the disease in an area, increased numbers of subacute and subclinical infections could happen over time, and that mortality rates decrease. In such circumstances, the clinical manifestations are more variable, and recognition of the disease becomes problematic in the field, emphasizing the need for implementation of appropriate surveillance programs to control the disease. This study provides the phylogenetic information about ASFV strains circulating in Southern areas of Vietnam during 2019 - 2020, which will be useful for ASF control program in Vietnam and neighboring countries.

Vietnam shares a cross-border with China, and illegal transport of pigs and pig products frequently occurs in the border provinces of both countries (Kreindel et al., 2018). On the other hand, Vietnam imports pork and other pork products from different European countries, such as Poland, Russia. The exact route of the introduction of ASFV into Vietnam remains unknown. According to recent molecular studies, some different ASFV strains circulate in China (Ge et al., 2018; 2019). These strains may represent multiple introductions of ASFV into China or intra-epidemic genome variation caused by a genetic mutation. To trace the source and extend the knowledge of ASFV evolution and epidemiology in Vietnam, we analyzed nucleotide and amino acid sequences of three defined regions of the genome B646L, E183L, and CP204L from the tested ASFV. Because all nucleotide and amino acid sequences for each genome region from all pigs in various cases obtained from Vietnam were identical, this study concluded that the ASF outbreaks in Vietnam and the surrounding areas were probably due to a single introduction of the virus. The genetic analysis results also reflected the rapid spread of pathogens within six months, spread to 63 provinces throughout the country and from a single source after entering Vietnam. ASFV is a pathogen that spread slowly in nature or under strict supervision. A nationwide outbreak of ASF indicated that the control of the epidemic in Vietnam was quite loose and less stringent. Vietnam has many small and household-scale farms, typically poor biosecurity, outdated facilities, limited breeding techniques and low awareness of veterinary regulations, which were significant contributors to the introduction, spread, and circulation of the disease. Besides, a lot of slaughterhouses and fresh meat markets are located close to the livestock sector, increasing the difficulty of disease control in Vietnam.

5. Conclusions

The results revealed that ASFV circulating in Southern Vietnam during 2019 - 2020 outbreaks belong to genotype II. The combination of molecular data and epidemiologic findings have confirmed that the ASFVs detected in Southern regions of Vietnam most probably originated or showed the same genetic relatedness to ASFVs detected in Northern Vietnam during 2019 and China in 2018. Analysis of the three independent genes of ASFV in this study and previous studies in Vietnam showed high stability of ASFV genome.

Conflict of interest

The authors declare no conflict of interest.

Acknowledgments

The study funded by the Scientific Research Fund of Nong Lam University, Ho Chi Minh City, Vietnam which was coded CS-SV20-CNTY-01.

References

Aguero, M., Fernandez, J., Romero, L., Sanchez Mascaraque, C., Arias, M., & Sanchez-Vizcaino, J. M. (2004). Highly sensitive pcr assay for routine diagnosis of African swine fever virus in clinical samples. *Journal of Clinical Microbiology* 41(9), 4431-4434.

Bastos, A. D. S., Penrith, M. L., Crucière, C., Edrich, J. L., Hutchings, G., Roger, F., Couacy-Hymann, E., & Thomson, G. R. (2003). Genotyping field strains of African swine fever virus by partial p72 gene characterisation. *Archives of Virology* 148(4), 693-706.

Dixon, L. K., Stahl, K., Jori, F., Vial, L., & Pfeiffer, D. U. (2020). African swine fever epidemiology and control. *Annual Review of Animal Biosciences* 8, 221-246.

FAO (Food and Agriculture Organization). (2020). *ASF situation in Asia update*. Retrieved March 5, 2020, from http://www.fao.org/ag/againfo/programmes/en/empres/ASF/2020/Situation_update_2020_03_05.html.

Firth, C., Kitchen, A., Shapiro, B., Suchard, M.A., Holmes, E.C., & Rambaut, A. (2010). Using time-structured data to estimate evolutionary rates of double-stranded dna viruses. *Molecular Biology and Evolution* 27(9), 2038-2051.

Gallardo, C., Fernández-Pinero, J., & Arias, M. (2019). African swine fever (ASF) diagnosis, an essential tool in the epidemiological investigation. *Virus Research* 271, 197676.

Gallardo, C., Mwaengo, D. M., Macharia, J. M., Arias, M., Taracha, E. A., Soler, A., Okoth, E., Martín, E., Kasiti, J., & Bishop, R. P. (2008). Enhanced discrimination of African swine fever virus isolates through nucleotide sequencing of the p54, p72, and pb602l (cvr) genes. *Virus Genes* 38(1), 85-95.

Gallardo, C., Reis, A. L., Kalema-Zikusoka, G., Malta, J., Soler, A., Blanco, E., Parkhouse, R. M. E., & Leitao, A. (2009). Recombinant antigen targets for serodiagnosis of African swine fever. *Clinical and Vaccine Immunology* 16(7), 1012-1020.

Gallardo, C., Soler, A., Nieto, R., Cano, C., Pelayo, V., Sánchez, M. A., Pridotkas, G., Fernandez-Pinero, J., Briones, V., & Arias, M. (2017). Experimental infection of domestic pigs with African swine fever virus lithuania 2014 genotype ii field isolate. *Transboundary and Emerging Diseases* 64(1), 300-304.

Ge, S., Li, J., Fan, X., Liu, F., Li, L., Wang, Q., Ren, W., Bao, J., Liu, C., Wang, H., Liu, Y., Zhang, Y., Xu, T., Wu, X., & Wang, Z. (2018). Molecular characterization of African swine fever virus, china, 2018. *Emerging Infectious Diseases* 24(11), 2131-2133.

Ge, S., Liu, Y., Li, L., Wang, Q., Li, J., Ren, W., Liu, C., Bao, J., Wu, X., & Wang, Z. (2019). An extra insertion of tandem repeat sequence in African swine fever virus, china, 2019. *Virus Genes* 55(6), 843-847.

Kreindel, S. , Pittiglio, C., Pinto, J., Lockhart, C., Calistri, P., Lubroth, J., & Correa, M. (2018). *African swine fever threatens people's republic of China - a rapid risk assessment of ASF introduction*. Rome, Italy: FAO.

Le, P. V., Jeong, G. D., Yoon, S. W., Kwon, H. M., Trinh, N. T. B., Nguyen, L. T., Bui, N. T. T., Oh, J., Kim, B. J., Cheong, M. K., Nguyen, T. V., Bae, E., Vu, H., T. T., Yeom, M., Na, W., & Song, D. (2019). Outbreak of African swine fever, Vietnam, 2019. *Emerging Infectious Diseases* 25(7), 1433-1435.

Mai, A. N. T., Vu, D. X., Nguyen, H. T. T., Nguyen, T. V., Trinh, N. T. B., Kim, J. Y., Kim, H. J., Cho, K. H., Nguyen, L. T., Bui, N. T. T., Jeong, G. D., Yoon, S. W., Truong, T., Ambagala, A., Song, D., & Le, P. V. (2021). Molecular profle of African swine fever virus (ASFV) circulating in Vietnam during 2019-2020 outbreaks. *Archives of Virology* 166(3), 885-890.

Nix, R. J., Gallardo, C., Hutchings, G., Blanco, E., & Dixon, L. K. (2006). Molecular epidemiology of African swine fever virus studied by analysis of four variable genome regions. *Archives of Virology* 151(12), 2475-2494.

OIE (World Organisation for Animal Health). (2019). *African swine fever situation*. Retrieved January, 2021, from https://www.oie.int/fileadmin/Home/eng/Health_standards/tahm/3.08.01_ASF.pdf?fbclid=IwAR0xd3mFl–ultXzS-GmCqjLdJVzgV6a13SrJI-sWi84jwKuFRf-qHcnOsg.

OIE (World Organisation for Animal Health). (2018). *African swine fever in Hungary*. Retrieved February, 2021, from https://www.oie.int/app/uploads/2021/03/report-47-global-situation-asf.pdf.

Quembo, C. J., Jori, F., Vosloo, W., & Heath, L. (2018). Genetic characterization of African swine fever virus isolates from soft ticks at the wildlife/domestic interface in mozambique and identification of a novel genotype. *Transboundary and Emerging Diseases* 65(2), 420-431.

Rowlands, R. J., Michaud, V., Heath, L., Hutchings, G., Oura, C., Vosloo, W., Dwarka, R., Onashvili, T., Albina, E., & Dixon, L. K. (2008). African swine fever virus isolate, Georgia, 2007. *Emerging Infectious Diseases* 14(12), 1870-1874.

Sanjuan, R., Nebot, M. R., Chirico, N., Mansky, L. M., & Belshaw, R. (2010). Viral mutation rates. *Journal of Virology* 84(19), 9733-9748.

Simulundu, E., Lubaba, C. H., Van Heerden, J., Kajihara, M., Mataa, L., Chambaro, H. M., Sinkala, Y., Munjita, S. M., Munang'andu, H. M., Nalubamba, K. S., Samui, K., Pandey, G. S., Takada, A., & Mweene, A. S. (2017). The epidemiology of African swine fever in "nonendemic" regions of Zambia (1989-2015): Implications for disease prevention and control. *Viruses* 9(9), 236.

Tran, T. H. T., Truong, D. A., Ly, V. D., Vu, H. T., Hoang, T. V., Nguyen, C. T., Chu, N. T., Nguyen, H. T., Pham, T. N., Nguyen, T., Yersin, A. G., & Dang, V. H. (2020). Genetic characterisation of African swine fever virus in outbreaks in ha nam province, red river delta region of vietnam, and activity of antimicrobial products against virus infection in contaminated feed. *Journal of Veterinary Research* 64(2), 207-213.

Quantities and antibiotic resistance of microorganisms in some microbial products for animals in Vietnam

Nhi T. T. Nguyen, Ngoc H. Le, & Hoa T. K. Ho*

Faculty of Animal Science and Veterinary Medicine, Nong Lam University, Ho Chi Minh City, Vietnam

ARTICLE INFO

Research Paper

Received: March 29, 2021
Revised: May 31, 2021
Accepted: June 10, 2021

Keywords

Antibiotic resistance
Bacillus
Lactobacillus
Probiotics

***Corresponding author**

Ho Thi Kim Hoa
Email: hoa.hothikim@hcmuaf.edu.vn

ABSTRACT

The aims of the study were to look into the quantities of live beneficial microorganisms and antibiotic resistance of bacterial strains in several probiotic products used for food animals in the market. Ten probiotic products that claim to contain beneficial bacteria and fungi were examined. Eight products are said on the label to contain *Lactobacillus* spp., nine contain *Bacillus* spp., five contain yeasts and two have molds. The results showed that eight products did not have the microbial quantities or/and composition of microorganisms as saying on their labels. Of eight products which claim to contain *Lactobacillus* spp., the bacteria were isolated from only four, of which three had *Lactobacillus* counts at least ten-fold as low as the numbers on the labels. Spore-forming bacilli were isolated from all nine *Bacillus*-containing products. However, two products had the bacterial counts at least 10-fold as low as the numbers printed on the labels. Among five products stated to contain yeasts, the organisms were recovered from samples of only one. Seven *Lactobacillus* and fifteen *Bacillus* isolates from all samples that had bacterial growth were tested for their susceptibility against seven common antibiotics using Kirby-Bauer disk diffusion method. The results revealed that all the *Lactobacillus* isolates showed susceptibility to the tested antibiotics except kanamycin. All 15 *Bacillus* isolates were susceptible to ampicillin, kanamycin, and ciprofloxacin; five isolates were intermediately resistant to tetracycline; one isolates resisted erythromycin, and one isolates was resistant to vancomycin. The results of this study would provide information for farm practice in choosing antibiotics used together with antibiotics to maintain or/and restore the gut microflora after antibiotic treatment.

Cited as: Nguyen, N. T. T., Le, N. H., & Ho, H. T. K. (2021). Quantities and antibiotic resistance of microorganisms in some microbial products for animals in Vietnam. *The Journal of Agriculture and Development* 20(3), 26-31.

1. Introduction

In the last two decades, the use of probiotics has become more and more popular in food-animal production. They are used for promoting animal health status and disease prevention, and for improvement of productivity. Probiotics have become one of the most potent alternatives to replace antibiotics in animal production. FAO/WHO has provided a definition of probiotics, which has been used as selection criteria for probiotic strains to be used in foods and dietary supplements. Probiotic strains for human use must be (i) sufficiently characterized; (ii) safe for the intended use; (iii) supported by at least one positive human clinical trial conducted ac-

cording to generally accepted scientific standards; and (iv) alive in the product at an efficacious dose throughout shelf life (Binda et al., 2020). Although the selection of beneficial bacteria for use in animals is not as strict as in humans, those criteria are still applied when a strain is studied for probiotic potential. Although most selected probiotic strains are safe, probiotics may possess undesirable properties such as virulence factors and transferable antimicrobial resistance (Alayande et al., 2020).

The objectives of the present study were to look into the quantities of live beneficial microorganisms and the resistance to some antibiotics of bacterial strains in several probiotic products used for food animals in the market.

2. Materials and Methods

Ten different products (named from A to J) containing beneficial microbes – *Lactobacillus* spp., Bacillus spp. and fungi were purchased from veterinary stores. They were all made in Vietnam and recommended to be used as supplements for food animals. Eight products are said on the label to contain *Lactobacillus* spp., nine contain *Bacillus* spp., five contain yeasts and two have molds.

2.1. Enumeration and isolation of the beneficial microbes from probiotic products

Ten-fold serial dilution of each sample was made by suspending one gram of each product into nine ml of sterilized MRS broth (de man, Rogosa, Sharpe; Oxoid, CM0359) or saline. Microbial enumeration was performed using conventional plate count method. One hundred µL of each dilution (10^{-1} to 10^{-6}) was spread on an appropriate agar plate to each group of examined microorganisms as described later. The process (weighing sample, making dilutions and inoculation) was repeated twice. If no growth were detected from the lowest dilution (10^{-1}) from one repeat, the process was done for the third time.

2.1.1. Lactic acid bacteria

MRS agar (de man, Rogosa, Sharpe; Oxoid; CM0361) was used for enumeration of lactobacilli (De Man et al., 1960). One hundred µL of each sample dilution in MRS broth was spread onto an MRS agar and incubated at 37°C/48 h under anaerobic condition (ThermoFisher, AN0025). For each sample, colonies on a plate that had a growth of 20 - 200 colonies were accounted. Three colonies from the counted plate were re-streaked onto new MRS agar plates and anaerobically incubated at 37°C/48 h. Each isolate was microscopically examined for Gram reaction and cell morphology. Test for catalase production was conducted by dripping two drops of hydrogen peroxide 3% onto bacteria on a glass slide. Isolates that were Gram-positive rods, non-spore forming and did not produce catalase was confirmed as Lactobacillus bacteria. Two isolates from each sample were kept in 15%-glycerin MRS broth at -20°C for further studies.

2.1.2. *Bacillus* spp.

TSA agar (Tryptone soya agar; Oxoid, CM0131) were used for enumeration of Bacillus spp. (Gorsuch et al., 2019). One hundred µL of each sample dilution in saline was spread onto a TSA plate and aerobically incubated at 37°C/48 h. Typical colonies of *Bacillus* bacteria were large, wrinkled, and saw-edged. For each sample, colonies on a plate that had a growth of 20 - 200 colonies were accounted. Three colonies from the counted plate were re-streaked onto new TSA agar plates and aerobically incubated at 37°C/24 h. Each isolate was microscopically examined for Gram reaction and cell morphology. *Bacillus* cells were large positive rods of which some were seen with endospores.

2.1.3. Yeasts and molds

Sabouraud dextrose agar (Oxoid, CM0041) containing chloramphenicol 5 mg/100 mL was used for growing yeasts and molds (Ladiges et al., 1974). One hundred µL of each sample dilution in saline was spread onto a Sabouraud plate and aerobically incubated at 30°C, and checked for fungal growth after one day, two days and a week. For each sample, colonies on a plate of 20 - 200 colonies were accounted, from which three colonies were re-streaked onto new agar sabouraud dextrose agar plates. Yeast colonies were large, smooth, raised, with even edges. Mold colonies was large, fuzzy, and pigmented. Two or three colonies from each sample was Gram-stained (yeasts) or Giemsa-stained (mold) and examined under a microscope at magnification 400x (Figure 1).

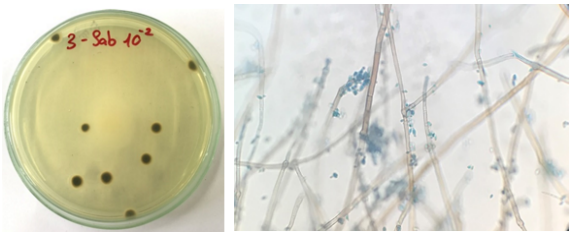

Figure 1. Mold colonies after one-day incubation (left) and Giemsa staining photo showing mold hyphae and spores (right; x400 magnification).

2.2. Antibiotic susceptibility testing

Two isolates of each microbe (*Lactobacillus* or *Bacillus*) from each sample (product) were tested for theirs susceptibility to seven antibiotics (ampicillin, amoxicillin/clavulanic, ciprofloxacin, erythromycin, kanamycin, tetracycline, vancomycin). The test was conducted using Kirby-Bauer disk diffusion method. The antibiotics belong to major groups which can be used for Gram-positive bacteria. Briefly, suspension of each isolate was made with saline to obtain turbidity equivalent to McFarland scale 0.5. The suspensions of *Lactobacillus* isolates each was spread evenly onto an MRS agar plate with a sterile cotton swab. *Bacillus* isolates were spread on Mueller-Hinton agar (MHA, Oxoid, CM0337). Antibiotic discs (Nam Khoa Biotek, Vietnam) were then placed on the surface of inoculated plates. MRS plates were anaerobically incubated at 37°C for 48 h (Anisimova & Yarullina, 2019). Plates of *Bacillus* isolates were aerobically incubated at 37°C/24 h (Jang et al., 2018).

After the incubation, the diameter (mm) of zone of inhibition (ZOI) was measured. Results were interpreted according to the recommendation by CLSI guidelines (Le & Nguyen, 2016; Sharma et al., 2017). Isolates with ZOI $\geq$ 20 mm diameter were considered as susceptible (S); ZOI between 15 and 19 mm were as intermediate (I); and ZOI $\leq$ 14 mm were resistant (R).

3. Results and Discussion

3.1. Enumeration and isolation of microorganisms

3.1.1. *Lactobacillus* spp.

The results are presented in Table 1. Of those four products, the number of lactobacilli recovered from one product (E) was ten-fold as high as that said on the label; from two products (F & G) it was more than ten-fold as low as the numbers on the labels; and from one product (H) the bacterial count was at the lower range of that announced by the manufacturer.

3.1.2. *Bacillus* spp.

Of the nine samples that contain *Bacillus* spp., the numbers of bacteria recovered from four samples were similar as it said on the product labels (product B, D, H, I). The other five were not. From four samples (products E, F, G, J), bacterial counts were higher (approximately 1 to 3 $\log_{10}$ CFU/g), whereas the count from sample C was 1 $\log_{10}$ CFU lower.

3.1.3. Yeast and mold

On the product labels, it was written that samples A and B contained both yeasts (*Saccharomyces cerevisiae* in A and *Torulopsis bovina* in B), and mold *Aspergillus oryzae*. However, the culture showed the growth of the molds but not the yeasts at all (after one week incubation). Furthermore, while the label of product A said that there were 2 x 10^6 *Aspergillus oryzae* CFU/g of the product, the actual count was 4 x 10^3 CFU/g. Similarly, it was 2 x 10^9 *Aspergillus oryzae* CFU/g on the label of product B, but the actual count was 8 x 10^6 CFU/g. It meant the actual viable counts of the molds from two samples were about 1,000-fold as low as it was written on the labels. Three samples (D, H and J) said to have yeast species *S. cerevisiae*. However, no growth was recovered from two samples D and H.

The enumeration and identification of probiotic microorganisms was carried out to evaluate the quality of the products which are available in the market. Four of the products claim to contained *Lactobacillus* spp., but none were recovered. There were five samples with revealed bacterial numbers were much lower than the numbers printed on product labels. In 2002, FAO/WHO gave a definition of probiotics as "live microorganisms which when administered in adequate amounts confer a health benefit on the host". In this document, it is recommended that minimum viable numbers of each probiotic strain at the end of the shelf-life should be described on the label. Of eight products saying to have *Lactobacillus* spp., only four did, of which the counts

Table 1. Microbial counts from probiotic products (CFU/g)

Sample	*Lactobacillus* spp.		*Bacillus* spp.	
	Label*	Counts	Label*	Counts
A	4.8 x 10^6	nd	No	-
B	2.0 x 10^7	nd	2.0 x 10^7	4.4 x 10^7
C	5.0 x 10^6	nd	5.0 x 10^6	5.0 x 10^5
D	10^6	nd	10^6	8.2 x 10^5
E	10^6	1.7 x 10^7	10^6	8.0 x 10^8
F	10^5	2.3 x 104	10^5	5.1 x 10^7
G	105	8.6 x 10^3	10^5	4.2 x 10^6
H	10^4 - 10^7	5.8 x 10^4	10^4 - 10^7	8.3 x 10^6
I	No	-	10^8	9.3 x 10^7
J	No	-	5.6 x 10^5	5.0 x 10^6

*The numbers of microbes stated on product labels; nd: No growth from 100 µL of 10-fold sample dilution; CFU: Colony forming unit.

of three were at least ten-fold as low as those on the labels. On the other hands, *Bacillus* spp. were isolated from all nine samples, of which two had their counts at least ten-fold as low as they were supposed.

So, samples of four products A, B, C and D did not have the counts of all strains as it printed on the labels, either not detected or much less. Samples of products E, F, G had less numbers of *Lactobacillus* than the label stated, and sample of product H did not have yeast as it is mentioned in the label. In summary, eight out ten products did not have the target microbes or/and the numbers of at least one strain were lower than it described on the label.

The facts that *Lactobacillus* spp. were not recovered from samples of four products, while *Bacillus* spp. were isolated from all would indicate difficulties producing and maintaining the survival of the lactic-acid-bacteria species. This is probably due to the anaerobic property of *Lactobacillus* spp.. Although a majority are aerotolerant, optimal growth and survival require anaerobic conditions. In contract, *Bacillus* spp. are aerobes and spore-formers. Therefore, they can grow best in the air and survive harsh environments. Aerobic metabolism and spore forming are among main advantageous traits of *Bacillus* strains for their use as probiotics for farm animals and aquatic animals, when cost of production (that determines the price of the product) and the storage conditions, the way of application are important factors. There were four products that did not meet the statement (on the labels) about the presence and quantities of all beneficial strains. This is a worldwide problem about probiotic market. As reviewed by De Simone (2019), current regulation of probiotics is inadequate to protect consumers. So, the source of probiotics (manufactories and/or stores) should be considered if one want to buy a probiotic product.

3.2. Antibiotic susceptibility of bacterial isolates

3.2.1. Antibiotic susceptibility of *Lactobacillus* isolates

All seven isolates showed susceptibility to the tested antibiotics except kanamycin (Table 2). Among seven isolates of *Lactobacillus*, two were susceptible to kanamycin, one resistant and the other showed intermediate sensitivity to the antibiotic. This finding was consistent with some previous studies, which reported that lactobacilli were highly resistant to aminoglycosides (gentamycin, kanamycin, streptomycin) that act by inhibiting synthesis of protein (Gueimonde et al., 2013).

3.3. Antibiotic susceptibility of *Bacillus* isolates

The test was performed on 15 *Bacillus* isolates. The results are presented in Table 3. All were susceptible to ampicillin, kanamycin, and ciprofloxacin. Five isolates showed intermediate susceptibility to tetracycline, one to amoxicillin/clavulanic and one to vancomycin. This results agreed with previous reports in the literature. For examples, 55.4% *Bacillus* cereus isolates from food samples by Tansuphasiri et al. (2006) and 33% of *B. subtilis* isolates from a study by

Table 2. Antibiotic sensitivity of *Lactobacillus* isolates (n = 7)

Antibiotics	Disc concentration (µg)	Isolates						
		1L	6L-1	6L-2	9L-1	9L-2	10L-1	10L-2
Ampicillin	10	S	S	S	S	S	S	S
Amoxicillin + Clavulanic	30	S	S	S	S	S	S	S
Vancomycin	30	S	S	S	S	S	S	S
Erythromycin	15	S	S	S	S	S	S	S
Kanamycin	30	S	I	S	I	I	I	R
Tetracycline	30	S	S	S	S	S	S	S
Ciprofloxacin	5	S	S	S	S	S	S	S

S: Susceptible; I: Intermediate; R: Resistant.

Table 3. Antibiotic sensitivity of *Bacillus* isolates (n = 15)

Antibiotics	Disc concentration (µg)	Number of isolates					
		S		I		R	
Ampicillin	10	15	100%	0	0%	0	0%
Amoxicillin + Clavulanic	30	14	93.3%	1	6.7%	0	0%
Vancomycin	30	13	86.6%	1	6.7%	1	6.7%
Erythromycin	15	14	93.3%	0	0%	1	6.7%
Kanamycin	30	15	100%	0	0%	0	0%
Tetracycline	30	10	66.7%	5	33.3%	0	0%
Ciprofloxacin	5	15	100%	0	0%	0	0%

S: Susceptible; I: Intermediate; R: Resistant.

Le & Nguyen (2016) showed resistance to oxytetracycline.

Antibiotic resistance of probiotic bacteria can be either or both intrinsic or/and acquired. One of the main functions of probiotics in prevention or/and treatment gastrointestinal disorders in humans and animals is to maintain or/and restore the gut microflora after antibiotic treatment. Therefore, intrinsic antibiotic resistance could be useful. However, when the resistance determinants are located on mobile genetic elements or plasmids, it raises great concerns on public health. Those resistant probiotics can spread resistance genes to others in the gut microflora via horizontal gen transfer, hence creating a reservoir of resistance for potential food or gut pathogens (Sharma et al., 2014). Therefore, in recognition of the importance of assuring safety, determination of antibiotic resistance patterns of probiotic strains should be carried out (FAO/WHO, 2002). The results in this study did not find resistance to the seven common antibiotics among *Lactobacillus* isolates, and most *Bacillus* isolates were susceptible to the drugs except a number of isolates showing intermediate resistance to tetracycline. This would provide information for farm practice in choosing products containing beneficial bacteria used together with antibiotics to maintain or/and restore the gut microflora after antibiotic treatment.

4. Conclusions

This was a small-scale study, which just looked at the quantities of microbial groups announced on the label, but not yet their benefits to animal health and productivity. Nevertheless, the results would provide some evidence for concerns about quality control of products containing beneficial microorganisms used for animals.

Conflict of interest

The authors declare no conflict of interest.

References

Alayande, K. A., Aiyegoro, O. A., & Ateba C. N. (2020). Probiotics in animal husbandry: Application and associated risk factors. *Sustainability* 12(3), 1087.

Anisimova, E. A., & Yarullina, D. R. (2019). Antibiotic resistance of *Lactobacillus* strains. *Current Microbiology* 76(12), 1407-1416.

Binda, S., Hill, C., Johansen, E., Obis, D., Pot, B., Sanders, M. E., Tremblay, A., & Ouwehand, A. C.

(2020). Criteria to qualify microorganisms as "probiotic" in foods and dietary supplements. *Frontiers in Microbiology* 11, 1662.

De Man, J. C., Rogosa M., & Sharpe M. I. (1960). A medium for the cultivation of *lactobacilli*. *Journal of Applied Bacteriology* 23(1), 130-135.

De Simone, C. (2019). The unregulated probiotic market. *Clinical Gastroenterology and Hepatology* 17(5), 809-817.

FAO/WHO (Food and Agriculture Organization/World Health Organization). (2002). *Guidelines for the evaluation of probiotics in food*. Paris, France: FAO.

Gorsuch, J. P., Jones, Z., Le Saint, D., & Kitts, C. L. (2019). Enumeration of industrial *Bacillus* assemblages in commercial products with customized plate-counting assays. *Journal of Microbiological Methods* 164, 105682.

Gueimonde, M., Sánchez, B., de los Reyes-Gavilán, C. G., & Margolles, A. (2013). Antibiotic resistance in probiotic bacteria. *Frontiers in Microbiology* 4, 202.

Jang, K., Lee, J., Lee, H., Kim, S., Ha, J., Choi, Y., Oh, H., Yoon, Y., & Lee, S. (2018). Pathogenic characteristics and antibiotic resistance of bacterial isolates from farmstead cheeses. *Korean Journal for Food Science of Animal Resources* 38(1), 203-208.

Ladiges, W. C., Foster, J. F., & Jorgensen II, J. J. (1974). Comparison of media for enumerating fungi in precooked frozen convenience foods. *Journal of Milk and Food Technology* 37(6), 302-304.

Le, Y. T. H., & Nguyen, H. D. (2016). Evaluation of the probiotic properties of *Bacillus* subtilis strains isolated from the Mekong Delta. *Can Tho University Journal of Science* 2, 26-32.

Sharma, C., Gulati, S., Thakur, N., Singh, B. P., Gupta, S., Kaur, S., Mishra, S. K., Puniya, A. K., Gill, J. P. S., & Panwar, H. (2017). Antibiotic sensitivity pattern of indigenous *lactobacilli* isolated from curd and human milk samples. *Biotech* 7(1), 53.

Sharma, P., Tomar, S. K., Goswami, P., Sangwan, V., & Singh, R. (2014). Antibiotic resistance among commercially available probiotics. *Food Research International* 57, 176-195.

Tansuphasiri, U., Khaminthakul, D., & Pandii, W. (2006). Antibiotic resistance of enterococci isolated from frozen foods and environmental water. *Southeast Asian Journal of Tropical Medicine and Public Health* 37, 162-170.

Efficacy of a commercial supplement added to drinking water in broilers fed aflatoxin-contaminated diets

Tung M. Che[1], Hien T. Le[2], Vi Q. Tran[2], Matthieu Le-Goff[3], & Phat T. Luong[2]

[1]Department of Animal Production, Nong Lam University, Ho Chi Minh City, Vietnam
[2]Olmix Asialand Vietnam, Binh Duong Province, Vietnam
[3]Olmix SA, ZA du Haut du Bois, Bréhan, France

ARTICLE INFO

Research Paper

Received: June 01, 2021
Revised: June 22, 2021
Accepted: June 29, 2021

Keywords

Aflatoxin
Broilers
Feed efficiency
Growth performance

***Corresponding author**

Che Minh Tung
Email: tung.cheminh@hcmuaf.edu.vn

ABSTRACT

The objective of the experiment was to evaluate effects of water supplementation with a commercial supplement (VitalSea®) on growth performance, mortality and serum concentrations of aspartate aminotransferase (AST) and lactate dehydrogenase (LDH) in broilers fed diets with aflatoxin (AF) contamination. A total of 960 day-old mixed-sex chicks (Ross 308, initial BW: 46.28 ± 0.25 g/chick) were randomly assigned to 1 of 4 treatments. The treatments included (1) basal diet without AF contamination and supplementation (negative control, NC), (2) AF-contaminated diet without supplementation (positive control, PC), (3) AF-contaminated diet + water supplementation with 0.5 mL VitalSea®/10 kg BW (VitalSea 1) and (4) AF-contaminated diet + water supplementation with 1.0 mL VitalSea®/10 kg BW (VitalSea 2). Each treatment was replicated with 8 pens of 30 birds (50% male, 50% female) each. Contaminated diets containing 30 µg AF/kg were fed to birds for Phase 1 (d 1-21) only. Water supplemented with VitalSea® was administered to birds for 5 days (d 22-26). In Phase 1 (d 1-21), there were no differences in ADG and ADFI among treatments ($P > 0.05$). In Phase 2 (d 22-35), there was a trend that the ADG of VitalSea 1 (68.66 g/d) and VitalSea 2 (68.56 g/d) was higher ($P < 0.06$) than that of the PC (62.61 g/d). Water supplemented with VitalSea® improved the FCR of broilers compared with the PC ($P < 0.01$). Over a 5-week study, broilers of the PC had a worse FCR than those of the other treatments ($P < 0.01$). At d 21, the serum LDH concentration of the PC was higher than that of the NC ($P = 0.026$). Briefly, addition of VitalSea® to drinking water for 5 days improved growth rate and feed efficiency of broilers fed AF-contaminated diets.

Cited as: Che, T. M., Le, H. T., Tran, V. Q., Le-Goff, M., & Luong, P. T. (2021). Efficacy of a commercial supplement added to drinking water in broilers fed aflatoxin-contaminated diets. *The Journal of Agriculture and Development* 20(3), 32-40.

1. Introduction

Aflatoxins (AF) are a group of mycotoxins naturally produced as secondary metabolites by the fungus *Aspergillus* and are potent hepatotoxins and carcinogens in the liver. Aflatoxins commonly contaminate a wide variety of feedstuffs, especially in tropical and subtropical regions of the world where conditions are favorable for the growth of mold (Molina-Alvarado et al., 2017; Nakavuma et al., 2020). Ditta et al. (2019) reported that globally about 25% of agricultural products were contaminated with AF and other mycotoxins in the world, especially in Africa, Asia and Latin America, resulting in decreased food/feed values and thereby causing economic

losses to farmers.

In chickens, it has been shown that the effects of AF include liver damage, decreased feed intake and growth rate, poor feed utilization and increased susceptibility to diseases. For instance, Raju and Devegowda (2000) showed that the final BW at 35 days of age in broilers fed a diet with 300 µg AFB_1/kg was reduced by 21%. Even feeding a diet containing as low as 20 µg AFB_1/kg for 3 weeks decreased the weight gain of broilers by 5% (Kana et al., 2010). Further, AF-contaminated diets fed to broilers also resulted in changes in serum levels of some biochemical parameters associated with liver health and functions (Yunus et al., 2011; Pizzolitto et al., 2013). Malekinezhad et al. (2021) found that feeding AF-contaminated diets increased the serum aspartate aminotransferase (AST), lactate dehydrogenase (LDH) and alanine aminotransferase (ALT).

There have been many chemical and biological techniques developed to detoxify AF-contaminated grains and complete feeds, with various effectiveness and ease of application. Thus, there is a need for new supplements or synergistic combinations to more efficiently alleviate the deleterious effects of AF and restore liver health and productivity. It has been shown that yeast extracts have the ability to reduce some of the adverse effects of aflatoxicosis in broilers and layers (Zaghini et al., 2005; Matur et al., 2010; Azizpour & Moghadam, 2015). Some plant extracts can also be used in poultry diets to counteract the toxicity of AF (Fouad et al., 2019). Recently, sulfated polysaccharides isolated from marine algae have been of potential interest because of their antioxidant, anticancer, antidiabetic, antimicrobial and gastroprotective effects (Manlusoc et al., 2019). In the present study, we hypothesized that the combination of marine sulfated polysaccharides ($MSP^{®}_{lipid}$), organic acids and yeast fractions could be an alternative solution to mitigate the negative impacts of AF on liver status and improve growth performance of broilers after exposure to AF-contaminated diets for 3 weeks. Therefore, the objective of the experiment was to evaluate effects of water supplementation with a commercial supplement (VitalSea®) on growth performance, mortality and serum concentrations of AST and LDH in broilers fed diets with a low level of AF contamination.

2. Materials and Methods

2.1. Experimental design, animals and housing

The experiment was conducted using 960 day-old mixed-sex chicks (Ross 308, initial BW: 46.28 ± 0.25 g/chick). The birds were randomly assigned to 1 of 4 treatments in a completely randomized design. The treatments included (1) basal diet without AF contamination and supplementation (negative control, NC), (2) AF-contaminated diet without supplementation (positive control, PC), (3) AF-contaminated diet + water supplementation with 0.5 mL VitalSea®/10 kg BW (VitalSea 1) and (4) AF-contaminated diet + water supplementation with 1.0 mL VitalSea®/10 kg BW (VitalSea 2). The birds were housed in floor pens in an open-sided house and each pen measured 2.5 m length x 1.2 m width. Each treatment had 8 replicate pens with 30 birds (50% male, 50% female) per pen. The experiment lasted for 5 weeks. The AF challenge model of the experiment is presented in Table 1.

2.2. Experimental diets and animal feeding

The experimental diets were formulated to meet the nutritional requirements of broilers during the experimental period (NRC, 1994). The birds were fed a 2-Phase feeding program: Phase 1 (1-21 d old) and Phase 2 (22-35 d old). The ingredient composition of the experimental diet is presented in Table 2. The AF-contaminated diets were obtained by including corn which was naturally contaminated with AF and its AF concentration was predetermined before the start of the experiment. Birds were fed the AF-contaminated diets during Phase 1 only and a normal diet during Phase 2. The analyzed AF concentration of the contaminated diets was 30 µg/kg (Table 3). The AF concentration of the non-contaminated Phase 1 and Phase 2 diets was 2 µg/kg and is presented in Table 3. Diets were in mash form and contained no antibiotics and mycotoxin binders. All birds had free access to water and feed at all times.

2.2.1. Feed sample and aflatoxin analyses

Feed samples were ground to pass through a 1-mm screen before analysis and analyzed according to the standard methods. Diet samples were

Table 1. The aflatoxin challenge model of the experiment

Age	Treatments			
	Negative control	Positive control	VitalSea 1	VitalSea 2
Phase 1 (d 1-21) Challenging period	Non-aflatoxin contaminated diet	Aflatoxin-contaminated diet		
Phase 2 (d 22-35)	Basal diet 2 without VitalSea®	Basal diet 2 without VitalSea®	Basal diet 2 + VitalSea® (0.5 mL/10 kg BW during 5 days, d 22-26)	Basal diet 2 + VitalSea® (1.0 mL/10 kg BW during 5 days, d 22-26)

Table 2. Ingredient composition of the experimental diets (as-fed basis)

Ingredients, %	Days of age	
	1 – 21 (Phase 1)	22 – 35 (Phase 2)
Corn, ground[1]	58.23	60.12
Soybean meal, 46%	35.60	33.50
Soybean oil	2.10	2.70
DL-Methionine, 99%	0.14	0.09
Lysine, 78.8%	0.20	0.08
Salt	0.30	0.30
Limestone	1.80	1.66
MCP (15, 23)	1.28	1.20
Vitamin and mineral premix[2,3]	0.25	0.25
Pigment	0.10	0.10

[1]Phase 1: Normal corn or aflatoxin (AF)-contaminated corn; Phase 2: normal corn only.
[2]Supplied per kg of feed (Phase 1): vitamin A (12000 IU), vitamin D3 (3500 IU), vitamin E (35 mg), vitamin K (4 mg), vitamin B1 (4 mg), vitamin B2 (7 mg), niacin (60 mg), vitamin B5 (17.5 mg), vitamin B6 (4 mg), vitamin B12 (15 µg), folic acid (1.3 mg), vitamin H (175 µg), Fe (60 mg), Cu (15 mg), Zn (80 mg), Mn (100 mg), I (1.5 mg), Se (0.25 mg), Co (0.3 mg).
[3]Supplied per kg of feed (Phase 2): vitamin A (10000 IU), vitamin D3 (3000 IU), vitamin E (25 mg), vitamin K (3.13 mg), vitamin B1 (3.13 mg), vitamin B2 (5 mg), niacin (44 mg), vitamin B5 (12.5 mg), vitamin B6 (3.13 mg), vitamin B12 (11 µg), folic acid (1.0 mg), vitamin H (125 µg), Fe (60 mg), Cu (15 mg), Zn (70 mg), Mn (90 mg), I (1.5 mg), Se (0.25 mg), Co (0.3 mg).

analyzed for DM (EC 152/2009), CP (AOAC 2001.11), crude fat (TCVN 4331:2001), crude fiber (AOCS Ba-6a-05), ash (EC 152/2009), Ca (GE297-ICP MS) and P (GE297-ICP MS). The nutrient analyses were performed by Upscience Vietnam in Binh Duong province, Vietnam. The aflatoxin concentrations of contaminated corn and feed samples were determined by LC/MS-MS method (Labocea, Britany, France). The analyzed nutrient composition and AF concentration of the experimental diets is presented in Table 3.

2.2.2. VitalSea® administration

Drinking water supplemented with VitalSea® was administered to birds for 5 consecutive days (d 22 to d 26) after 21-d exposure to AF-contaminated diets. The VitalSea® was added to drinking water at 0.5 mL of VitalSea® per 10 kg of BW in the VitalSea 1 treatment and at 1.0 mL of VitalSea® per 10 kg of BW in the VitalSea 2 treatment. The VitalSea® contained $MSP^{®}_{lipid}$, yeast fractions and a blend of organic acids. This product was provided by Olmix Asialand Co. Ltd, Binh Duong province, Vietnam.

2.2.3. Assessment of growth performance, flock uniformity and mortality rate

The initial BW of chicks in each pen was recorded at the beginning of the experiment. Subsequent measurements of the bird weights and feed intake were determined at 21 and 35 days of age. The ADG, ADFI and FCR were calculated on a per-pen basis. Day old chicks were weighed individually and subsequently at 21 and 35 days of age for measurement of flock uniformity. The flock uniformity was calculated as the percent of the flock that was within ± 10% of the mean BW.

Table 3. Analyzed nutrient composition and aflatoxin concentration of the experimental diets (as-fed basis)[1]

Items	Phase 1		Phase 2
	Negative control	Positive control	
ME, kcal/kg[2]	3000	3000	3050
DM, %	88.45	89.09	88.39
Crude protein, %	23.59	22.40	22.02
Crude fat, %	3.89	3.95	4.57
Crude fiber, %	2.66	2.35	2.42
Ash, %	5.94	5.88	5.69
Ca, %	1.01	0.99	0.88
Total phosphorus, %	0.62	0.60	0.61
Aflatoxin, µg/kg[3]	2.00	30.00	2.00

[1]The analysis was performed by Upscience Vietnam in Binh Duong province, Vietnam.
[2]Calculated.
[3]Analyzed by Labocea laboratory (Britany, France).

Table 4. Effects of water supplementation with VitalSea® on live body weight of broilers (g/bird) fed aflatoxin-contaminated diets

Age, d	Treatments[1]				SEM	*P*
	NC	PC	VitalSea 1	VitalSea 2		
1	46.19	46.20	46.36	46.39	0.088	0.278
21	767.28	765.46	774.87	795.85	9.843	0.136
35	1675.39^{ab}	1636.53^{b}	1726.32^{ab}	1754.94^{a}	29.487	0.039

[1]8 replicate pens/treatment and 30 birds/pen; NC: negative control; PC: positive control; VitalSea 1: 0.5 mL of VitalSea® per 10 kg of live BW; VitalSea 2: 1.0 mL of VitalSea® per 10 kg of live BW; VitalSea® was administered to broilers from d 22-26.
[a-b]Within a row, means without a common superscript differ ($P < 0.05$).

The number of dead or removed birds from each pen was recorded daily to calculate the mortality rate.

2.2.4. Blood collection and measurements of serum AST and LDH

Two male birds per pen were randomly selected for collection of blood samples from a wing vein at 21 days of age and subsequent blood samples were taken from the same birds at 26 and 35 days of age. Two milliliters of blood from each bird were collected into a tube containing no anticoagulant. The blood was allowed to clot at room temperature and stored at 4°C before separation of serum by centrifugation (3000 x g for 10 min at room temperature). Serum concentrations of AST and LDH were measured by specific commercial kits (AFG Bioscience, IL, USA) using an autoanalyzer (Biotek, Vermont, USA).

2.2.5. Statistical analysis

Data were analyzed as a completely randomized design by ANOVA using the GLM procedure (SAS Inst. Inc., Cary, NC). The pen was considered the experimental unit for live BW, ADFI, ADG and FCR, whereas one bird was considered the experimental unit for the other parameters. When a significant F value for treatment means was observed in the analysis of variance, the treatment means were compared using Tukey's test. To test the effect of AF contamination on the mortality of broilers during the AF exposure period (Phase 1), the mortality data were pooled from the 3 treatments with AF-contaminated diet. The flock uniformity and mortality rate among the treatments was compared by the Chi-square test. Treatment effects were considered significant at $P < 0.05$, whereas a trend for a treatment effect was noted when $P < 0.1$.

3. Results

3.1. Growth performance

No differences in the BW of broilers were found at 1 and 21 days of age among treatments ($P > 0.05$; Table 4). At d 35, the BW of birds in

Table 5. Effects of water supplementation with VitalSea® on growth performance of broilers (g/bird) fed aflatoxin-contaminated diets

Age, d	Treatments[1]				SEM	*P*
	NC	PC	VitalSea 1	VitalSea 2		
D 1-21						
ADFI, g	46.44	46.73	47.89	47.76	0.554	0.182
ADG, g	33.99	33.87	34.15	34.71	0.449	0.572
FCR	1.367	1.380	1.402	1.376	0.009	0.060
D 22-35						
ADFI, g	120.57	121.41	121.75	126.33	2.122	0.238
ADG, g	64.92	62.61	68.66	68.56	1.584	0.029
FCR	1.860^{ab}	1.943^{b}	1.776^{a}	1.845^{a}	0.025	0.001
D 1-35						
ADFI, g	73.52	74.19	74.90	75.75	0.889	0.345
ADG, g	45.29	44.43	46.77	46.76	0.665	0.047
FCR	1.624^{a}	1.670^{b}	1.602^{a}	1.620^{a}	0.011	0.001

[1]8 replicate pens/treatment and 30 birds/pen; NC: negative control; PC: positive control; VitalSea 1: 0.5 mL of VitalSea® per 10 kg of live BW; VitalSea 2: 1.0 mL of VitalSea® per 10 kg of live BW; VitalSea® was administered to broilers from d 22-26.
[a-b]Within a row, means without a common superscript differ ($P < 0.05$).

the VitalSea 2 group (1754.94 g/bird) was higher ($P < 0.05$) than that of birds in the PC group (1636.53 g/bird). There were no differences in ADFI among treatments at any Phases or for the overall period ($P > 0.05$; Table 5).

In Phase 1, no differences in ADG were found among treatments ($P = 0.572$, Table 5). Broilers of the VitalSea 1 group tended to have a higher FCR than that of the NC group ($P < 0.06$). In Phase 2, water supplementation with VitalSea® tended to increase the ADG of broilers compared with the PC group ($P < 0.06$). The VitalSea 1 and VitalSea 2 groups also had a better FCR than the PC group ($P < 0.01$). For the overall period, the ADG of broilers consuming water with VitalSea 1 (46.77 g/d) and VitalSea 2 (46.76 g/d) tended to be higher ($P < 0.09$) than that of broilers in the PC group (44.43 g/d). In addition, the FCR of the PC group (1.670) was higher than that of the NC (1.624), VitalSea 1 (1.602) and VitalSea 2 (1.620) groups ($P < 0.01$).

3.2. Flock uniformity and mortality rate

There were no differences in the flock uniformity of broilers among treatments at d 1 and d 21 ($P > 0.05$; Figure 1). At d 35, no differences were found for the flock uniformity of broilers among treatments ($P > 0.05$), although the flock uniformity of broilers in the VitalSea 1 group (61.9%) was numerically higher than that of broilers in the NC (58.6%), PC (54.5%) and VitalSea 2 (56.4%) groups. As shown in Figure 2A, the mortality rate of the NC group (2.5%) was lower ($P < 0.05$) than the average mortality rate of the 3 AF-contaminated groups (5.7%) during d 1-21 (period of AF exposure). No differences ($P > 0.05$) in the mortality rate were observed among treatments during d 22-35 (Figure 2B).

3.3. Serum concentrations of AST and LDH

At 21 days of age, there were no differences in the serum concentration of AST among treatments ($P = 0.118$; Table 6). However, the serum LDH concentration of broilers in the PC group (2214.4 U/L) was higher ($P = 0.026$) than that of broilers in the NC group (2078.1 U/L), but was not different from that of broilers in the VitalSea 1 (2122.0 U/L) and VitalSea 2 (2144.7 U/L) groups ($P > 0.05$). At 26 and 35 days of age, no differences in the serum concentrations of AST and LDH were found among treatments ($P > 0.05$).

4. Discussion

Aflatoxins are a common contaminant of poultry feeds in the tropical and subtropical areas. For example, Shareef (2010) found that AF was a major mycotoxin group (91.1%) with an average concentration of 179.1 µg/kg in different poultry feed samples collected in Pakistan. In Vietnam, a 5-year survey (from 2012-2017) showed that the total AF incidence and total AF mean

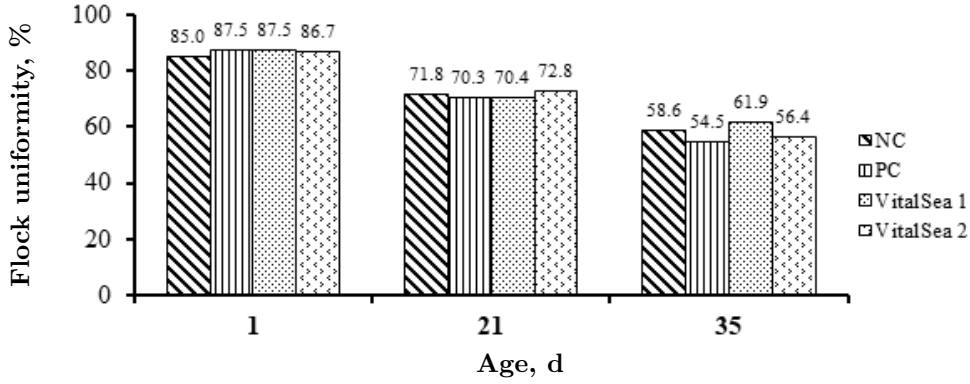

Figure 1. Effects of water supplementation with VitalSea® on the flock uniformity of broilers fed aflatoxin-contaminated diets ($P > 0.05$). NC: negative control; PC: positive control; VitalSea 1: 0.5 mL of VitalSea® per 10 kg of live BW; VitalSea 2: 1.0 mL of VitalSea® per 10 kg of live BW; VitalSea® was administered to broilers from d 22-26; There were 240 birds/treatment.

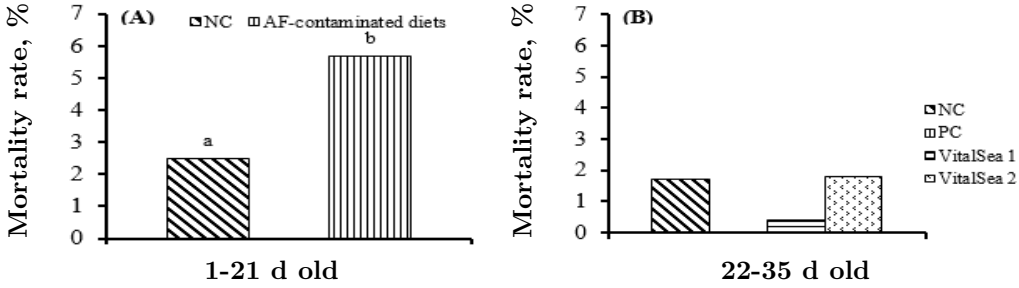

Figure 2. Effects of water supplementation with VitalSea® on the mortality rate of broilers fed aflatoxin-contaminated diets. (A) AF exposure period: NC (non-AF contaminated diet) vs. 3 AF-contaminated diets (PC, VitalSea 1, VitalSea 2). (B): NC: negative control; PC: positive control; VitalSea 1: 0.5 mL of VitalSea® per 10 kg of live BW; VitalSea 2: 1.0 mL of VitalSea® per 10 kg of live BW; VitalSea® was administered to broilers from d 22-26. There were 240 birds/treatment. [a,b]Means with different superscript letters differ ($P < 0.05$).

Table 6. Serum concentration of aspartate aminotransferase (AST) and lactate dehydrogenase (LDH) of broilers fed aflatoxin-contaminated diets with and without water supplementation of VitalSea®

Age, d	Treatments[1]				SEM	*P*
	NC	PC	VitalSea 1	VitalSea 2		
D 21						
AST, U/L	280.8	232.9	277.4	318.9	28.648	0.118
LDH, U/L	2078.1^{b}	2214.4^{a}	2122.0^{ab}	2144.7^{ab}	32.712	0.026
D 26						
AST, U/L	208.9	194.4	195.8	216.7	7.876	0.150
LDH, U/L	909.1	991.9	946.4	1012.5	39.007	0.240
D 35						
AST, U/L	270.8	266.8	256.6	270.7	21.397	0.963
LDH, U/L	828.5	972.0	899.0	1035.2	93.382	0.394

[1]16 birds/treatment; NC: negative control; PC: positive control; VitalSea 1: 0.5 mL of VitalSea® per 10 kg of live BW; VitalSea 2: 1.0 mL of VitalSea® per 10 kg of live BW; VitalSea® was administered to broilers from d 22-26.
[a-b]Within a row, means without a common superscript differ ($P < 0.05$).

concentration of corn samples were 27% and 16 µg/kg, respectively (Molina-Alvarado et al., 2017). Aflatoxins are of major importance because of their toxicity. Feeding AF-contaminated

feedstuffs to animals impaired feed intake, feed efficiency and/or animal health (Dersjant-Li et al., 2003; Magnoli et al., 2011; Yunus et al., 2011). According to Rawal et al. (2010), AF contamination is practically unavoidable universally. Therefore, the combination of different bioactive ingredients that can not only reduce the toxic effects of AF but also enhance liver functions and gut health could be a promising strategy to improve the overall health and performance of animals.

Our study showed that feeding a diet containing 30 µg AF/kg can result in negative effects on health and feed efficiency of young broilers. As shown in Figure 2A, broilers fed AF-contaminated diets had a higher mortality rate than those fed the NC diet during the AF exposure period. Furthermore, consuming the AF-contaminated diets for 21 days post-hatching also reduced the overall feed efficiency of broilers compared with the NC and VitalSea® groups (Table 5). According to Richard (2007) and Denli et al. (2009), AF toxicity is affected by different factors including AF level, duration of dietary exposure, species, sex, breed and age of animals. For instance, the autopsy of dead birds in our study revealed that 78% of dead birds fed the AF-contaminated diets showed paleness and yellow discoloration of the liver. It was also observed that the birds with yellowish colored liver died mainly during d 1-11 (68.8%) as compared with d 12-21 (31.2%). Young animals are often more susceptible to AF than older ones due to the lack of well-developed hepatic enzymatic systems required to detoxify mycotoxins (Kermanshahi, 2007; Ditta et al., 2019). Besides, the results of our study agree with those of previous studies. Yang et al. (2012) showed that diets contaminated with 36.9 µg AFB_1/kg decreased the weight gain, feed consumption and duodenal villus height of broilers during 1-21 days of age. It was also reported that diets containing 20 and 22 µg AFB_1/kg reduced the apparent digestibility of ducks and growth performance of broilers, respectively (Han et al., 2008; Saminathan et al., 2018). Additionally, although AF-contaminated diet did not affect the serum AST, it did increase the serum concentration of LDH at d 21 (Table 6). This implies that consuming the AF-contaminated diet, to a certain extent, might have caused liver malfunction and/or damage leading to the release of LDH into the bloodstream. Liver lesions such as fat vacuoles and hepatocellular necrosis with perilobular location were observed in broilers fed a diet containing 50 µg AFB_1/kg (Magnoli et al., 2011). Valchev et al. (2014) reported that AF not only caused liver lesions but also increased the serum level of LDH. Generally, diets contaminated with AF increased the FCR, mortality rate and serum LDH concentration of broilers.

In the present study, addition of VitalSea® to the drinking water for 5 consecutive days immediately after 21 days of AF exposure improved the final BW, growth rate and feed efficiency of broilers for both Phase 2 and the overall period (Table 5). This improvement may be associated with the bioactive components combined in the VitalSea®, such as $MSP^{®}_{lipid}$, yeast fractions and a blend of organic acids. Aflatoxins are known to alter the synthesis, absorption and transport of lipids to extra-hepatic tissues. Their metabolites can significantly increase the hepatic lipid peroxide level which negatively affects cellular membrane integrity leading to cell damage. For instance, Liu et al. (2018) showed that feeding 40 µg AFB_1/kg to broilers decreased the ADG and FCR, and increased the intestinal lesions. It has been shown that the use of MSP can improve not only lipid metabolism but also antioxidant capacity in animals (Manlusoc et al., 2019). Bussy et al. (2020) reported that DigestSea®, a product containing $MSP^{®}_{lipid}$, improved liver function and laying performance of turkey breeders. In addition, the combination of MSP® and organic acids was also found to improve the FCR of broilers during the finishing period (Che et al., 2019). In recent years, yeast extracts have been of potential interest due to their AF detoxification ability and positive effects on gut health. Matur et al. (2010) showed that dietary supplementation of *S. cerevisiae* extract reduced the toxic effects of AF on pancreatic lipase and chymotrypsin activity in laying breeder hens. Also, it was suggested that yeast cell wall could partially protect the growth performance and intestinal health of broilers concurrently challenged with AF and necrotic enteritis (Liu et al., 2018). Briefly, VitalSea® with a combination of different bioactive compounds showed its effectiveness in ameliorating the productivity of broilers after 3-week exposure to AF.

5. Conclusions

Feeding AF-contaminated diets negatively affected the productivity and health of broilers not only during the AF exposure but also in the

subsequent period. Water supplementation with VitalSea® can help restore the performance of broilers after AF exposure. As contamination of poultry feeds with AF is quite common in the tropical countries and other parts of the world, the addition of VitalSea® to drinking water could be a useful tool in supporting the liver health and growth performance of broilers.

Conflicts of interest

The authors declare no conflicts of interest.

References

Azizpour, A., & Moghadam, N. (2015). Effects of yeast glucomannan and sodium bentonite on the toxicity of aflatoxin in broilers. *Bazilian Journal of Poultry Science* 17, 7-13.

Bussy, F., Le-Goff, M., Biesse, M., Guriec, N., Delarue, J., Mathiaud, O., and Collén, P. N. (2020). An algal extract improves liver function and laying performance of turkey breeders. *Journal of US-China Medical Science* 17, 250-256.

Che, T. M., Le, H. T., Tran, V. Q., Berdeaux, D., Meallet, V., & Guillaume, M. (2019). Use of marine sulfated polysaccharide as an alternative to antibiotics in the diet of broilers. *The Journal of Agriculture and Development* 18(3), 1-26.

Denli, M., Blandon, J. C., Guynot, M. E., Salado, S., & Perez, J. F. (2009). Effects of dietary AflaDetox on performance, serum biochemistry, histopathological changes, and aflatoxin residues in broilers exposed to aflatoxin B1. *Poultry Science* 88(7), 1444-1451.

Dersjant-Li, Y., Verstegen, M. W. A., & Gerrits, W. J. J. (2003). The impact of low concentrations of aflatoxin, deoxynivalenol or fumonisin in diets on growing pigs and poultry. *Nutrition Research Reviews* 16(2), 223-239.

Ditta, Y. A., Mahad, A., & Bacha, U. (2019). Aflatoxins: their toxic effect on poultry and recent advances in their treatment. In P. B., Njobeh, & F., Stepman (Eds).. *Mycotoxins: Impact and management strategies* (125-147). London, UK: IntechOpen.

Fouad, A. M., Ruan, D., El-Senousey, H. K., Chen, W., Jiang, S., & Zheng, C. (2019). Harmful effects and control strategies of aflatoxin B_1 produced by *Aspergillus flavus* and *Aspergillus parasiticus* strains on poultry: Review. *Toxins* 11, 176.

Han, X. Y., Huang, Q. C., Li, W. F., Jiang, J. F., & Xu, Z. R. (2008). Changes in growth performance, digestive enzyme activities and nutrient digestibility of cherry valley ducks in response to aflatoxin B1 levels. *Livestock Science* 119, 216-220.

Kana, J. R., Teguia, A., & Tchoumboue, J. (2010). Effect of dietary plant charcoal from *Canarium schweinfurthii* Engl. and maize cob on aflatoxin B_1 toxicosis in broiler chickens. *Advances in Animal Biosciences* 1, 462–463.

Kermanshahi, H., Akbari, M. R., Maleki, M., & Behgar, M. (2007). Effect of prolonged low level inclusion of aflatoxin B_1 into diet on performance, nutrient digestibility, histopathology and blood enzymes of broiler chickens. *Journal of Animal and Veterinary Advances* 6(5), 686-692.

Liu, N., Wang, J. Q., Jia, S. C., Chen, Y. K., & Wang, J. P. (2018). Effect of yeast cell wall on the growth performance and gut health of broilers challenged with aflatoxin B_1 and necrotic enteritis. *Poultry Science* 97, 477-484.

Magnoli, A. P., Monge, M. P., Miazzo, R. D., Cavaglieri, L. R., Magnoli, C. E., Merkis, C. I., Cristofolini, A. L., Dalcero, A. M., & Chiacchiera, S. M. (2011). Effect of low levels of aflatoxin B1 on performance, biochemical parameters, and aflatoxin B_1 in broiler liver tissues in the presence of monenin and sodium bentonite. *Poultry Science* 90, 48-58.

Malekinezhad, P., Ellestad, L. E., Afzali, N., Farhangfar, S. H., Omidi, A., & Mohammadi, A. (2021). Evaluation of berberine efficiency in reducing the effects of aflatoxin B_1 and ochratoxin A added to male broiler rations. *Poultry Science* 100, 797-809.

Manlusoc, J. K. T., Hsieh, C. L., Hsieh, C. Y., Salac, E. S. N., Lee, Y. T., & Tsai, P. W. (2019). Pharmacologic application, potentials of sulfated polysacchride from marine algae. *Polymers* 11, 1163.

Matur, E., Ergul, E., Akyazi, I., Eraslan, E., & Cirakli, Z. T. (2010). The effects of *Saccharomyces cerevisiae* extract on the weight of some organs, liver, and pancreatic digestive enzyme activity in breeder hens fed diets contaminated with aflatoxins. *Poultry Science* 89(10), 2213-2220.

Molina-Alvarado, A., Zamora-Sanabria, R., & Granados-Chinchilla, F. (2017). A focus on aflatoxins in feedstuffs: Levels of contamination, prevalence, control strategies, and impacts on animal health. In Abdulra'uf, L. (Ed.). *Aflatoxin: Control analysis, detection and health risks* (115-152). London, UK: IntechOpen.

Nakavuma, J. L., Kirabo, A., Bogere, P., Nabulime M. M., Kaaya, A. N., & Gnonlonfin, B. (2020). Awareness of mycotoxins and occurrence of aflatoxins in poultry feeds and feed ingredients in selected regions of Uganda. *International Journal of Food Contamination* 7, 1-10.

NRC (National Research Council). (1994). *Nutrient requirements of poultry* (9^{th} ed.). Washington DC, USA: National Academy Press.

Pizzolitto, R. P., Armando, M. R., Salvano, M. A., Dalcero, A. M., & Rosa, C. A. (2013). Evaluation of *Saccharomyces cerevisiae* as an antiaflatoxicogenic agent in broiler feedstuffs. *Poultry Science* 92, 1655-1663.

Raju, M. V. L. N., & Devegowda, G. (2000). Influence of esterified-glucomannan on performance and organ morphology, serum biochemistry and haematology in

broilers exposed to individual and combined mycotoxicosis (aflatoxin, ochratoxin and T-2 toxin). *Bristish Poultry Science* 41, 640-650.

Rawal, S., Ji, E. K., & Roger, C. (2010). Aflatoxin B_1 in poultry: Toxicology, metabolism and prevention. *Research in Veterinary Science* 89(3), 325-331.

Richard, J. L. (2007). Some major mycotoxins and their mycotoxicoses - An overview. *International Journal of Food Microbiology* 119(1-2), 3-10.

Saminathan, M., Selamat, J., Abbasi Pirouz, A., Abdullah, N., & Zulkifli, I. (2018). Effects of nano-composite adsorbents on the growth performance, serum biochemistry, and organ weights of broilers fed with aflatoxin-contaminated feed. *Toxins* 10, 345.

Shareef, A. M. (2010). Molds andmycotoxins in poultry feeds fromfarms of potentialmycotoxicosis. *Iraqi Journal of Veterinary Sciences* 24(1), 17-25.

Valchev, I., Kanakov, D., Hristov, T. S., Lazarov, L., Binev, R., Grozeva, N., & Nikolov, Y. 2014. Investigations on the liver function of broiler chickens with experimental aflatoxicosis. *Bulgarian Journal of Veterinary Medicine* 17(4), 302-313.

Yang, J., Bai, F., Zhang, K., Lv, X., Bai, S., Zhao, L., Peng, X., Ding, X., Li, Y., & Zhang, J. (2012). Effects of feeding corn naturally contaminated with AFB_1 and AFB_2 on performance and aflatoxin residues in broilers. *Czech Journal of Animal Science* 57(11), 506-515.

Yunus, A. W., Razzazi-Fazeli, E., & Bohm, J. (2011). Aflatoxin B_1 in affecting broiler's performance, immunity, and gastrointestinal tract: A review of history and contemporary issues. *Toxins* 3, 566-590.

Zaghini, A., Martelli, G., Roncada, P., Simioli, M., & Rizzi, L. (2005). Mannanoligosaccharides and aflatoxin B_1 in feed for laying hens: Effects on egg quality, aflatoxins B_1 and M_1 residues in eggs, and aflatoxin B_1 levels in liver. *Poultry Science* 84(6), 825-832.

Genetic relationship analysis of *Dendrobium anosmum* Lindl. var. semialba based on the chloroplast *matK* and *rbcL* genes

Dien T. K. Pham[1*], Biet V. Huynh[2], & Truong Mai[1]

[1]Institute of Tropical Biology, Vietnam Academy of Science and Technology, Ho Chi Minh City, Vietnam
[2]Research Institute for Biotechnology and Environment, Nong Lam University, Ho Chi Minh City, Vietnam

ARTICLE INFO

Research Paper

Received: April 29, 2021
Revised: May 25, 2021
Accepted: June 02, 2021

Keywords

Chloroplast
Dendrobium anosmum Lindl. var. semialba
Genetic relationship
matK
rbcL

***Corresponding author**

Pham Thi Kieu Dien
Email: kieudien93@gmail.com

ABSTRACT

Dendrobium anosmum Lindl. var. semialba has variants of flower shapes. Currently, it has high economic value and is favored on the market. In this study, the genetic relationship of *Dendrobium anosmum* Lindl. var. semialba species was determined based on the analysis of chloroplast *matK*, *rbcL* gene sequences. The *matK* and *rbcL* genes of twelve species were amplified and their DNA sequenced. These DNA sequences were compared, calculated genetic distance and constructed phylogenetic tree. The results showed that 100% of samples were amplified and sequenced successfully. The analysis of *matK* sequences showed that 12 species had very high genetic similarity with the low genetic distance of 0 - 0.001; the nucleotide sequences were almost unchanged except for one variable nucleotide position in TB1 and TB1 was in a separate branch of the phylogenetic tree. The analysis of *rbcL* sequences showed that all species had a low genetic distance of 0 - 0.012 and had 7 mutant positions in nucleotide sequences of TB1 and TB5. These species were in a separate branch of the phylogenetic tree while the other species were grouped in the other branch of the phylogenetic tree. The study provided a reliable molecular database of the *Dendrobium anosmum* Lindl. var. semialba for identification, classification, biodiversity assessment and conservation of genetic resources.

Cited as: Pham, D. T. K., Huynh, B. V., & Mai, T. (2021). Genetic relationship analysis of *Dendrobium anosmum* Lindl. var. semialba based on the chloroplast *matK* and *rbcL* genes. *The Journal of Agriculture and Development* 20(3), 41-49.

1. Introduction

The orchid family (Orchidaceae) is one of the largest families of flowering plants in the world. There are 20,000 species in 850 genera in this family. *Dendrobium*, one of the largest genera in Orchidaceae, having more than 1,100 species identified, distributed in many parts of the world. Southeast Asia can be considered as the homeland of *Dendrobium* with hundreds of species, especially there are more than 100 species in Vietnam, widely distributed in all regions of the country (Hazlina et al., 2013; Xu et al., 2013; Tran et al., 2018). *Dendrobium anosmum* Lindl. is widely grown and has high economic value because of the thick leaves, arranging in 2 rows along the body and the beautiful flowers (Cao, 2018). In particular, the rare native *Dendrobium anosmum* Lindl. var. semialba, being from the natural forests of the Di Linh plateau Lam Dong province, have been cultivated domestically. It is very popular in the market today thanks to its characteristic aroma and unique variation of the flower.

Characteristically, *Dendrobium* species have a

wide geographical distribution and ability to produce a large number of hybrids with different morphologies. The high morphological diversity is one of the difficulties in taxonomy, especially the taxonomy based on morphology. The taxonomy of species is complex also because of the large distribution region (Xiaohua et al., 2009). Besides comparative vegetative anatomy and plant systematics, genetics has been used as a powerful tool for taxonomy and studying genetic relationships among *Dendrobium* species (Hazlina et al., 2013; Moudi et al., 2013a). Accurate genetic relationship information has been essential for the conservation of genetic resources, identification of plant varieties, selection of parents for propagation (Hazlina et al., 2013; Tran et al., 2018).

Currently, molecular techniques are widely used in the genetic analysis of orchids. The common molecular data used in plant systematics come from two sources: chloroplast DNA (cpDNA) and nuclear ribosomal DNA (nrDNA). Chloroplast DNA has been the most extensively used source of data in plant phylogenetic analysis. In particular, *matK* and *rbcL* are chloroplast genes having high effectiveness in genetic correlation analysis (Hollingsworth, et al., 2009; Moudi et al., 2013b; An et al., 2019). These makers have been successfully applied in many studies about genetic relationships and taxonomy of rice, Apocynaceae, Acacia, Orchidaceae, Araliaceae, etc. (Cabelin & Alejandro, 2016; Jin et al., 2017; Ismail et al., 2020).

This study aimed to determine the genetic relationship among twelve species of the rare native *Dendrobium anosmum* Lindl. var. semialba based on the data of *matK* and *rbcL* DNA barcoding markers, which supports selective breeding and conservation of genetic resources.

2. Materials and Methods

2.1. Plant materials

Leaves of twelve *Dendrobium anosmum* Lindl. var. semialba species were collected from Son Dien village and Tam Bo village, Di Linh district, Lam Dong province, Vietnam, which were listed in the Table 1. There was a negative control sample (SD1) having a normal flower and a positive control sample (SD2) having a variant flower.

2.2. Isolation of DNA, amplification, and sequencing

Genomic DNA was extracted from 50 mg of fresh leaf explant by ISOLATE II Plant DNA kit (Bioline, UK). The isolated DNA was stored at - 20°C. The primer sets used for amplification of *matK* and *rbcL* gene were *matK*-390F (50 - eCGATCTATTCATTCAATATTTC - 30) and *matK*-1326R (50 - TCTAGCACACGAAAGTCGAAGT - 30) for *matK*, *rbcL*-aF (50 - ATGTCACCACAAACAGAGACTAAAGC - 30) and *rbcL* - ajf634R (50 - GAAACGGTCTCTCCAACG CAT - 30) for *rbcL*. A PCR reaction mixture of 50 µL comprised as follows: 2 µL of template DNA (200 ng), 1 µL of both forward and reverse primers (20 µM), 25 µL MyTaq Mix (2X) and the rest was added with deionized distilled water. PCR cycling conditions involved initial denaturation at 95°C for 1 min; followed by 35 cycles of denaturation at 95°C for 30 sec, annealing at 45°C (*matK*) or 55°C (*rbcL*) for 15 sec, and extension at 72°C for 10 sec. After 35 cycles, the PCR reaction products were held at 4°C. The PCR products were examined by electrophoresis on 1.5% agarose gel. Red gel dye was used to detect DNA lines under UV light. The band size of amplified products was determined by using a 100 bp ladder. The PCR products of *matK* and *rbcL* genes were purified. After that, the nucleotide sequences of the purified DNA were determined by Sanger sequencing ABI Genetic Analyzers 3730 XL (1st Base, Singapore).

2.3. DNA sequence data analysis

The *matK*, *rbcL* nucleotide sequences from the sequencing results of twelve *Dendrobium anosmum* Lindl. var. semialba species and the *matK*, *rbcL* nucleotide sequences of one species *Dendrobium anosmum* in the Genbank database were cut to the same size and were analyzed by Molecular Evolutionary Genetics Analysis version 7.0 (Kumar et al., 2016). The nucleotide sequences were aligned with ClustalW. The genetic distance was computed by Jukes-Cantor method. The Maximum Likelihood (ML) was used for the construction of phylogenetic trees. 1000 bootstrap replicates were executed to estimate the robustness of the ML trees (Thompson et al., 2002; Ijaz et al., 2019).

Table 1. Plant materials of species examined in this study

Sample ID	Species	Flower shape	Collection site
SD1	*Dendrobium anosmum* Lindl. (negative control)	Normal	Son Dien commune, Di Linh district, Lam Dong province, Vietnam
SD2	*Dendrobium anosmum* Lindl.var. semialba (positive control)	Variant	Son Dien commune, Di Linh district, Lam Dong province, Vietnam (received from M.M Gryshko Botanical Garden, Ukraine)
TB1	*Dendrobium anosmum* Lindl.var. semialba	Variant	Tam Bo commune, Di Linh district, Lam Dong province, Vietnam
SD3	*Dendrobium anosmum* Lindl.var. semialba	Variant	Son Dien commune, Di Linh district, Lam Dong province, Vietnam
TB2	*Dendrobium anosmum* Lindl.var. semialba	Variant	Tam Bo commune, Di Linh district, Lam Dong province, Vietnam
SD4	*Dendrobium anosmum* Lindl.var. semialba	Variant	Son Dien commune, Di Linh district, Lam Dong province, Vietnam
TB3	*Dendrobium anosmum* Lindl.var. semialba	Variant	Tam Bo commune, Di Linh district, Lam Dong province, Vietnam
TB4	*Dendrobium anosmum* Lindl.var. semialba	Variant	Tam Bo commune, Di Linh district, Lam Dong province, Vietnam
SD5	*Dendrobium anosmum* Lindl.var. semialba	Variant	Son Dien commune, Di Linh district, Lam Dong province, Vietnam
TB5	*Dendrobium anosmum* Lindl.var. semialba	Variant	Tam Bo commune, Di Linh district, Lam Dong province, Vietnam
SD6	*Dendrobium anosmum* Lindl.var. semialba	Variant	Son Dien commune, Di Linh district, Lam Dong province, Vietnam
TB6	*Dendrobium anosmum* Lindl.var. semialba	Variant	Tam Bo commune, Di Linh district, Lam Dong province, Vietnam

3. Results and Discussion

3.1. PCR amplification

The amplification success rate of the *matK* gene from twelve species of *Dendrobium anosmum* Lindl. var. semialba was 100% (Figure 1). The length of the *matK* sequences from amplification using a pair of primer *matK* - 390F and *matK* - 1326R was 936 bp. This result was similar to the study of other authors in the *matK* gene amplification (Wattoo et al., 2016). This result proved that the pair of primer *matK* - 390F and *matK* - 1326R at 45°C annealing temperatures, PCR reaction components, and thermal cycle were suitable for *matK* gene amplification in the present study.

The *rbcL* gene of all samples successfully amplified by the pair of primer *rbcL* - aF and *rbcL* - ajf634R at the annealing temperature of 55°C. The length of the *rbcL* sequences was 654 bp. It

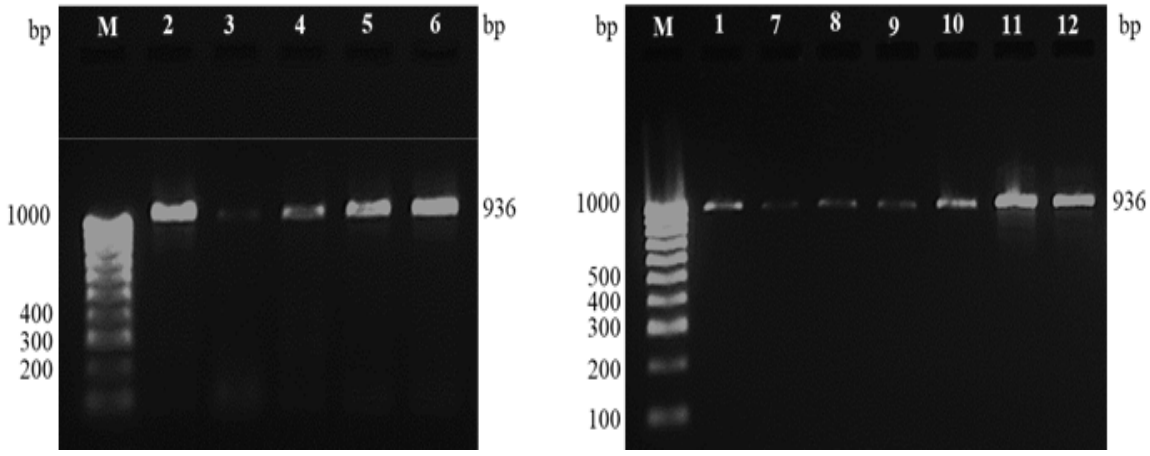

Figure 1. Electrophoresis of *matK* gene PCR products of twelve *Dendrobium anosmum* Lindl. var. semialba species. M is a 100 bp ladder, the number above each lane from 1 to 12 in turn are SD1, SD2, TB1, SD3, TB2, SD4, TB3, TB4, SD5, TB5, SD6, TB6 species).

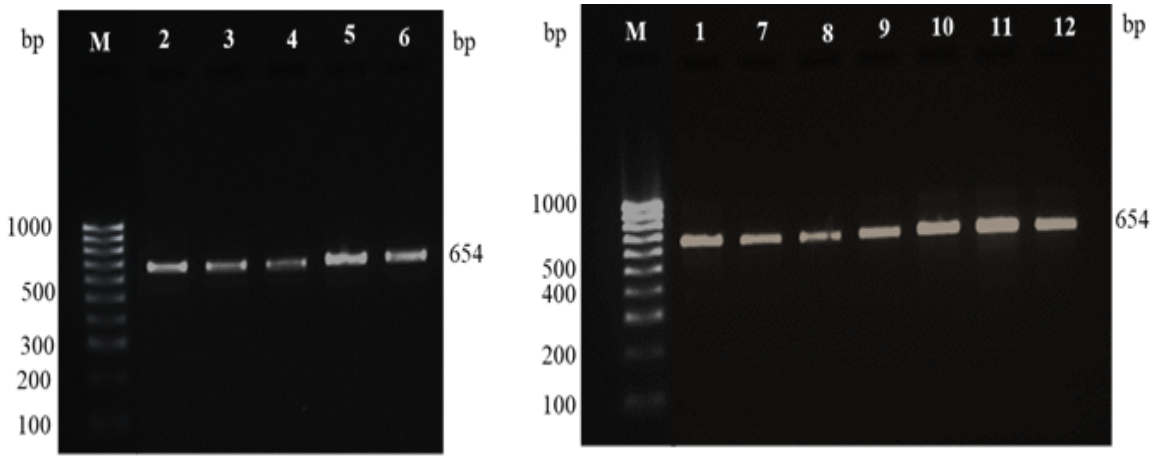

Figure 2. Electrophoresis of *rbcL* gene PCR products of twelve *Dendrobium anosmum* Lindl. var. Semialba species. M is a 100 bp ladder, the number above each lane from 1 to 12 in turn are SD1, SD2, TB1, SD3, TB2, SD4, TB3, TB4, SD5, TB5, SD6, TB6 species).

was expressed as a single line being dark bright on agarose gel (Figure 2). This proved that the PCR products had high quality for sequencing. This result was similar to the result in the study of Steven & Subramanyam (2009).

3.2. Genetic relationship analysis

The length of the *matK* sequences eliminated low-quality ends was 750 bp. The *matK* sequence was proved to be useful for *Dendrobium* species identification and reconstructing phylogeny (Asahina et al., 2010; Chattopadhyay et al., 2017). Among the chloroplast genes, *matK* is one of the most rapidly evolving genes. It has a length of about 1550 bp and encodes the enzyme maturase which is involved in the splicing of type - II introns from RNA transcripts. The rate of *matK* evolution was found suitable for resolving intergeneric as well as interspecies relationships in many angiosperms (Vijayan & Tsou, 2010). The results of aligning the *matK* sequences showed that there was only one varied nucleotide position, accounting for 0.13% *matK* sequences were analyzed (Table 2). It was a replacement of Thymine with Guanine at nucleotide positions 686 of TB1 species. The nucleotide sequences of the others were completely similar. Research by Asahina et al. (2010) also showed that individuals of the same species *D.*

Table 2. Nucleotide sequences variation in *matK*, *rbcL* gene of twelve species of *Dendrobium anosmum* Lindl. var. semialba and *Dendrobium anosmum* in the NCBI database (DA)

Species	Position[1]							
	matK	*rbcL*						
	686	281	297	369	370	422	441	469
SD1	T	C	T	T	A	G	T	A
SD2	T	C	T	T	A	G	T	A
SD3	T	C	T	T	A	G	T	A
SD4	T	C	T	T	A	G	T	A
SD5	T	C	T	T	A	G	T	A
SD6	T	C	T	T	A	G	T	A
TB1	G	A	G	T	A	T	C	C
TB2	T	C	T	T	A	G	T	A
TB3	T	C	T	T	A	G	T	A
TB4	T	C	T	T	A	G	T	A
TB5	T	A	G	C	C	T	C	C
TB6	T	C	T	T	A	G	T	A
DA	T	C	T	T	A	G	T	A

[1]Variable nucleotide positions are indicated at the top.

Figure 3. Phylogenetic tree constructed using *matK* sequences of twelve species of *Dendrobium anosmum* Lindl. var. semialba in this present study and one species of *Dendrobium anosmum* in the NCBI database (DA). Bootstrap values (%) are shown on each branch. The indicated scale represents 0.0001 nucleotide substitution per site.

moniliforme (Linn.) Swartz, D. pulchellum Roxburgh ex Lindley, *D. tosaense* Makino had no variation in the *matK* nucleotide sequence. However, there was a higher variability in *matK* sequences among *Dendrobium* species with up to 24 distinct nucleotide positions. The genetic distances between 13 species calculated using *matK* sequences were extremely low from 0 to 0.001 (Table 3). This result proved that the genetic relationship among *Dendrobium anosmum* Lindl. var. semialba species having variant flower, control species and standard species on Genbank was very close.

Data from *matK* sequence analysis were used to construct the phylogenetic tree. SD1 species having a normal flower, SD2, SD3, TB2, SD4, TB3, TB4, SD5, TB5, SD6, TB6 species having variant flower and a standard species (DA) from Genbank were gathered together with a 100% bootstrap supporting rate in the phylogenetic

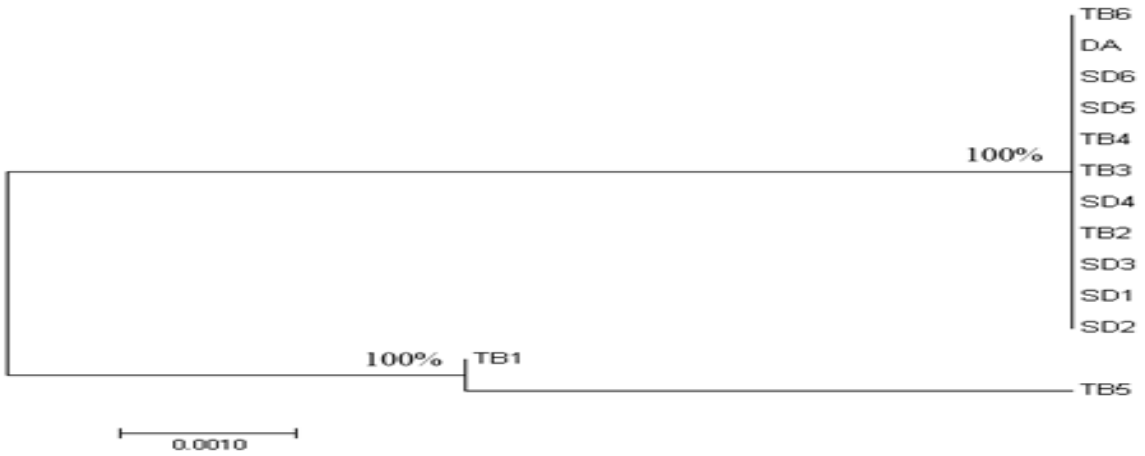

Figure 4. Phylogenetic tree constructed using *rbcL* sequences of twelve species of *Dendrobium anosmum* Lindl. var. semialba in this present study and one species of *Dendrobium anosmum* in the NCBI database (DA). Bootstrap values (%) are shown on each branch. The indicated scale represents 0.001 nucleotide substitution per site.

tree constructed using *matK* sequences, while only TB1 species was on a separate clade of the phylogenetic tree with a 100% bootstrap supporting rate (Figure 3). By contrast, another study demonstrated that 27 distinct species belonging to the same genus *Dendrobium* were grouped into many clades in the phylogenetic trees constructed based on *matK* data with a high bootstrap rate (Srikulnath et al., 2015). Therefore, the branching level of the phylogenetic tree constructed using *matK* sequences belonging to different species of genus *Dendrobium* is probably higher than that belonging to similar species of this genus.

After removing low-quality ends of amplified products of *rbcL* gene, the *rbcL* sequences were used to analyze have a length of 582 bp. *rbcL* chloroplast gene encoding ribulose-1,5-bisphosphate carboxylase/oxygenase large subunit is the most commonly sequenced gene for phylogenetic studies of plants, especially the species of Orchidaceae family (Moudi et al, 2013b). The *rbcL* region from thirteen species *Dendrobium anosmum* Lindl. var. semialba were aligned in Table 2. The number of variable sites was seven sites in *rbcL* sequences of TB1 and TB5 and the variation rates were very low. TB1 has five single-nucleotide substitution sites, accounting for 0.86% *rbcL* sequences were analyzed. These sites were as follows: 281 (replacement of Cytosine with Adenine), 297 (replacement of Thymine with Guanine), 422 (replacement of Guanine with Thymine), 411 (replacement of Thymine with Cytosine), 469 (replacement of Adenine with Cytosine). TB5 has the most single-nucleotide substitution sites with seven sites, accounting for 1.2% *rbcL* sequences were analyzed. In addition to variable sites such as TB1, TB5 had two other variable sites were 369 (replacement of Thymine with Cytosine) and 370 (replacement of Adenine with Cytosine). Similar results between *Dendrobium* species as well as between individuals of the same species were demonstrated in the study of Asahina et al. (2010). Zhu et al. (2018) suggested that *rbcL* is unable to distinguish D. officinale from five closely related species of it. The *rbcL* gene has high conservation at the family level. Taxodiaceae (redwood) family had only minor sequence differences in their cp *rbcL* genes compared to species in the Cupressaceae (Chattopadhyay et al., 2017).

Nucleotide change plays an important role in determining genetic distance and phylogenetic origin. The *rbcL* sequences analysis showed that the genetic distances among thirteen species were low from 0 to 0.012 (Table 4). These results indicated that thirteen species in this study were closely related. From the phylogenetic trees reconstructed based on the *rbcL*, thirteen species were divided into two branches. SD1, SD2, SD3, TB2, SD4, TB3, TB4, SD5, SD6, TB6 and a species from Genbank were located in a branch; while TB1 and TB5 were located in the other branch of phylogenetic tree with a bootstrap value of 100% (Figure 4).

Table 3. Genetic distances among twelve species of *Dendrobium anosmum* Lindl. var. semialba in this present study and one species of *Dendrobium anosmum* in the NCBI database (DA) based on the *matK* sequences

Species	SD1	SD2	SD3	SD4	SD5	SD6	TB1	TB2	TB3	TB4	TB5	TB6	DA
SD1													
SD2	0.000												
SD3	0.000	0.000											
SD4	0.000	0.000	0.000										
SD5	0.000	0.000	0.000	0.000									
SD6	0.000	0.000	0.000	0.000	0.000								
TB1	0.001	0.001	0.001	0.001	0.001	0.001							
TB2	0.000	0.000	0.000	0.000	0.000	0.000	0.001						
TB3	0.000	0.000	0.000	0.000	0.000	0.000	0.001	0.000					
TB4	0.000	0.000	0.000	0.000	0.000	0.000	0.001	0.000	0.000				
TB5	0.000	0.000	0.000	0.000	0.000	0.000	0.001	0.000	0.000	0.000			
TB6	0.000	0.000	0.000	0.000	0.000	0.000	0.001	0.000	0.000	0.000	0.000		
DA	0.000	0.000	0.000	0.000	0.000	0.000	0.001	0.000	0.000	0.000	0.000	0.000	

Table 4. Genetic distances among twelve species of *Dendrobium anosmum* Lindl. var. semialba in this present study and one species of Dendrobium anosmum in the NCBI database (DA) based on the *rbcL* sequences

Species	SD1	SD2	SD3	SD4	SD5	SD6	TB1	TB2	TB3	TB4	TB5	TB6	DA
SD1													
SD2	0.000												
SD3	0.000	0.000											
SD4	0.000	0.000	0.000										
SD5	0.000	0.000	0.000	0.000									
SD6	0.000	0.000	0.000	0.000	0.000								
TB1	0.009	0.009	0.009	0.009	0.009	0.009							
TB2	0.000	0.000	0.000	0.000	0.000	0.000	0.009						
TB3	0.000	0.000	0.000	0.000	0.000	0.000	0.009	0.000					
TB4	0.000	0.000	0.000	0.000	0.000	0.000	0.009	0.000	0.000				
TB5	0.012	0.012	0.012	0.012	0.012	0.012	0.003	0.012	0.012	0.012			
TB6	0.000	0.000	0.000	0.000	0.000	0.000	0.009	0.000	0.000	0.000	0.012		
DA	0.000	0.000	0.000	0.000	0.000	0.000	0.009	0.000	0.000	0.000	0.012	0.000	

4. Conclusions

In summary, this study demonstrated that the *matK* and *rbcL* region sequence analyses were simple, quick, and highly reliable. Regarding species discrimination, *rbcL* gave better resolution than *matK* in identifying *Dendrobium anosmum* Lindl. var. semialba species. There was a close genetic relationship among *Dendrobium anosmum* Lindl. var. semialba species based on the low genetic distance and the minor nucleotide variation in the *matK* and *rbcL* sequences.

Conflict of interest

The authors declare no conflict of interest.

Acknowledgments

The authors gratefully acknowledge financial support from the Ho Chi Minh City Foundation for Science and Technology Development, Department of Science and Technology (DOST), 2018-2021.

References

An, J., Moon, J. C., Kim, J. H., Kim, G. S., & Jang, C. S. (2019). Development of DNA-based species-specific real-time PCR markers for four berry fruits and their application in commercial berry fruit foods. *Applied Biological Chemistry* 62(1), 1-7.

Asahina, H., Shinozaki, J., Masuda, K., Morimitsu, Y., & Satake, M. (2010). Identification of medicinal *Dendrobium* species by phylogenetic analyses using *matK* and *rbcL* sequences. *Journal of Natural Medicines* 64(2), 133-138.

Cabelin, V. L. D., & Alejandro, G. J. D. (2016). Efficiency of *matK*, *rbcL*, *trnH-psbA*, and *trnL-F* (cpDNA) to molecularly authenticate Philippine ethnomedicinal Apocynaceae through DNA barcoding. *Pharmacognosy Magazine* 12(46), 384-388.

Cao, B. P. (2018). Physiological and biochemical changes of micropropagated *Dendrobium anosmum* Lindl. in ex vitro acclimatization process. *Science and Technology Development Journal-Natural Sciences* 2(3), 59-67.

Chattopadhyay, P., Banerjee, G., & Banerjee, N. (2017). Distinguishing orchid species by DNA barcoding: Increasing the resolution of population studies in plant biology. *Omics: A Journal of Integrative Biology* 21(12), 711-720.

Hazlina, N., Wahba, L. E., Fadelah, A., & Wickneswari, R. (2013). Genetic relationships among 81 *Dendrobium* accessions from Malaysia. *Malaysian Applied Biology* 42(1), 35-40.

Hollingsworth, P. M., Forrest, L. L., Spouge, J. L., Hajibabaei, M., Ratnasingham, S., Bank, M. van der, Chase, M. W., Cowan, R. S., Erickson, D. L., Fazekas, A. J., Graham, S. W., James, K. E., Kim, K. J., Kress, W. J., Schneider, H., AlphenStahl, J. van, Barrett, S. C. H., Berg, C. van den, Bogarin, D., Burgess, K. S., Cameron, K. M., Carine, M., Chacón, J., Clark, A., Clarkson, J. J., Conrad, F., Devey, D. S., Ford, C. S., Hedderson, T. A. J., Hollingsworth, M. L., Husband, B. C., Kelly, L. J., Kesanakurti, P. R., Kim, J. S., Kim, Y. D., Lahaye, R., Lee, H. L., Long, D. G., Madriñán, S., Maurin, O., Meusnier, I., Newmaster, S. G., Park, C. W., Percy, D. M., Petersen, G., Richardson, J. E., Salazar, G. A., Savolainen, V., Seberg, O., Wilkinson, M. J., Yi, D. K., & Little, D. P. (2009). A DNA barcode for land plants. *Proceedings of the National Academy of Sciences* 106(31), 12794-12797.

Ijaz, S., Haq, I. U., & Babar, M. (2019). Jukes-cantor evolutionary model-based phylogenetic relationship of economically important ornamental palms using maximum likelihood approach. *Applied Ecology and Environmental Research* 17(6), 14859-14865.

Ismail, M., Ahmad, A., Nadeem, M., Javed, M. A., Khan, S. H., Khawaish, I., Sthanadar, A. A., Qari, S. H., Alghanem, S. M., Khan, K. A., Khan, M. F., & Qamer, S. (2020). Development of DNA barcodes for selected Acacia species by using *rbcL* and *matK* DNA markers. *Saudi Journal Biological Science* 27(12), 3735-3742.

Jin, W. T., Schuiteman, A., Chase, M. W., Li, J. W., Chung, S. W., Hsu, T. C., & Jin, X. H. (2017). Phylogenetics of subtribe Orchidinae sl (Orchidaceae; Orchidoideae) based on seven markers (plastid *matK*, *psaB*, *rbcL*, *trnL-F*, *trnH-psba*, and nuclear nrITS, Xdh): implications for generic delimitation. *BMC Plant Biology* 17(1), 222.

Kumar, S., Stecher, G., & Tamura, K. (2016). MEGA7: molecular evolutionary genetics analysis version 7.0 for bigger datasets. *Molecular Biology and Evolution* 33(7), 1870-1874.

Moudi, M., Go, R., Yien, C. Y. S., & Saleh, M. N. (2013a). A review on molecular systematic of the genus *Dendrobium* Sw. *Acta Biologica Malaysiana* 2(2), 71-78.

Moudi, M., Yien, C. Y. S., Nazre, M., Abdullah, J. O., & Go, R. (2013b). Phylogenetic analysis among four sections of Genus *Dendrobium* Sw. (Orchidaceae) in Peninsular Malaysia using *rbcL* sequence data. *International Journal of Bioassays* 2(06), 932-937.

Srikulnath, K., Sawasdichai, S., Jantapanon, T. K., Pongtongkam, P., & Peyachoknagul, S. (2015). Phylogenetic relationship of *Dendrobium* species in Thailand inferred from chloroplast *matK* gene and nuclear rDNA ITS region. *The Horticulture Journal* 84(3), 243-252.

Steven, G. N., & Subramanyam, R. (2009). Testing plant barcoding in a sister species complex of pantropical *Acacia* (Mimosoideae, Fabaceae). *Molecular Ecology Resources* 9(1), 172-180.

Thompson, J. D., Gibson, T. J., & Higgins, D. G. (2002). Multiple sequence alignment using ClustalW

and ClustalX. *Current Protocols in Bioinformatics* 1, 2-3.

Tran, D. D., Khuat, T. H., La, N. T., Nguyen, T. T. T., Pham, H. B., Nguyen, K. T, Tran, D. H., Do, T. M., & Tran, K. D. (2018). Identification of Vietnamese native *Dendrobium* species based on ribosomal DNA internal transcribed spacer sequence. *Advanced Studies in Biology* 10(1), 1-12.

Vijayan, K., & Tsou, C. H. (2010). DNA barcoding in plants: Taxonomy in a new perspective. *Current Science* 99(11), 1530-1541.

Wattoo, J. I., Saleem, M. Z., Shahzad, M. S., Arif, A., Hameed, A., & Saleem, M. A. (2016). DNA Barcoding: Amplification and sequence analysis of *rbcL* and *matK* genome regions in three divergent plant species. *Advancements in Life Sciences* 4(1), 3-7.

Xiaohua, J., Singchi, C., & Yibo, L. (2009). Taxonomic revision of *Dendrobium moniliforme* complex (Orchidaceae). *Scientia Horticulturae* 120(1), 143-145.

Xu, J., Han, Q. B., Li, S. L., Chen, X. J., Wang, X. N., Zhao, Z. Z., & Chen, H. B. (2013) Chemistry, bioactivity and quality control of *Dendrobium*, a commonly used tonic herb in traditional Chinese medicine. *Phytochemistry Reviews* 12, 341-367.

Zhu, S., Niu, Z., Xue, Q., Wang, H., Xie, X., & Ding, X. (2018). Accurate authentication of Dendrobium officinale and its closely related species by comparative analysis of complete plastomes. *Acta Pharmaceutica Sinica B* 8(6), 969-980.

Accumulation and distribution of lead (Pb) in different tissues of Lucky bamboo plants (*Dracaena sanderiana*)

Lien B. Ho[1,2*], Biet V. Huynh[3], & Tuyen C. Bui[4]

[1]Faculty of Management Sciences, Thu Dau Mot University, Binh Duong, Vietnam
[2]Faculty of Biological Sciences, Nong Lam University, Ho Chi Minh City, Vietnam
[3]Research Institute for Biotechnology and Environment, Nong Lam University, Ho Chi Minh City, Vietnam
[4]Faculty of Environment and Natural Resources, Nong Lam University, Ho Chi Minh City, Vietnam

ARTICLE INFO

Research Paper

Received: April 29, 2021
Revised: June 08, 2021
Accepted: June 18, 2021

Keywords

Anatomical structure
Cell walls
Distribution
Dracaena sanderiana
Lead (Pb)

***Corresponding author**

Ho Bich Lien
Email: lienhb@tdmu.edu.vn

ABSTRACT

Lucky bamboo plants (*Dracaena sanderiana*) were used to study the accumulation and distribution of lead (Pb) in tissues of root, stem and leaf, as well as the impact of lead accumulation on the anatomical structure of these tissues. *Dracaena sanderiana* plants were exposed to $Pb(NO_3)_2$ solution at the Pb concentrations of 0; 200; 400; 600; 800; 1,000; 2,000; 3,000 and 4,000 mg/L for 60 days. The results showed that the more the Pb concentration was used, the more the amount of lead was accumulated and deposited. The tolerance limit of *Dracaena sanderiana* was 800 mg/L of Pb in water. The lethal concentration for plants was 4,000 mg/L Pb. When the concentrations of Pb in the solution were higher than the tolerance limit of the plant, the growth of *Dracaena sanderiana* could be inhibited. *Dracaena sanderiana* could accumulate up to 39,235 mg/kg Pb in the presence of Pb at 800 mg/L. Lead was accumulated mainly in roots (97.5%) and deposited mainly in the cell walls and the spaces between cells in tissues of roots. In the stems and leaves of *Dracaena sanderiana*, lead accumulation was limited and distributed mainly around vascular bundles. Lead accumulation caused changes in the anatomical structure of root, stem and leaf tissues. The accumulation and distribution of Pb is mainly in the cell walls and the space of cells; it could be a detoxification mechanism for Pb of *Dracaena sanderiana*.

Cited as: Ho, L. B., Huynh, B. V, & Bui, T. C. (2021). Accumulation and distribution of lead (Pb) in different tissues of Lucky bamboo plants (*Dracaena sanderiana*). *The Journal of Agriculture and Development* 20(3), 50-60.

1. Introduction

Today, the continuous development of science and technology has brought many economic benefits to humans. However, this also makes the environment more seriously polluted. In the world, the pollution of heavy metals, especially lead (Pb) pollution is becoming increasingly popular due to the massive development of human, agricultural and industrial activities (ATSDR, 1993). Lead is the most dangerous substance in the environment, and has caused deleterious effects not only to the environment, but also to the public's health (EPA, 2000). Thus, the search for Pb treatment methods has to be taken in priority in many countries.

Different methods of lead decontamination are available, the most commonly is physical chemistry. They can process the contaminated soil in-situ or ex-situ by using techniques involving chemicals, such as chelating and physical methods such as pumping or heating. Recently, a technique based on the use of plants has been developed for remediation of soil and water. This technique is well known "phytoremediation" that is less invasive and less expensive than the physical

and chemical techniques (EPA, 2000), but it involves the identification of plant species with particular capabilities. To be used in lead decontamination, the plants should tolerate the presence of high concentrations. In addition, they must be capable of accumulating the contaminant into their roots or in their shoots and have detoxifying mechanisms. However, these plant species were rather limited. Finding out plant species that represent its lead removal ability to reduce environmental pollution is one of the most interesting subjects towards scientists.

Recently, the research of Hao (2011) indicated a plant's ability in absorbing Cu, Ni, Hg, Cd and Cr for the process of phytoremediation, namely, Lucky bamboo plants (*Dracaena sanderiana*). Sereshi et al. (2014) had also shown that *Dracaena sanderiana* has the ability to grow well in garbage wastewater. However, the accumulation and distribution of lead by *Dracaena sanderiana* has not been researched yet.

Consequently, this study has been conducted to determine the accumulation and distribution of lead in *Dracaena sanderiana* plants as well as the impact of Pb on changes in the anatomy structure of those tissues.

2. Material and Methods

2.1. Plant materials and experiment

Lucky bamboo plants (*Dracaena sanderiana*) were collected, cut into sections about 45 cm, and were cultivated in greenhouse at Thu Dau Mot University, Binh Duong, Vietnam. Plants were cultivated in distilled water for 60 days in order to obtain homogeneous plants. Eighty one cloned plants selected by tree height, root length, number of leaves, and healthy condition, were transplanted to plastic pots containing 15 L $Pb(NO_3)_2$ solution (Merck), pH level of 4.5 with the following Pb concentrations: 0; 200; 400; 600; 800; 1,000; 2,000; 3,000 and 4,000 mg/L. The experiment was conducted for 60 days, after this period, plants were harvested and subsequently divided into roots, stems and leaves. The experimental design was completely randomized with three replicates. Every 10 days, experimental plants were evaluated for the total content of Pb in plant parts and after 60 days experimental plants were evaluated for Pb distribution and anatomy structure. Experimental solution didn't change for 60 days.

2.2. Determination total content of Pb in parts of *Dracaena sanderiana*

Plant materials including roots, stems and leaves were collected at 7 time periods (0, 10, 20, 30, 40, 50 and 60 days) and washed 3 times with distilled water, oven dried at 70°C for 24 h, then milled. Approximately 1 g of milled plants was placed in 100 mL digest tubes, added with 10 ml HNO_3, 2 mL $HCLO_4$ and 2 mL H_2O_2 then digested at 180°C until the samples were completely digested. The concentration of Pb in digestates was determined by AAS (Atomic Absorption Spectrometer) (Shimadzu, Japan).

2.3. Determination of Pb distribution in roots, stems and leaves tissues of *Dracaena sanderiana*

The observations of lead on plant tissues were made using histochemical methods which are considered to be fast, simple and accurate (Glater & Hernandez, 1972; Tung & Temple, 1996). Sodium rhodizonate is a specific good chromophoric reagent which gives red to blackish brown color with a buffer solution at pH of 2.8. Lucky bamboo plant parts (roots, stems and leaves) of each treatment Pb level were fixed by formaldehyde acid acetic for 24 h. The aim of the fixation was to obtain the same tissue as the original one. Then, samples were cut thin with a hand microtome. Thin sections are then soaked in a solution of sodium rhodizonate 0.2% (added one drop of acetic acid buffer solution of pH 2.8) for 30 min. Tissue samples were then rinsed with distilled water and placed in an object glass and observed on a microscope.

2.4. Determination of changes in anatomical structure of roots, stems and leaves tissues of *Dracaena sanderiana*

Experimental plants were taken from each treatment Pb level and then separated according to the roots, stems and leaves, which were then cleaned with distilled water and soaked in a solution of formaldehyde acetic acid for 24 h. Plant parts that have been fixed in formaldehyde acetic acid solution were then cut as thin as possible using a hand microtome, then stained in double with methylene blue and carmine red. Protocol for implementing a temporary microscope template was made according to the method of Hoang

& Nguyen (2004). The samples were observed by using a light microscope. Parameters measured were profile anatomical structure of roots, stems and leaves. Measurements were conducted on the thickness of tissues. These observations were conducted using Optika B - 383PL microscope (linked with a computer).

2.5. Data analysis and statistical analysis

Anatomical tissues size was measured by Optika Vision Pro software. Values are calculated as the mean of 3 repetitions. All data were averaged and statistically processed using Statgraphics centurion XVI software. Least significant difference (LSD) test was used to compare Pb contents in roots, stems and leaves of plants on different treatments.

3. Results and Discussion

3.1. Accumulation of Pb in *Dracaena sanderiana* plants

Results obtained from Figure 1, 2, 3 showed that levels of Pb in solution affected accumulated Pb ability in parts of *Dracaena sanderiana* plants. Pb content accumulated in roots, stems and leaves at different Pb levels tended to increase along with increasing Pb concentration and indicated a significant difference at 5% level according to the LSD test. The more Pb concentration increases, the more content of Pb accumulated in plants. However, contents of Pb in roots weren't significant difference in longer Pb exposure time (Pb contents was accumulated in the roots at concentrations 200; 400; 600; 800; 1,000 and 2,000 mg/L had significant difference at 5% level ($P < 0.05$) at 0 to 40 days, but wasn't significant difference at 50 days and 60 days) (Figure 1). This showed that *Dracaena sanderiana* may have a certain accumulation threshold. If accumulated content of Pb in plants surpasses the threshold, plants will halt absorption Pb from outside.

The tolerance limit of Pb in solution of *Dracaena sanderiana* was 800 mg/L (Ho et al., 2019). When the concentrations of Pb in the medium were higher than the tolerance limit of the plant, the growth of *Dracaena sanderiana* could be inhibited. The lethal concentration of Pb was 4,000 mg/L (All of the plants died at this level at 30 days). The highest Lead accumulation capacity in roots of *Dracaena sanderiana* was 38,518 mg/kg dw for the solution with Pb concentrations < 1,000 mg/L and 60,570 mg/kg dw for the solution with Pb concentrations > 1,000 mg/L (at 60 days of the experiment). Compared with Pteris vittata with accumulated Pb content in the roots 3,157 mg/kg dw at 3,000 mg/kg level (Tran et al., 2011), *Dracaena sanderiana* has a higher ability for accumulation Pb in the roots. Lead concentrations 2,000 mg/kg, 3,000 mg/kg and 4,000 mg/kg also significantly inhibited the growth of Pteris vittata. *Lantana camara* L. could tolerate Pb at a pollution level of 4,000 mg/L. After 1 day contacting with this Pb level, *Lantana camara* L. could accumulate 5,252 mg/kg dw Pb in the roots (Diep & Garnier-Zarli, 2007) and thus *Dracaena sanderiana*'s accumulation ability is lower than it (1,009 mg/kg dw in 1 day). Lead accumulation capacity in stems and leaves of *Dracaena sanderiana* was also shown to be higher than in some plant species such as *Chrysopogon zizanioides*, *Ricinus communis*, *Conyza canadensis*, *Oryza sativa*, *Pfaffia glomerata*, *Elsholtzia splendens* (Kumar & Prasad, 2018), with the highest Pb content in stem was 2,263 mg/kg dw (at 4,000 mg/L) and in leaves was 389.52 mg/kg dw (at 2,000 mg/L).

Pb content in parts of *Dracaena sanderiana* at all concentrations of Pb arranged in the order of roots > stems > leaves. At Pb levels from 200 to 4,000 mg/L, accumulated Pb content in roots, stems and leaves was 97.50%, 1.95% and 0.55%. Similar results were also reported in many plants such as *Lantana camara* L. (Diep & Garnier-Zarli, 2007), *Armeria maritima*, *Agrostis tenuis* and *Cardaminopsis halleri* (Dahmani et al., 2000). This result showed that the Pb transportation capacity of *Dracaena sanderiana* was limited only with upper organs as stems and leaves. Thus, *Dracaena sanderiana* could use phytostabilization or phytofiltration mechanism for absorptionPb. According to these two mechanisms, absorbed Pb was accumulated mainly in the roots.

3.2. Distribution of Pb in *Dracaena sanderiana* plants

3.2.1. Distribution of lead in roots tissues

Staining sodium rhodizonate gives red to blackish brown color in tissues where lead has accumulated. The appearance of red stains found in two forms as diffusive or granular deposits (Glater &

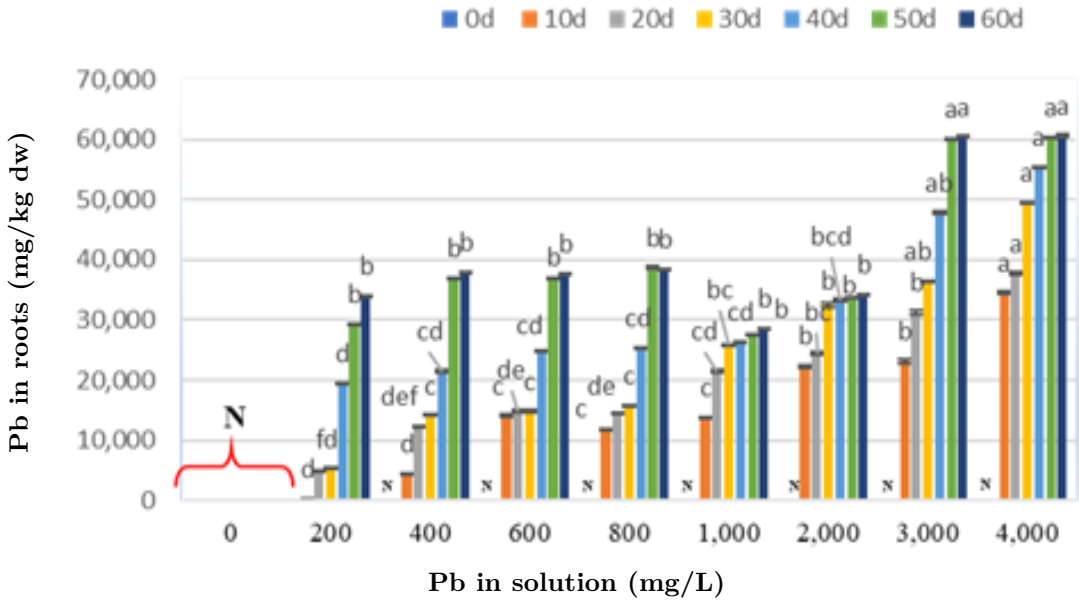

Figure 1. Accumulation of Pb in roots (mg/kg dry weight) of *Dracaena sanderiana*.
Note: Data in chart columns with different letters indicate a significant difference at 5% level according to LSD test; N: negative; dw: dry weight, analysis threshold = 0.006 mg/L); d: day.

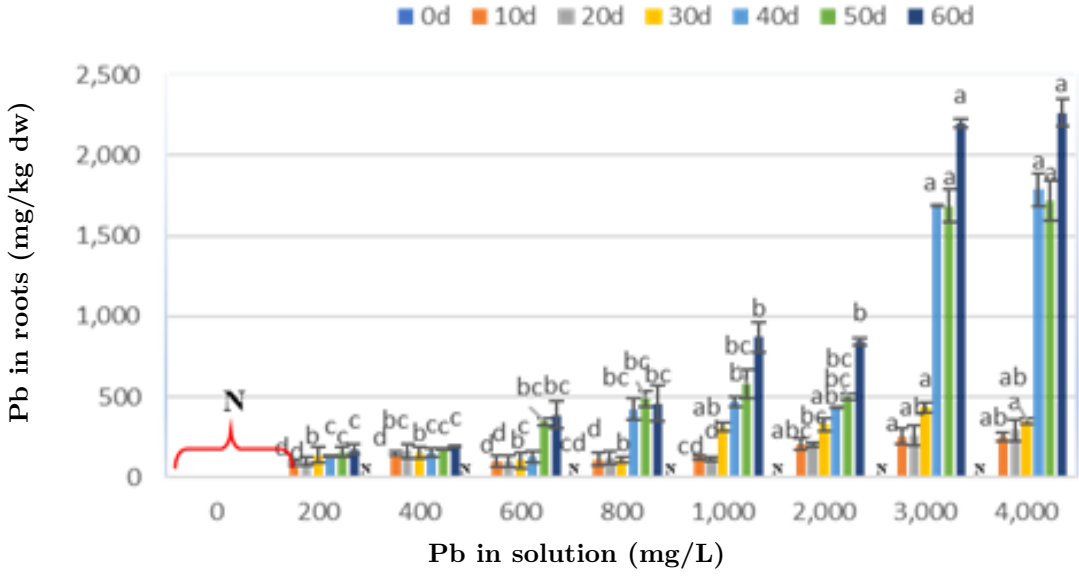

Figure 2. Accumulation of Pb in stems (mg/kg dry weight) of *Dracaena sanderiana*.
Note: Data in chart columns with different letters indicate a significant difference at 5% level according to LSD test; N: negative; dw: dry weight, analysis threshold = 0.006 mg/L); d: day.

Hernandez, 1972). At the root tissues could be seen that Pb deposited mainly in granular form (Fig 4A).

In the root tissues of *Dracaena sanderiana*, Pb was distributed mainly in the spaces between cells and linked to the cell walls (Figure 4B). This distribution could be mainly way to distribute Pb in the root tissues and be a tolerance and limitation strategy for Pb toxicity (Al-Saadi et al., 2013). Pb binds to the cell walls because of high affinity with components such as lignin, pectin, polysaccharide, cellulose (Krzesłowska et al., 2009). More

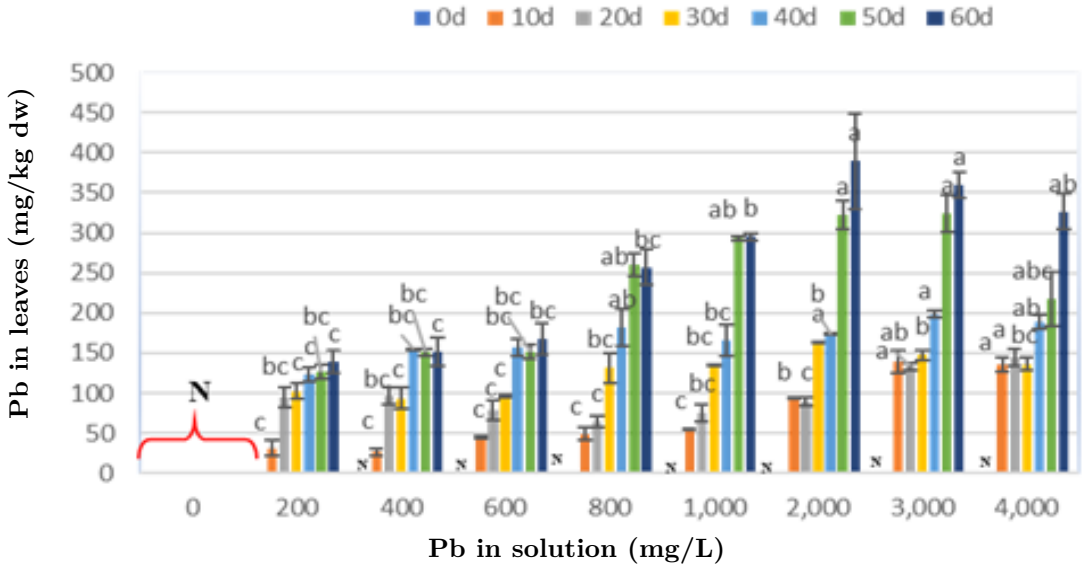

Figure 3. Accumulation of Pb in leaves (mg/kg dry weight) of *Dracaena sanderiana*.
Data in chart columns with different letters indicate a significant difference at 5% level according to LSD test; N: negative; dw: dry weight, analysis threshold = 0.006 mg/L); d: day.

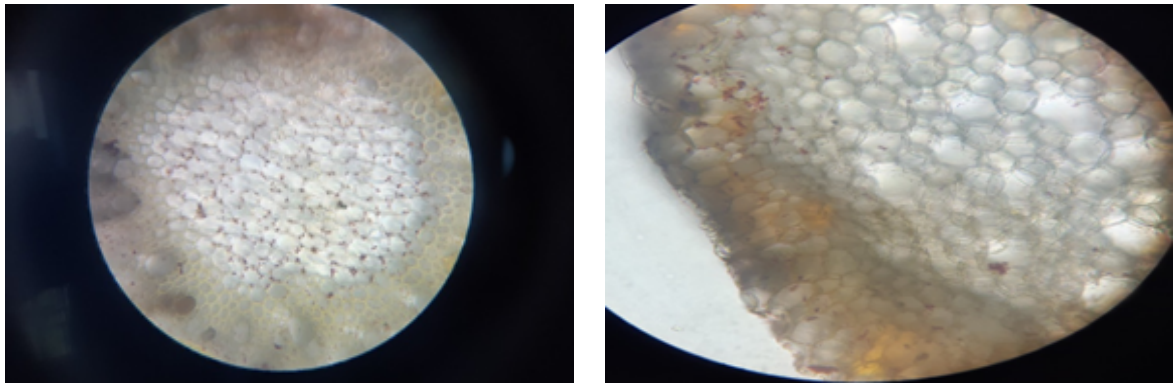

(A) (B)

Figure 4. Distribution of Pb in root tissues *Dracaena sanderiana* plants: (A) Pb granular form (10X); (B) Distribution of Pb in epidermis and parenchyma at 800 mg/L Pb (40X); Bar: 1.1mm and 0,4mm; E: epidermis; P: parenchyma.

than 90% of Pb accumulated in the roots was found insoluble in the spaces between cells and tightly bound to the cell walls (Jiang & Liu, 2010).

In the roots, Pb tended to move to the xylem tissue to be transported to stems and leaves. However, Pb mobility is limited by the endodermis barrier. So lead accumulation increases in the endodermis, especially on the casparian strip with dark red color (Figure 5A). At lethal concentration (4000 mg/L), endodermis barrier is broken and Pb infiltrates through casparian into tissues (Figure 5B) The endodermis acts as a barrier to the migration of Pb from roots to stems and leaves (Azmat et al., 2006). This may partly explain for the result that the content of Pb accumulates in roots higher than in stems and leaves.

3.2.2. Distribution of Pb in stems tissues

The Pb form deposited mainly in the stem as a diffuse form and a small part showed in granular form. In the stem, Pb content accumulated and deposited the most around the vascular bun-

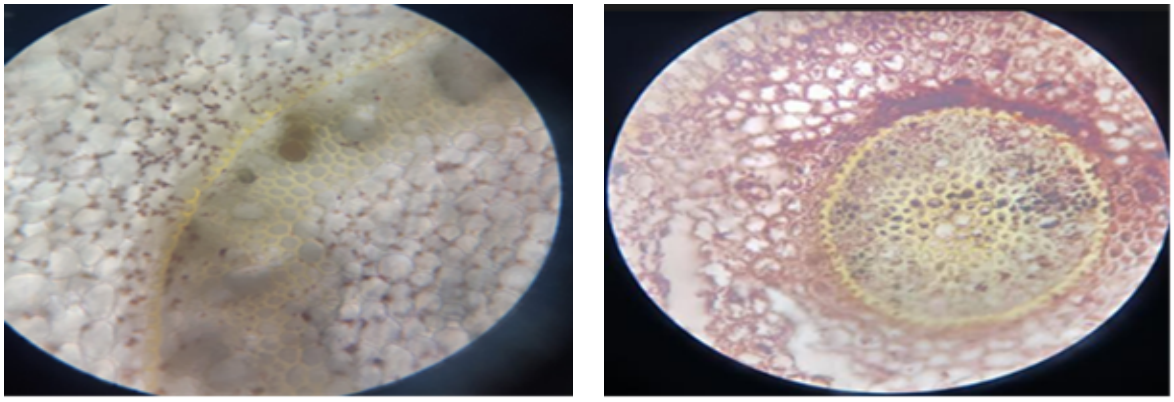

(A) (B)

Figure 5. Distribution of Pb in root tissues of *Dracaena sanderiana* plants. (A) Distribution of Pb at endodermis at 1000 mg/L Pb (40X); (B) Distribution of Pb at lethal concentration (4000 mg/L) (40X); Bar: 0,4mm; En: Endodermis; C: Casparian strip.

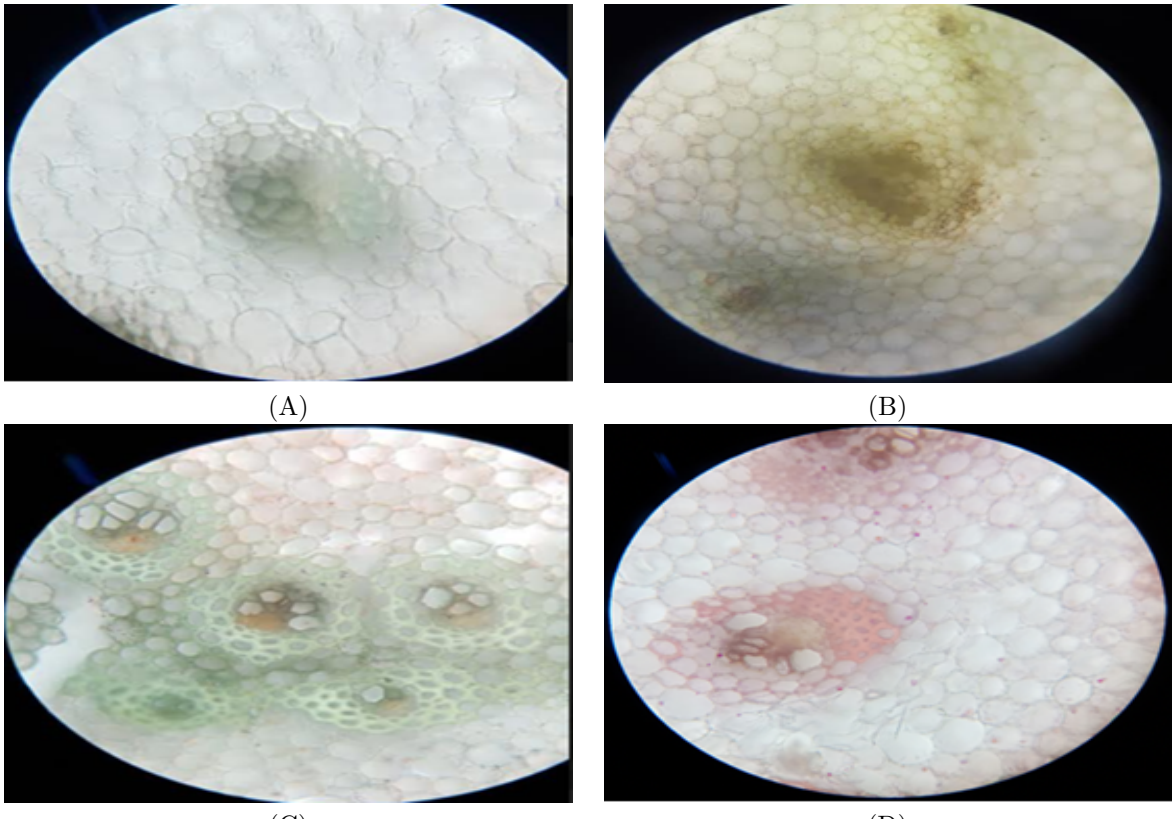

(A) (B)

(C) (D)

Figure 6. Distribution of Pb in stems tissues of *Dracaena sanderiana* plants. (A, B, C and D: control, 400 mg/L, 800 mg/L and 2000 mg/L; VB: vascular bundles; Bar: 0.4 mm; (40X).

dles and tended to diffuse to nearby tissues (Figure 6B, 6C, 6D). Lead content accumulated also increased with the concentration of lead treated (Figure 6). High concentration of lead deposited on the vascular bundles could exceed the tolerance of plants and reduce vascular size and expand the xylem space. This phenomenon has also been identified in the study of Al-Saadi et al.

(2013).

3.2.3. Distribution of Pb in leaves tissues

According to the observation of Pb distribution in leaf tissues (Figure 7), red marks didn't detected in leaf tissues of *Dracaena sanderiana* that exposed lead at a concentration of 200 mg/L to 2000 mg/L. Red marks only detected at concentrations of 3000 mg/L and 4000 mg/L. The results showed that the color in leaves tissues is not different between control, concentration of 200 mg/L and concentration of 2000 mg/L (Figure 7A, 7B, 7C). In contrast, red marks were detected at concentration of 3000 mg/L Pb and observed in vascular bundles (Figure 7d). It is possible that the concentration of lead accumulated very low in leaves at treatment concentrations is less than 3000 mg/L so the color has not been seen.

3.3. Response of plant tissues to lead accumulation

3.3.1. Response of root tissues

This study examined the effect of toxic Pb on *Dracaena sanderiana*. The results showed that Pb markedly affect the treatmented *Dracaena sanderiana* plants as compared to the control. A pronounced effect of Pb on plant roots tissues structure of *Dracaena sanderiana* showed the rapid respond to accumulated Pb, through a increasing in size of tissues. Epidermis, parenchyma, xylem and pith tissues were increased 1.36 - 2.48; 1.01 – 1.55; 1.01 – 122 and 1.01 – 1.55 times, respectively when were observed at 200 – 400 mg/L Pb (Figure 8). These tissues tended to increase when Pb levels in solution increase, especially to the epidermis and parenchyma tissues. These results could be explained that lead accumulation in root tissues accelerates maturation of cells as well as the formation of secondary cell walls. When plant cells are exposed to Pb, the synthesis polysaccharides in cell walls increase as resulting for significant thickening of the cell walls (Raven et al., 1999).

Thicker root tissues could also be the detoxification way for Pb of *Dracaena sanderiana* in order to create the physical barrier and reduce migration of Pb to the upper parts of the plants. Similar results were also reported by Tupan & Azrianingsih (2016) who said that the size of parenchyma and endodermis tissues of Thalassia hemprichii roots have increased in Pb poisoning condition. In 250 mg/L Pb, the number of xylem tissue layers in Lens culinaris increased more than three times compared to the control (Azmat et al., 2006). In addition, the thickening of the cell walls also creates more sites for Pb binding and thus increases extracellular sequestration (Gomes et al., 2011). Thicker cell walls have also been detected in *F. hygrometrica protonemata* (Krzesłowska et al., 2009).

3.3.2. Response of stem tissues

Epidermis tissue and vascular bundles in the stems at Pb levels of 200, 400, 600 and 800 mg/L were thicker than 1.05 - 1.18 times and 1.02 - 1.10 times as compared to the control plant (Figure 9). The size of the epidermis tissue and vascular bundle were decreased when Pb concentrations above 800 mg/L. In contrast, xylem tube diameter of stems in all Pb levels increased 1.08 - 1.36 times as compared to the control treatment.

At lower concentrations (200, 400, 600, 800 mg/L), the thicker epidermis tissue could be the result of stimulation when the presence of lead in low concentrations was diffused from vascular tissue leading to more maturation of the cell walls. Krzesłowska et al. (2010) suggested that, when a small amount of lead penetrates in the cell membranes, it interacts with cellular components and increases the thickness of the cell walls. He also reported that the presence of low levels of Pb will stimulate the growth of plants. However, at higher lead levels (1000, 2000, 3000 and 4000 mg/L), the epidermis, cell layer occupying and including vascular size decreased. These changes may be due to the effects of toxic lead thresholds when linked to cell walls that do not make cells thicker which disrupt hormonal balance. The effect on water hydrolysis of cells as causes the cells lose much water (Gomes et al., 2011).

Dracaena sanderiana is a plant that can survive in both soil and water environments. When living in a water environment, the *Dracaena sanderiana* itself, like other aquatic plants, needs a large intercellular space to bring oxygen to the roots. Therefore, *Dracaena sanderiana* has many vascular bundles in the stem anatomy structure. Vascular bundle size tends to increase lead concentration to 800 mg/L. This change may be the way to the tree against the loss of oxygen. Al-Saadi et al. (2013) found changes in intercellular spaces in the stem of a aquatic plant *Potamoge-*

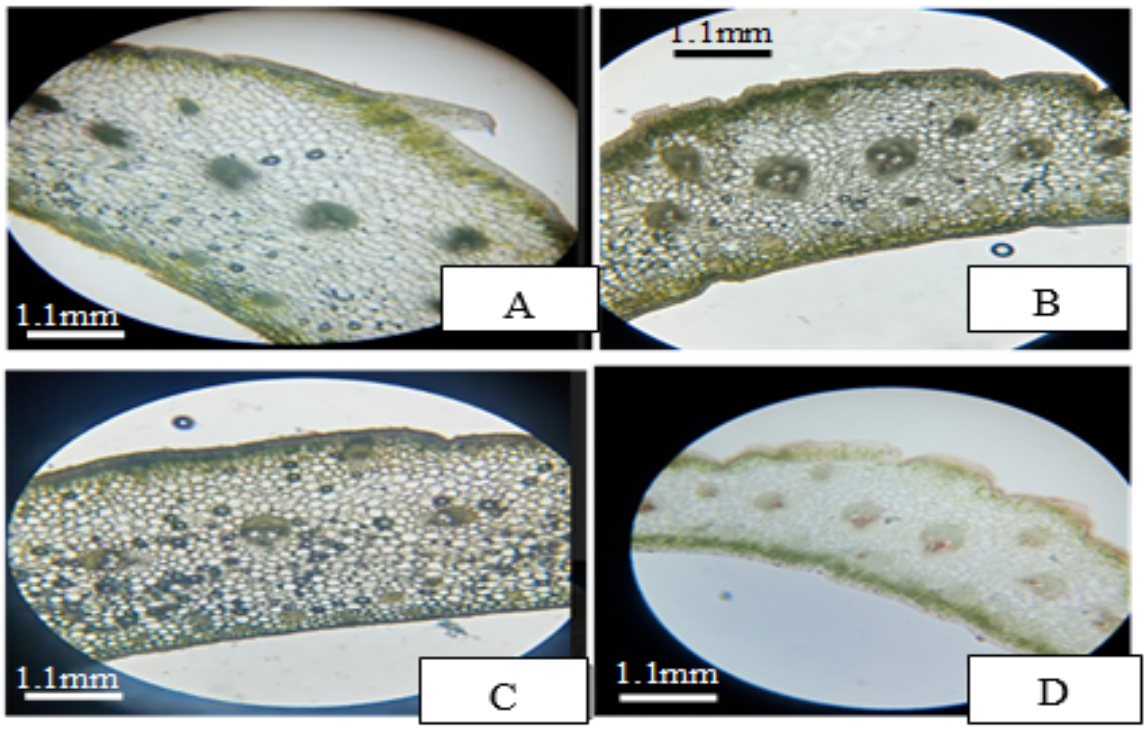

Figure 7. Distribution of Pb in leaves tissues of *Dracaena sanderiana* plants. (A): Control; (B): 200 mg/L; (C): 2000 mg/L; (D): 3000 mg/L; Bar: 1.1mm; (10X).

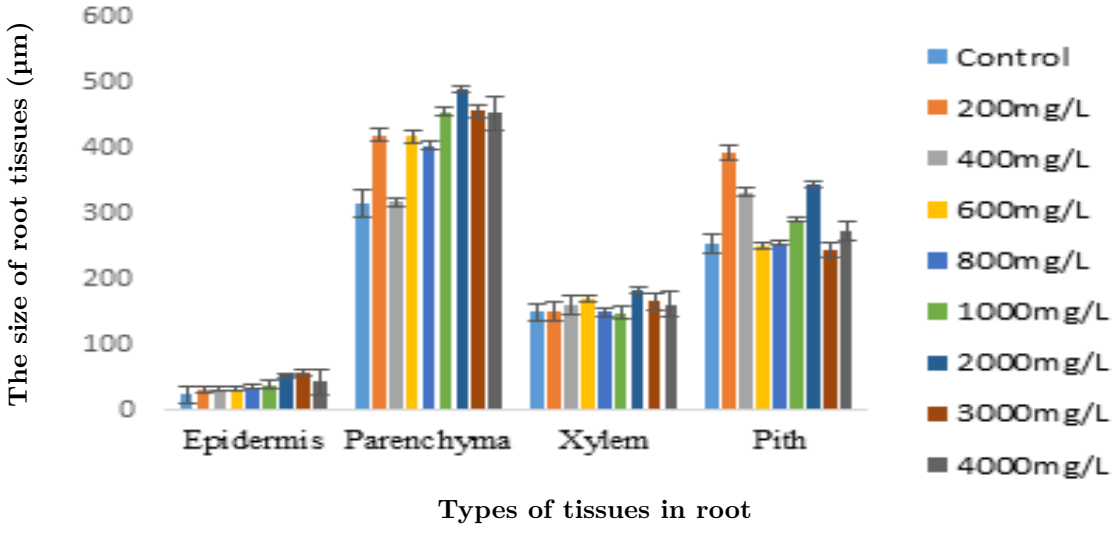

Figure 8. Changes in the anatomical tissues structure of Dracaena sanderiana roots.

ton sp. and concluded that the change is because Pb is transported in the intercellular space so the intercellular space must expand to prevent oxygen loss (Al-Saadi et al., 2013). The increased size of vessels can be an important strategy of live plants in the wetland environment not only facilitates the transport of oxygen in the tree, but also increases the potential for carrying oxygen to the root zone.

3.3.3. Response of leaf tissues

The size of the upper epidermis, parenchyma and vascular bundle was greater than the con-

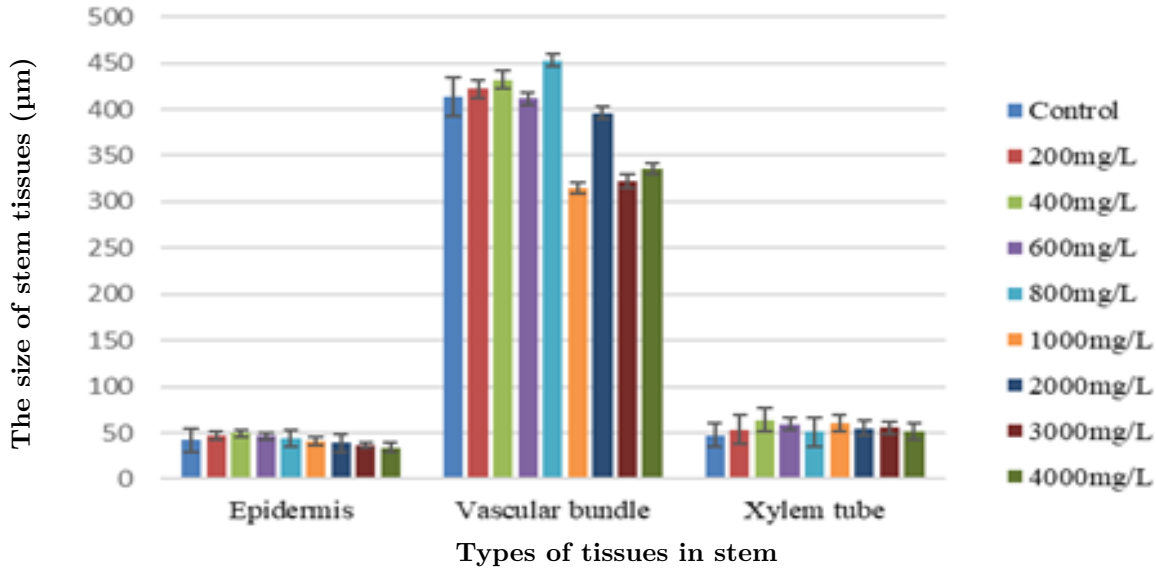

Figure 9. Changes in the anatomical tissues structure of *Dracaena sanderiana* stem.

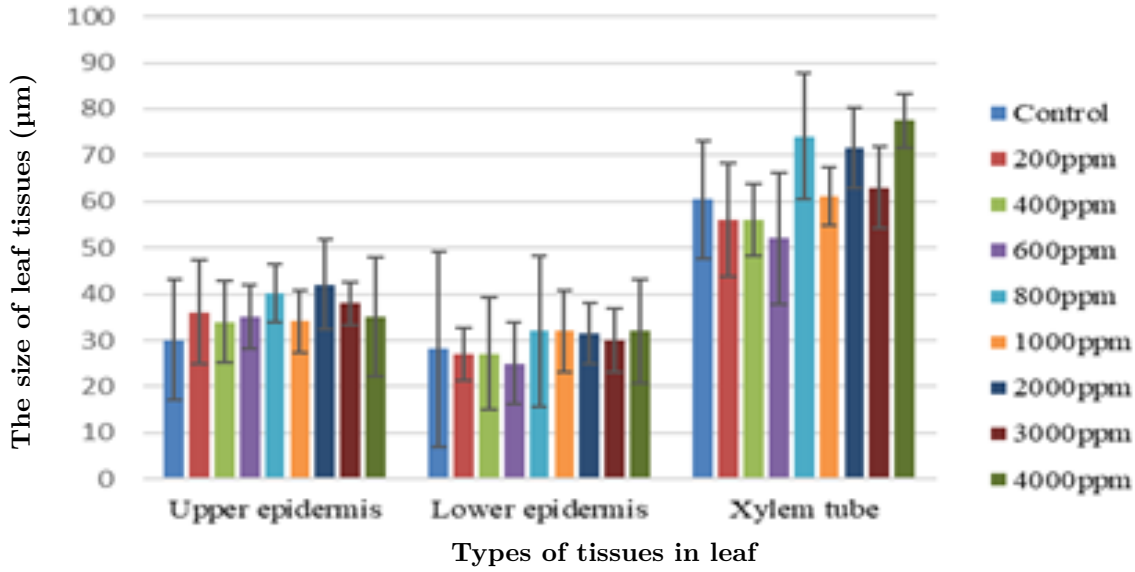

Figure 10. Changes in the upper epidermis, lower epidermis and xylem tissues structure of *Dracaena sanderiana* leaf.

trol 1.13 - 1.32 times; 1.37 - 3.95 times and 1.06 - 1.55 times, respectively (Figure 10, 11). However, the increase in size in these tissues varies with lead concentration and depends on the type of tissue. The structure of other types of tissue such as the lower epidermis, vascular bundle also changes with the concentration of lead. The size of the lower epidermis and xylem at 200, 400 and 600 mg/L Pb decreased greatly compared to the control. Otherwise at 800, 1000, 2000, 3000 and 4000 mg/L Pb, they increase greatly compared to the control (1.13 - 1.14 times) (Figure 10). This proves that the leaves of *Dracaena sanderiana* trees have a reaction to lead. When plants are contaminated with lead, plants have some lead-resistant mechanisms, isolating lead in vacuole is one of those mechanisms. To accumulate lead in vacuoles, the vacuole size must stretch and change the leaf anatomical structure. The change in leaf anatomical structures may be related to

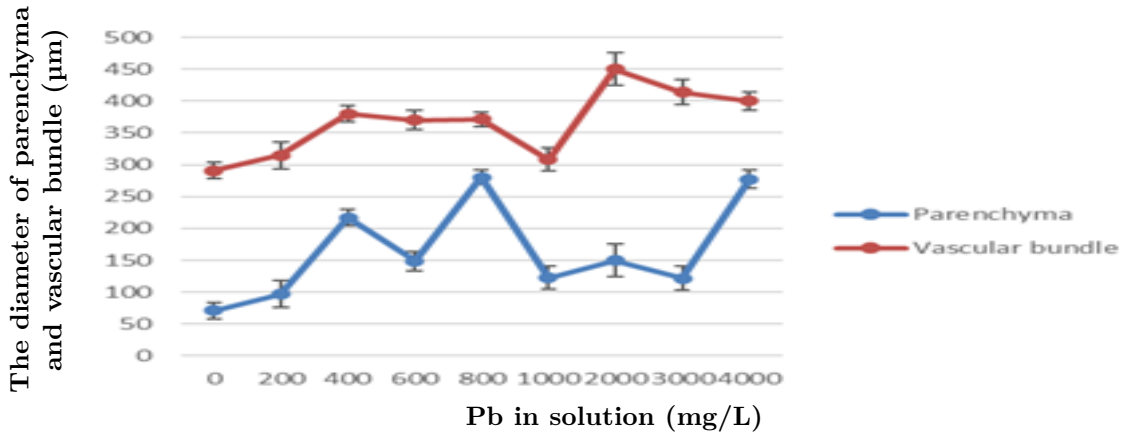

Figure 11. Changes in the parenchyma and vascular tissues structure of *Dracaena sanderiana* leaf.

lead content in the leaves. In this study, the results changed significantly in epidermal size and leaf tissue may be related to this problem. The change in leaf anatomical structure is significant at lead concentrations of 2000, 3000 and 4000 mg/L and this is also the concentration at which leaves accumulate the most lead content.

With the results of the surgery leaves obtained showed that the leaf has many characteristics adapted to high lead environment. Leaf epidermis, parenchyma and vascular bundle increased more than to help plants accumulate lead, and limit evapotranspiration, increasing the ability to accumulate water to detoxify the tree, on the other hand, the increased vascular bundle diameter helps facilitate transport oxygen to the roots zone (compared to the control treatment).

4. Conclusions

Lucky bamboo plants (*Dracaena sanderiana*) have the ability to accumulate and distribute lead in roots, stems and leaves tissues. Pb content is accumulated mainly in the roots and increases with the increase in concentration of Pb. In the roots, Pb is deposited mainly on cell walls and intercellular. In stems and leaves, Pb deposited mainly around the vascular bundles. The distribution of Pb made the anatomical structure of the roots, stems and leaves change markedly. With the capacity for accumulation and distribution of Pb, *Dracaena sanderiana* can become a well bio-accumulated plant as well as a biofilter plant for lead heavy metal pollution.

Conflict of interest

The authors declare no conflict of interest.

Acknowledgements

This research was financially supported by Thu Dau Mot University under grant number DT. 21.1-036.

References

Al-Saadi, S. A. A. M., Al-Asaadi, W. M., & Al-Waheeb, A. N. H. (2013). The effect of some heavy metals accumulation on physiological and anatomical characteristic of some *Potamogeton* L. plant. *Journal of Ecology and Environmental Sciences* 4(1), 100-108.

ATSDR (Agency for Toxic Substances and Disease Registry). (1993). *Toxicological profile for lead.* Georgia, USA: U.S. Department of Health and Human Services, Public Health Service.

Azmat, R., Haider, S., & Askari, S. (2006). Phytotoxicity of Pb: I effect of Pb on germination, growth, morphology and histomorphology of *Phaseolus mungo* and *Lens culinaris. Pakistan Journal of Biological Sciences* 9(5), 979-984.

Dahmani-Muller, H., van Oort, F., Gélie, B., & Balabane, M. (2000). Strategies of heavy metal uptake by three plant species growing near a metalsmelter. *Environmental Pollution* 109(2), 231-238.

Diep, H. M. T., & Zarli, E. G. (2007). *Lantana camara* L., plant accumulating lead from soils for decontamination. *Science and Technology Development Journal* 10(1), 13-24.

EPA (Environmental Protection Agency). (2000). *Introduction to phytoremediation.* Ohio, USA: National Risk Management Research Laboratory Office of Research and Development U.S. Environmental Protection Agency.

Glater, R. A. B., & Hernandez, L. (1972). Lead detection in living plant tissue using a new histochemical method. *Journal of the Air Pollution Control Association* 22(6), 463-467.

Gomes, M. P., de Sa e Melo Marques, T. C. L. L., de Oliveira Goncalves Nogueira, M., de Castro, E. M., & Soares, A. M. (2011). Ecophysiological and anatomical changes due to uptake and accumulation of heavy metal in *Brachiaria decumbens*. *Scientia Agricola* 68(5), 566-573.

Hao, T. Y. (2011). Removal of heavy metals copper and chromium (VI) using hydroponically cultivated plants *Dracaena surculosa* and *Dracaena sanderiana* (Unpublished doctoral dissertation). University of Technology Malaysia, Johor, Malaysia.

Ho, L. B., Huynh, B. V., & Bui, T. C. (2019). Assessment accumulation potential of lead by Lucky bamboo plants (*Dracaena sanderiana*). *Science and Technology Journal of Agriculture & Rural Development* 16, 3-12.

Hoang, S. T., & Nguyen, N. P. (2004). *Morphology - Plant anatomy*. Ha Noi, Vietnam: Publishing of University of Education.

Jiang, W., & Liu, D. (2010). Pb-induced cellular defense system in the root meristematic cells of *Allium sativum* L. *BMC Plant Biology* 10, 40.

Krzesłowska, M., Lenartowska, M., Mellerowicz, E. J., Samardakiewicz, S., & Wozny, A. (2009). Pectineus cell wall thickenings formation a response of moss protonemata cells to lead. *Environmental and Experimental Botany* 65(1), 119-131.

Krzesłowska, M., Lenartowska, M., Samardakiewicz, S., Bilski, H., & Wozny, A. (2010). Lead deposited in the cell wall of *Funaria hygrometrica* protonemata is not stable–a remobilization can occur. *Environmental Pollution* 158(1), 325-338.

Kumar, A., & Prasad, M. N. V. (2018). Plant-lead interactions: Transport, toxicity, tolerance, and detoxification mechanisms. *Ecotoxicology and Environmental Safety* 166, 401-418.

Raven, P. H., Evert, R. F., & Eichhorn, S. E. (1999). *Biology of plants* (6^{th} ed.). New York, USA: W. H. Freeman & Company Worth.

Sereshi, H., Eskandarpour, N., Samadi, S., & Aliakbarzadeh, G. (2014). Investigation on *Dracaena sanderiana* phytoremediation ability for Hg and Cd using multivariate task specific ionic liquid-based dispersive liquid-liquid microextraction. *International Journal of Environmental Research* 8(4), 1075-1084.

Tran, T. V., Nguyen, K. T ., Do, A. T. & Dinh, K. D. (2011). The study about the resistibility and absorptivity of the Pteris vittata fern to Pb and Zn. *Vietnam Journal of Science and Technology* 49(4), 101-109.

Tung, G., & Temple, P. J. (1996). Uptake and localization of lead in corn (*Zea mays* L.) seedling, a study by histochemical and electron microscopy. *The Science of the Total Environment* 188(2-3), 71-85.

Tupan, C. I., & Azrianingsih, R. (2016). Accumulation and distribution of lead heavy metal in the tissues of roots, rhizomes and leaves of seagrass *Thalassia hemprichii*. *AACL Bioflux* 9(3), 580-589.

Influence of spray-drying conditions on the physicochemical properties of red-fleshed dragon fruit (*Hylocereus polyrhizus*) powder made from peel and flesh

Trang T. N. Tran, Quan A. Do, Ngoan H. Nguyen, Tram N. Pham, Trang L. H. Do, Diep T. N. Duong*, & Binh Q. Hoang

Faculty of Chemical Engineering and Food Technology, Nong Lam University, Ho Chi Minh City, Vietnam

ARTICLE INFO

Research Paper

Received: December 04, 2020
Revised: March 09, 2021
Accepted: March 20, 2021

Keywords

Physicochemical
Pitaya
Powder
Spray-drying

***Corresponding author**

Duong Thi Ngoc Diep
Email: duongngocdiep@hcmuaf.edu.vn

ABSTRACT

Pitaya production has been increasing, that offers abundant material for food processing. New product development would greatly add value for this produce. The present study focused on the effects of spray-drying conditions such as coating material concentration and spray-drying temperature on the physicochemical characteristics of red-fleshed dragon fruit powder made from peel and flesh. The sample quality was influenced by two experimental factors, which were the maltodextrin concentration and the spray-drying inlet temperature. The samples spray-dried at 140°C to 150°C with 15% maltodextrin (w/w) gave the powder with the highest betacyanin, polyphenol, and vitamin C retention results (97.62 - 98.86%, 90.66 - 91.63%, and 63.40 - 63.68%, respectively). The moisture content, water activity and solubility of the sample was 3.88% to 4.27%, 0.26 to 0.28 and 99%, respectively. Red-fleshed dragon fruit powder made from flesh and peel has numerous potentials in the beverage industry.

Cited as: Tran, T. T. N., Do, Q. A., Nguyen, N. H., Pham, T. N., Do, T. L. H., Duong, D. T. N., & Hoang, B. Q. (2021). Influence of spray-drying conditions on the physicochemical properties of red-fleshed dragon fruit (*Hylocereus polyrhizus*) powder made from peel and flesh. *The Journal of Agriculture and Development* 20(3), 61-67.

1. Introduction

Red-fleshed dragon fruit, also known as red pitaya, is a member of the Cactaceae family and the order of Caryophyllales. With the specific purple-red color of the peel and flesh, delicate and appetizing flavor, high nutritional and functional potentials (Stintzing et al., 2003), red-fleshed dragon fruits are widely cultivated on a large scale throughout countries that possess tropical and subtropical climate, including Vietnam. Red-fleshed dragon fruit is well-known for its outstanding pharmacological benefits. Both the flesh and peel are rich in polyphenol and antioxidants, with the peel exhibiting higher antioxidant activities (Wu et al., 2006). Although the ideal weather pattern can benefit the cultivation of such fruit, it still leaves some negative effects on other related aspects as the fruit is usually consumed fresh, including difficulties regarding storage conditions and transportation, etc. For that reason, processes that can turn fresh fruits into commercialized products play an important role in building up the values for agricultural commodities. Fruit powder is an excellent option in response to the trend towards healthier and more natural products for consumers. The quality of the product will hardly reach the requirement if the processing is not controlled well. Because of this, the study utilized peel as an alternative source to partly replace the flesh in making red dragon fruit powder by spray-drying, thus reduce

the loss of by-products and lower the price of the finish powder. The present research was carried out to assess the physicochemical properties of pitaya fruit powder with emphasis on the physicochemical properties of water activity, moisture content, solubility, etc. by varying concentrations of the coating materials (maltodextrin) and inlet temperatures of spray drying.

2. Materials and Methods

2.1. Materials

Red-fleshed pitaya used in the present study was purchased locally from Thu Duc wholesale market in Ho Chi Minh City within a week of harvesting. The selected fruits were fresh and ripe, with no defect of physical injures and fungi (Figure 1). One standardized fruit weighed approximately 450 g with the ratio of flesh: peel equaled 4:1. The Brix values of the peel and flesh were 5.0°Bx and 12°Bx respectively. The pH values for flesh and peel were 4.58 and 4.94, respectively. The betacyanin, ascorbic acid, and total phenolic contents were 12.74 mg/100 g, 16.25 mg AA/100 g, and 57.29 mg GAE/100 g in the flesh, respectively and were 3.75 mg/100 g, 10.63 mg AA/100 g, and 25.25 mg GAE/100 g in the peel, respectively. The peel, flesh, and scale (the prominent, green parts located on the fruit's skin) were separated and stored at -18°C until use.

A B

Figure 1. (A) Flesh and (B) peel of red dragon fruit.

Enzyme Pectinex Ultra SP-L liquid was produced by Novozymes group (Bagsvaerd, Denmark), distributed by Brenntag Vietnam Company Limited (Ho Chi Minh City). Enzyme pectinase is an enzyme of the polygalacturonase group. The enzyme has its activity of 3800 PGNU per mL (polygalacturonase activity per mL). Enzyme is stored at 10 - 12°C. The activity of this product is stable over wide pH (2.8 - 6.5) and temperature (15 - 55°C) ranges.

Chemicals: gallic acid 99%, folin-ciocalteu 99%, ascorbic acid 99,7% (Merck, Germany), sodium carbonate 98%, sodium metabisulfite, citric acid anhydrous, disodium hydrogen phosphate, iodine, potassium iodide (Xilong, China), ethanol 99% (Chemos, Vietnam), maltodextrin DE 10 (Himedia, India).

Equipment: electronic scale (Ohaus Corp.pine Brook, USA), water bath (Schutzart, Germany), balances (Sartorius, Japan), vortex, UV-vis spectrophotometer (Jenway, USA), spray-dryer KD-400 (Vietnam), blender (Phillip, Netherland), juicer (Vietnam), Z206A centrifuge (Hermle, Germany), IKA T18 digital Ultra Turrax homogenizer (IKA, Germany), Chroma meter CR-400 (Konica Minolta, Japan).

2.2. Sample preparation

2.2.1. Flesh extract preparation

The flesh after thawing was ground by a juicer to eliminate the seeds then mixed with water to the ratio of 1:1 (w/w). Pectinex Ultra SPL of 0.2% (w/w) concentration was added. The puree was hydrolyzed at 45°C for 60 min (a result of the preliminary test). After that, the sample was inactivated at 100°C for 1 min, then filter through cheesecloth. The obtained solution was stored at 10°C until use.

2.2.2. Peel extract preparation

The peel was mixed with water to the ratio of 1:1 (w/w) and crushed by a blender. Pectinex Ultra SPL of 0.4% (w/w) concentration was added to the peel solution. The puree was hydrolyzed at 45°C for 120 min (a result of the preliminary test). After that, the sample was inactivated at 100°C for 1 min, then centrifuged at 5000 rpm for 10 min and filtrated through a 102-filter paper with a diameter pore of 15 - 20 µM to get the peel extract. The obtained solution was refrigerated at 10°C until use.

2.2.3. Powder preparation

The extracts of flesh and peel puree were mixed to the ratio of 4:1 (w/w), this ratio was obtained based on the natural proportion between flesh and de-scaled peel of standardized red-fleshed

dragon fruit. The mixture was added with different concentrations of maltodextrin and homogenized at 5000 rpm for 5 min. The sample was dried at 150°C in a spray-dryer KD-400 equipped with a diameter nozzle in the Chemical Department of Nong Lam University, Ho Chi Minh City, as the feed flow rate of 500 mL/h was controlled by the pump rotation speed at 2.5 rpm and compressor air pressure of 2.1 kgf/cm^2. The powder samples were stored in a screw-capped amber bottle at -18°C until further analysis.

2.3. Experiment design

2.3.1. Effect of maltodextrin concentration on physico-chemical of powder

This experiment was investigated by an experimental single factor. Maltodextrin concentration with 3 levels (10%, 15%, and 20%, w/w) was surveyed. Sample preparation was followed in section 2.2. The physicochemical properties of powder including betacyanin retention, total phenolic content retention, vitamin C retention, moisture content, water activity, solubility, L*, C, and H° were recorded.

2.3.2. Effect of drying temperature on physicochemical of powder

After the maltodextrin concentration was chosen (section 2.3.1), inlet air temperature with 3 levels (140, 150, and 160°C) was investigated. Sample preparation was followed section 2.2. The physicochemical properties of powder were including betacyanin retention, total phenolic content retention, vitamin C retention, moisture content, water activity, solubility, L*, C, and H° recorded.

2.3.3. Analytical methods

Moisture Content: The moisture was determined by infrared moisture drying balance MX-50 (0.01%/max 51g), Sartorius, Japan. One gram of sample was weighed and dried until a constant weight was obtained.

Water Activity: The water activity was determined by using a water activity meter AquaLab-DewPoint 4Te (Decagon Devices Inc., Pullman, WA, USA) at 25°C ± 0.5.

Color measurement: The color of the pitaya powder was measured by using a Chroma meter CR-400 (Konica Minolta, Japan). The lens of the color reader was put upon the powder to obtain the L*, C, and H° values for the powder.

Solubility: The water solubility was performed using the method described by Reddy et al. (2015) with a few modifications. A sample of 0.5 g was mixed with 6 mL of distilled water and then centrifuged at 5000 rpm for 10 min. After centrifugation, the suspension was placed in a dish and dried at 105°C for 4 h to obtain constant dry solids weight. The solubility (%) was determined as:

$$\text{Solubility (\%)} = \frac{\text{Weight of dry solids in the supernatant}}{\text{Weight of dry sample}} \times 100$$

Total betacyanin content: The total betacyanin content of the dragon fruit sample was determined by a colorimetric method (Rebecca et al., 2008). The sample was weighed and diluted in water, followed by vortexing, then centrifuged at 5000 rpm for 10 min. The supernatant was collected and filtrated using filter paper. The absorption value was analyzed by a spectrophotometer (Spectronic UV-Vis Genesys 10S Thermo, USA) at a wavelength of 538 nm. The proportion of betacyanin retention: = (BC_1/BC_0) × 100, where BC_1 is the betacyanin content after spray-dried, BC_0 is the betacyanin content before the spray-dried interval.

Total phenolic content: Polyphenols in red dragon fruits were determined by the Folin-Ciocalteau method (Singleton et al., 1999). In a tube, 1 mL of distilled water was mixed well with 1 mL of the diluted sample and 0.5 mL of Folin-Ciocalteau 10% and left for 6 min. Continue to add 1.5 mL of 20% Na_2CO_3 and 1 mL of distilled water, then left for another 2 h in darkness. The absorption value was analyzed by a spectrophotometer at a wavelength of 760 nm. The total phenolic content was calculated based on the standard curve for polyphenols and expressed by GAE/100 g dry solid. Proportion TPC retention: = (TPC_1/TPC_0) × 100, where TPC_1 is the total phenolic content after spray-dried, TPC_0 is the total phenolic content before spray-dried interval.

Ascorbic acid content (UV-VIS method): The method used to determine total ascorbic acid content was described by Kapur et al. (2012). In a tube, 0.23 mL of 3% bromine water was added into 4 mL of sample solution, 0.13 mL of 10% thiourea. Then 1 mL of 2, 4-DNPH solution was added. Samples were kept at 37°C temperature for 3 h in a water bath. After that, samples were

cooled in an ice bath for 30 min and treated with 5 mL chilled 85% H_2SO_4. The absorption value was analyzed by a spectrophotometer at a wavelength of 521 nm. The total ascorbic content was calculated based on the standard curve for ascorbic acid and expressed by AAE/100 g dry solid. Proportion AAC retention = $(AAC_1/AAC_0) \times 100$, where AAC_1 is the total ascorbic acid content after spray-dried, AAC_0 is the total ascorbic acid content before spray-dried interval.

Ascorbic acid content (HPLC method): The method followed Uckoo et al. (2011) with some modifications. In a tube, an aliquot of 0.5 g powder sample was homogenized (8000rpm, 1 min) in 3% metaphosphoric acid. The supernatant was diluted with ortho-phosphoric acid 3 mM and filtered through a 0,45 µM PTFE membrane. The HPLC operation systems (LC-20AD, Shimadzu, Japan) including pump (SIL-20A), detector (UV-VIS SPD-20A), degasser (DGU-20A3). The mobile phase A was provided with ortho-phosphoric acid 3 mM and the stationary phase was column C18 reverse (Inertsil, ODS 3, Japan). An isocratic mobile phase was run at a flow rate of 1.0 mL/min. An injection volume of 1.0 µL was used. The ascorbic acid was detected at 254 nm.

2.4. Statistical analysis

All experiments were carried out 2 times. Data and results were analyzed by using JMP 10.0 software and p-value ($P < 0.05$) and ANOVA One-way analysis of variance (ANOVA) to determine the significant differences ($P < 0.05$) between the means. Results are presented as mean ± standard deviation.

3. Results and Discussion

3.1. Effect of maltodextrin concentration on physicochemical of powder

The results of this experiment were as listed in Table 1.

Overall, all values of antioxidant compounds increased with maltodextrin concentration from 10% to 15% and decreased with maltodextrin concentration from 15% to 20% (Figure 2). The highest values of betacyanin, polyphenol, and vitamin C were obtained at 15% maltodextrin concentration (98.73%, 97.35%, and 63.73%, respectively). This can be explained by the protective ability of maltodextrin as a coating material towards sensitive compounds like antioxidants, but if the maltodextrin concentration was too high, it increased the viscosity of the feed solution and reduced the efficiency of the spray-drying process. All samples had similar values of moisture content (4.07 - 4.99%), water activity (0.26 - 0.28), and solubility (99.13 - 99.94). L^* value of the sample with 20% maltodextrin concentration was higher and significantly different ($P < 0.05$) from the other two samples.

A B C

Figure 2. Spray-dried powder with (A) 10%, (B) 15%, and (C) 20% maltodextrin concentration supplement.

C and H^o values between the three samples were not significantly different from each other ($P < 0.05$). An increase in L^* values (72.97 - 76.45) and a decrease in Chroma values (30.38 - 28.24) were observed while H^o remained stable (approximately 359.77). This result indicated that all samples almost had the same light purple-red color and the color intensity got lighter as the maltodextrin concentration increased from 10% to 20%. This can be explained by the influence of the white color of maltodextrin on the color of the samples, the higher the concentration of maltodextrin, the lighter the color of the powder samples. The sample with 15% maltodextrin concentration had the highest physicochemical properties.

3.2. Effect of drying temperature on physicochemical of powder

In general, the increase in temperature from 140°C to 150°C witnessed an increase in physicochemical properties, with betacyanin retention increased from 97.62% to 98.76%, polyphenol retention increased from 98.19% to 98.31% and vitamin C retention increased from 63.40% to 63.68% (Table 2). However, when the drying temperature continued increasing, the physicochemical values started to drop, at this time the betacyanin retention, polyphenol retention, vitamin C retention were 95.63%, 92.42%, and 58.63%, re-

Table 1. Effect of maltodextrin concentration on physicochemical properties of red-fleshed dragon fruit powder

Attributes	Maltodextrin concentration (%)		
	10	15	20
Betacyanin retention (%)	$74.39^{c} \pm 0.34$	$98.73^{a} \pm 0.18$	$84.87^{b} \pm 0.63$
Polyphenol retention (%)	$83.24^{b} \pm 0.29$	$97.35^{c} \pm 0.60$	$96.92^{c} \pm 0.47$
Vitamin C retention (%)	$59.42^{b} \pm 0.62$	$63.73^{a} \pm 1.31$	$63.32^{ab} \pm 1.80$
Moisture content (%)	$4.99^{a} \pm 0.16$	$4.13^{b} \pm 0.79$	$4.07^{b} \pm 0.07$
Water activity	$0.28^{a} \pm 0.01$	$0.26^{a} \pm 0.01$	$0.28^{a} \pm 0.02$
Solubility (%)	$99.13^{a} \pm 0.95$	$99.94^{a} \pm 1.52$	$99.45^{a} \pm 1.48$
L^{*}	$72.97^{a} \pm 0.39$	$73.24^{a} \pm 0.85$	$76.45^{b} \pm 0.01$
C	$30.38^{a} \pm 0.48$	$30.16^{a} \pm 0.70$	$28.24^{a} \pm 0.82$
H^{o}	$359.76^{a} \pm 0.33$	$359.78^{a} \pm 0.54$	$359.76^{a} \pm 0.64$

$^{a, b, c}$Denote the statistically significant difference at $P < 0.05$. N = 2.

Table 2. Effect of inlet temperature on physicochemical properties of red-fleshed dragon fruit powder

Attributes	Inlet temperature (°C)		
	140	150	160
Betacyanin retention (%)	$97.62^{a} \pm 0.85$	$98.76^{a} \pm 0.28$	$95.63^{b} \pm 0.43$
Polyphenol retention (%)	$98.19^{a} \pm 0.74$	$98.31^{a} \pm 0.12$	$92.42^{b} \pm 0.70$
Vitamin C retention (%)	$63.68^{a} \pm 0.15$	$63.40^{a} \pm 0.64$	$58.63^{b} \pm 0.55$
Moisture content (%)	$4.27^{a} \pm 0.86$	$3.88^{a} \pm 0.09$	$3.29^{a} \pm 0.04$
Water activity	$0.26^{a} \pm 0.02$	$0.28^{a} \pm 0.06$	$0.28^{a} \pm 0.07$
Solubility (%)	$99.03^{a} \pm 1.26$	$98.72^{a} \pm 0.91$	$99.13^{a} \pm 1.03$
L^{*}	$72.97^{a} \pm 0.34$	$72.21^{a} \pm 0.37$	$72.57^{a} \pm 0.45$
C	$31.85^{a} \pm 0.38$	$32.37^{a} \pm 0.44$	$33.04^{a} \pm 0.21$
H^{o}	$359.75^{a} \pm 0.01$	$359.76^{a} \pm 0.01$	$359.74^{a} \pm 0.01$

$^{a, b, c}$Denote the statistically significant difference at $P < 0.05$. N = 2.

spectively. This phenomenon occurred due to the sensitivity of polyphenol compounds over temperature. High temperature can easily destroy product's components that are not heat-resistant, thus leads to the decrease of these values. The drying temperature increased (from 140°C to 160°C) leaded to a decrease in moisture content (4.27 - 3.29%) (Figure 3). However, this range of temperature showed slightly no change in water activity (0.26 - 0.28) and solubility (98.72 - 99.13%). L^{*}, C, and H^{o} values between three samples were not significantly different from each other ($P < 0.05$). This result indicated that inlet drying temperature did not show any influences on the color of the powder. The samples spray-dried at 140°C and 150°C had the highest physicochemical properties.

Analytical results by HPLC showed that the samples analyzed (experiment 2.3.2) had peak area decreasing in the direction of increasing drying temperature, this showed that the vitamin C content in samples decreased gradually with the increasing of drying temperature (Figure 4). This result is consistent with the result obtained from UV-VIS analysis. Thus, analysis attributes such as betacyanin content, total phenolic content, ascorbic acid content by UV-VIS spectroscopy method are acceptable and still show the impact on the experimental factors of the physicochemical properties of dragon fruit powder.

Figure 3. Powder spray-dried at (A) 140°C, (B) 150°C, and (C) 160°C.

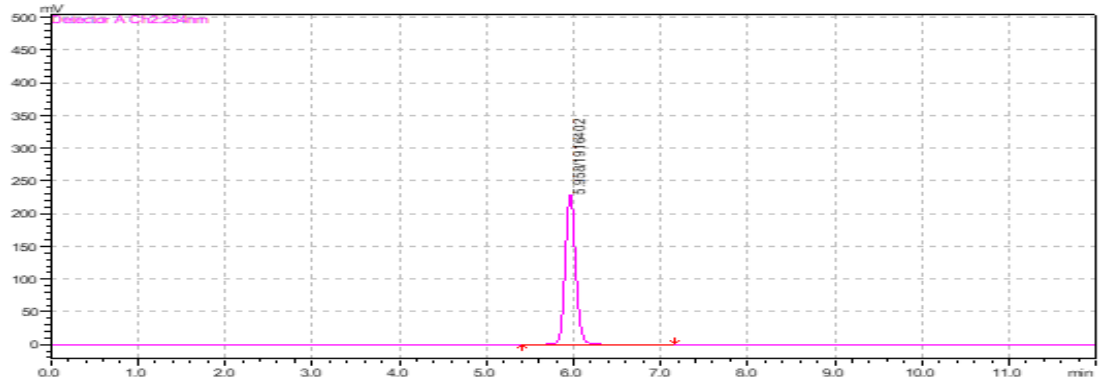

The peak of standard ascorbic acid.

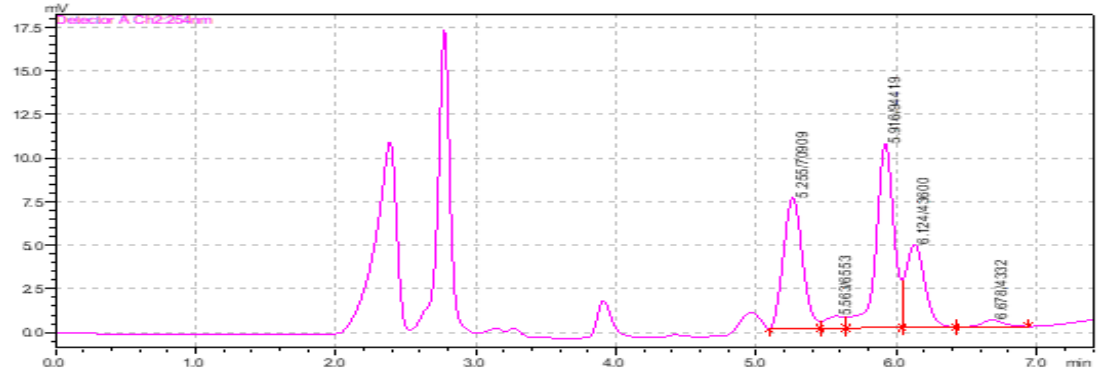

The peak of ascorbic acid of powder spray-dried at 140°C.

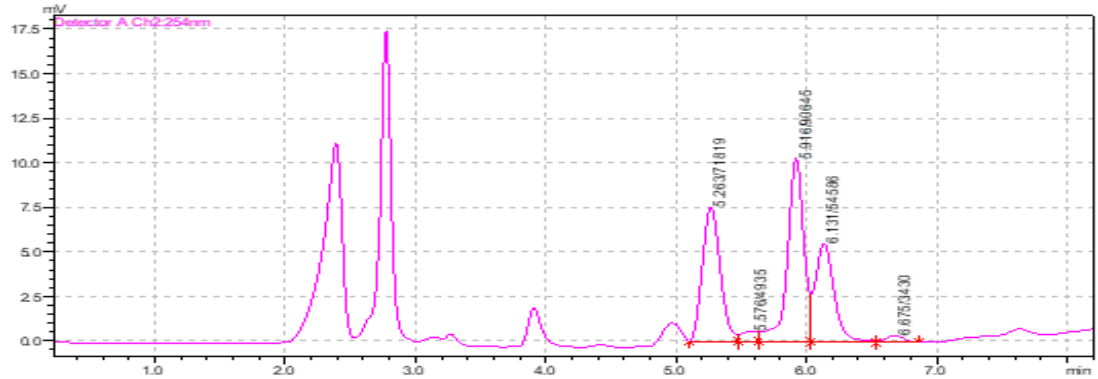

The peak of ascorbic acid of powder spray-dried at 150°C

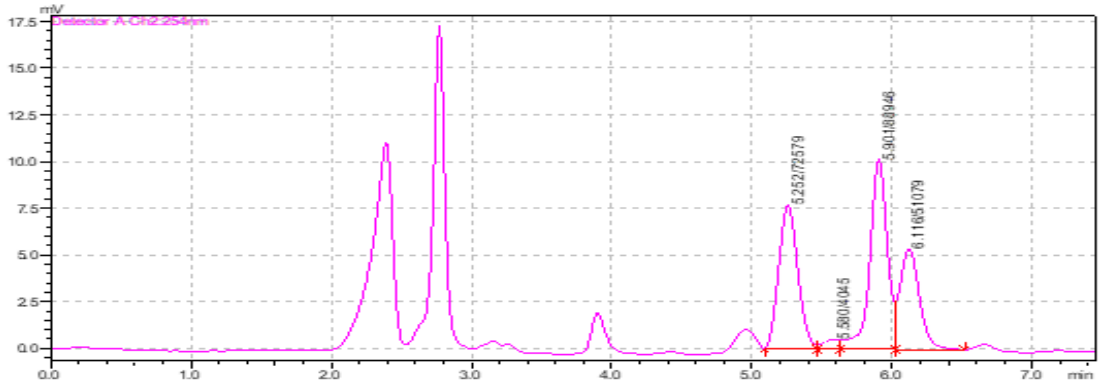

The peak of ascorbic acid of powder spray-dried at 160°C.

Figure 4. The peaks of ascorbic acid of samples under different drying temperatures.

4. Conclusions

The physicochemical properties such as betacyanin retention, polyphenol retention, and vitamin C retention varied depending on the maltodextrin concentration and inlet spray-drying temperature. Moisture content also showed variations. However, water activity and solubility did not show any significant changes in values between samples with different maltodextrin concentrations or inlet spray-drying temperatures. Moreover, unlike C and Ho values which remained stable under different maltodextrin concentrations and inlet temperatures, L^* value of samples with 20% maltodextrin concentration was significantly higher than the other samples. The best spray-drying conditions in relation to physicochemical properties of the powder were 140°C to 150°C inlet temperature and 15% maltodextrin concentration, with 97.62 - 98.76% betacyanin retention, 98.19 - 98.31% polyphenol retention, 63.40 - 63.68% vitamin C retention, 3.88 - 4.27% moisture content, 72.21 - 72.97 in L^* value. Spray-drying is a convenient method to process red-fleshed dragon fruit into powder. Maltodextrin is also a good coating material to protect sensitive constituent components. Further recommendations include more research on the ratio of the peel and flesh solution before spray-drying or using other materials as microencapsulating agents to optimize the value of the powder.

Conflict of interest

The authors declare no conflict of interest.

Acknowledgments

The authors would like to thank Nong Lam University, Ho Chi Minh City for sponsoring our research (project number: CS-SV19-CNTP-03).

References

Kapur, A., Hasković, A., Čopra-Janićijević, A., Klepo, L., Topčagić, A., Tahirović, I., & Sofić, E. (2012). Spectrophotometric analysis of total ascorbic ccid content in various fruits and vegetables. *Bulletin of the Chemists and Technologists of Bosnia and Herzegovina* 38, 39-42.

Rebecca, O. P. S., Zuliana, R., Boyce, A. N., & Chandran, S. (2008). Determining pigment extraction efficiency and pigment stability of dragon fruit (*Hylocereus polyrhizus*). *Journal of Biological Sciences* 8(7), 1174-1180.

Reddy, C. K., Pramila, S., & Haripriya, S. (2015). Pasting, textural and thermal properties of resistant starch prepared from potato (*Solanumtuberosum*) starch using pullulanase enzyme. *Journal of Food Science and Technology* 52(3), 1594-1601.

Singleton, V. L., Orthofer, R., & Lamuela-Raventós, R. M. (1999). Analysis of total phenols and other oxidation substrates and antioxidants by means of folinciocalteu reagent. In Minor, D. L., & Colecraft, H. M. (Eds.). *Methods in Enzymology* (152-178). Massachusetts, USA: Academic Press.

Stintzing, F. C., Schieber, A., & Carle, R. (2003). Evaluation of colour properties and chemical quality parameters of cactus juices. *European Food Research and Technology* 216, 303-311.

Uckoo, R. M., Jayaprakasha, G. K., Nelson, S. D., & Patil, B. S. (2011). Rapid simultaneous determination of amines and organic acids in citrus using high-performance liquid chromatography. *Talanta* 83(3), 948-954.

Wu, L. C., Hsu, H. W., Chen, Y. C., Chiu, C. C., Lin, Y. I., & Ho, J. A. A. (2006). Antioxidant and antiproliferative activities of red pitaya. *Food Chemistry* 95(2), 319-327.